ABSTRACT

Title of Dissertation:	CYCLING AROUND THE CLOCK: MODELING BIKE SHARE TRIPS AS HIGH-FREQUENCY SPATIAL INTERACTIONS
	Zheng Liu, Doctor of Philosophy, 2023
Dissertation directed by:	Assistant Professor Taylor Oshan, Department of Geographical Sciences

Spatial interactions provide insights into urban mobility that reflects urban livability. A range of traditional and modern urban mobility models have been developed to analyze and model spatial interaction. The study of bike-sharing systems has emerged as a new area of research, offering expanded opportunities to understand the dynamics of spatial interaction processes. This dissertation proposes new methods and frameworks to model and understand the high-frequency changes in the spatial interaction of a bike share system. Three challenges related to the spatial and temporal dynamics of spatial interaction within a bike share system are discussed via three studies: 1) Predicting spatial interaction demand at new stations as part of system infrastructure expansion; 2) Understanding the dynamics of determinants in the context of the COVID-19 pandemic; and 3) Detecting events that lead to changes in the spatial interaction process of bike share trips from a model-based proxy. The first study proposes a hybrid strategy to predict 'cold start' trips by comparing flow interpolation and spatial interaction methods. The study reveals 'cold start' stations

with different classifications based on their locations have different best model choices as a hybrid strategy for the research question. The second study demonstrates a disaggregated comparative framework to capture the dynamics of determinants in bike share trip generation before, during, and after the COVID-19 lockdown and to identify long-term bike share usage behavioral changes. The third study investigates an event detection approach combining martingale test and spatial interaction model with specification evaluation from simulated data and explorative examination from bike share datasets in New York City, Washington, DC, and San Francisco. Results from the study recognize events from exogenous factors that induced changes in spatial interactions which are critical for model evaluation and improvement toward more flexible models to high-frequency changes. The dissertation elaborated and expanded the spatial interaction model to more effectively meet the research demands for the novel transportation mode of bike-share cycling in the context of a high-frequency urban environment. Taken as a whole, this dissertation contributes to the field of transportation geography and geographic information science and contributes methods toward the creation of improved transport systems for more livable cities.

CYCLING AROUND THE CLOCK:
MODELING BIKE SHARE TRIPS AS HIGH-FREQUENCY SPATIAL INTERACTIONS

by

Zheng Liu

Dissertation submitted to the Faculty of the Graduate School of the
University of Maryland, College Park, in partial fulfillment
of the requirements for the degree of
Doctor of Philosophy
2023

Advisory Committee:
Dr. Taylor Oshan, Chair
Dr. Kathleen Stewart
Dr. Yiqun Xie
Dr. Giovanni Baiocchi
Dr. Vanessa Frias-Martinez

Dedication

To my parents,

Honglei Zheng (郑红雷) *and Guangdou Liu* (刘光斗),

for their unconditional support and love through the journey.

Acknowledgements

First and foremost, I would like to express my profound gratitude to my doctoral advisor, Dr. Taylor Oshan. Without his unwavering support and guidance, I would not have been able to successfully navigate the challenges of the PhD program and reach the finish line. Dr. Oshan provided me with invaluable feedback on my research helping me to refine my ideas and develop a clear focus for my dissertation. Beyond his professional expertise, Dr. Oshan was a constant source of encouragement and support throughout my time in the program, always taking the time to offer a listening ear or a word of wisdom when needed.

In addition to my gratitude towards Dr. Oshan, I would like to express my sincere appreciation to my dissertation committee members, Dr. Kathleen Stewart, Dr. Yiqun Xie, Dr. Giovanni Baiocchi, and Dr. Vanessa Frias-Martinez. Their constructive comments and feedback on my dissertation have been invaluable in helping me to improve my work. Moreover, I am deeply grateful to each of them for the advice, encouragement, and opportunities they have provided throughout my PhD journey. Their mentorship and support have been instrumental in shaping my academic growth and development, and I am honored to have had them as my committee members.

My thanks go to all friends in the Center for GIS, Zhiyue, Hai, Jeff, Peiqi, Xin, Yuehui, Weiye, Riccardo, Federico, and Xiaoguo for the wonderful work and life experiences. My thanks also go to all the colleagues in the Oshan group, Mengyu, Victor, and Ushashi, for discussing my research and providing me with substantial help in the development of my dissertation.

I would like to thank to Guimin, Yunting, Yimeng, Junchuan, Lei, Xiuxia, Xiaodong, Yu, Ruomin, Fengyu, Yuqian, Jeremiah, Tianyu, as well as faculty and cohorts from the MSGIS program who offered me unforgettable memories and made my PhD life not alone. Special thanks to all my friends from the Lakeside North community, Yao, Jiaming, Aolin, Yanjia, Cheng, and Yuhan, who left the most pieces of memories ever since my life in the US. Beyond the fun times, their support has been invaluable in helping me navigate the many challenges that life has thrown my way.

A special thanks to my girlfriend, Diyang Cui. From the very beginning of our story, she has been there for me, providing the emotional support and motivation I needed to push through even the most difficult moments. I am eternally grateful to her for all that she has done for me, and my gratitude to her has no expiration date.

Finally, I am indebted to my parents for offering solid backing for me. Their constant love and encouragement have been a source of strength for me during the six years that I lived on the other side of the world pursuing my degree.

Table of Contents

List of Tables

List of Figures

List of Abbreviations

COVID-19: Coronavirus disease caused by the SARS-CoV-2 virus

DC: Washington, DC

GBFS: General Bikeshare Feed Specification

GPS: the Global Positioning System

ICT: Information and Communications Technology

IOT: Internet of Things

LASSO: Least Absolute Shrinkage and Selection Operator

LSTM: Long Short-Term Memory

NYC: New York City

OD: Origin-destination

OK: Ordinary Kriging

POI: Point of interest

RK: Regression Kriging

RNN: Recurrent Neural Networks

SI: Spatial interaction

US: the United States

VIF: Variance Inflation Factor

Chapter 1: Introduction

1.1 Background and motivation

The increasing trend of urbanization in the past century has resulted in over half of the world's population now living in cities (United Nations, Department of Economic and Social Affairs, Population Division, 2019). This rapid urbanization has created a pressing need to gain a deeper understanding of urban infrastructure, population distribution, and job opportunities, which are crucial indicators of urban livability (Bassolas et al., 2019). A key aspect of this livability is the rising human mobility within urban areas, which serves as an essential observation for urban planners. Thus, it has become increasingly important to investigate and anticipate human mobility both within and between cities. Spatial interactions or origin-destination flows, which refer to the movement of people and goods between locations, are vital indicators of urban socio-economic activities and provide insights into the interdependence between different places. Studying spatial interactions of human mobility can gain valuable insights into the factors that influence urban livability and create more sustainable and equitable cities for all.

The study of spatial interaction and mobility has long been a central focus of transportation and geographical science, as understanding and predicting the flows of people, goods, and information across space is vital for numerous fields, including urban planning, transportation, and regional development. A range of methods have been developed to analyze and model spatial interaction, including both traditional approaches and new techniques that leverage recent advances in computing and artificial intelligence. Traditional methods such as spatial interaction models (Fotheringham & O'Kelly, 1989; Oshan, 2020; Wilson, 1971) are widely used to understand the

spatial interaction generation process in telecommunication, commodity goods, and migration in the past decades. These models use statistical techniques to estimate the flows of people or goods between different locations, based on factors such as distance, accessibility, and infrastructure. In recent years, modern urban mobility methods such as deep learning have gained attention in the study of spatial interaction, due to the development of more powerful computing resources and the increased use of artificial intelligence. Among the different targets of urban mobility models, there are (1) trip-based origin-destination (OD) demand (Z. Cheng et al., 2021; Ke et al., 2019; L. Liu et al., 2019; Y. Wang et al., 2019; Xiong et al., 2020); (2) location-based demand (Ai et al., 2019; P.-C. Chen et al., 2020; Geng et al., 2019; S. Guo et al., 2019; Li & Axhausen, 2020; Lin et al., 2019; Z. Pan et al., 2020; Ren, Chen, et al., 2019; Sun et al., 2020; Y. Yang et al., 2020); and (3) volumetric demand (L. Cai et al., 2020; Cui et al., 2019; Do et al., 2019; Ma et al., 2019; Qu et al., 2019; Ren, Cheng, et al., 2019; Shleifer et al., 2019; B. Yang et al., 2019; Y. Zhang et al., 2020; Zhang & Xin, 2020). Trip-based OD demand, also referred to spatial interaction in geography and other disciplines, has focused on enhancing predictions with the recent advances in statistical learning and deep learning at various temporal scales utilizing big geospatial data.

The availability of geo-located traces from Information and Communications Technologies (ICTs) has revolutionized the study of urban mobility, providing much greater spatiotemporal resolution than was previously possible. However, the use of individual-level traces from mobile phone records can be limited by concerns around privacy and consistency of data availability. As a result, anonymous flow records from transportation systems have become a popular choice for mobility modeling studies. Historically, public transportation systems such as buses, rail, and taxicabs have formed the backbone of cities, by facilitating interaction and providing an affordable and reliable alternative to private transportation. More recently, bike share systems have emerged as a new

form of transportation that can be more easily changed or expanded due to their lightweight and affordable infrastructure. Docked bike share systems, in particular, have become popular in many cities, offering daily trips with detailed time information that create new opportunities to study the dynamics of spatial interaction processes. Many articles have been dedicated to build the relationship between bike-share trips and its determinants. Factors related to socio-demographics, public transit, system infrastructure, street features, land use or places of interests, and weather are frequently included in the regression model with bike-share trip demand (Hu et al., 2022; A. Li et al., 2020; Maas et al., 2021; Noland et al., 2016; Ross-Perez et al., 2022; Schimohr & Scheiner, 2021; X. Wang et al., 2021; Younes et al., 2020; Zacharias & Meng, 2021).

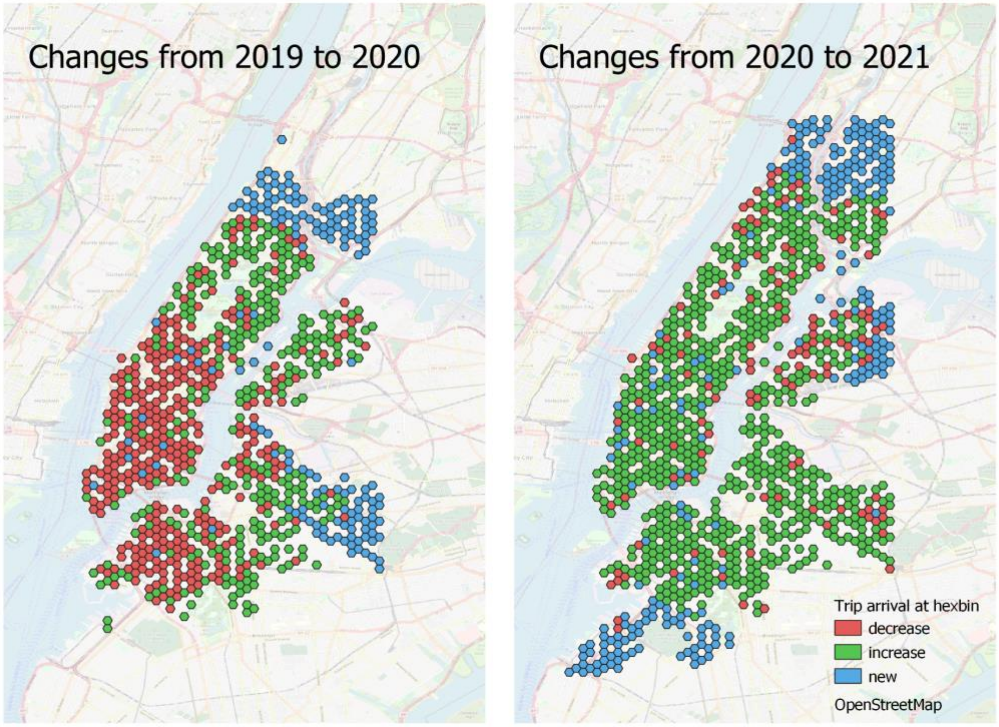

Figure 1. Citi Bike trip arrival changes from 2019 to 2020 and 2020 to 2021 in NYC, with each hexagon categorized primarily as decreasing trips, increasing trips, and new stations installed.

This dissertation aims to address unsolved challenges that arise for this new form of transportation by proposing new methods and frameworks to model and understand the high-frequency changes

in the spatial interaction from a bike share system. Taking the New York City (NYC) system demonstrated in Figure 1 above as an example, there are several types of changes from 2019 to 2021. The blue hexagons contained new stations installed within the year, the red hexagons experienced a decrease in trip arrivals compared to the previous year, and the green hexagons marked an increase in the total trip arrivals. This exploratory data analysis from the NYC system has shown at least two challenges to predict the associated spatial interaction flows. The first challenge is the changing layout of the stations, which does not allow the direct application of models like Recurrent Neural Networks (RNN) or Long Short-Term Memory (LSTM) networks that take historical flows as input. A new approach is needed to deal with trips at those new stations. The second challenge stems from the changes associated with the COVID-19 pandemic as the total trips in 2020 dropped slightly compared to 2019 but total trips in 2021 exceeded those from 2019. In Table 1 below, changes in the total trips and trip duration across three years suggest the spatial interaction model calibrated before the pandemic may no longer be valid for the post-pandemic era (Werner et al., 2022). Such changes also imply that the health benefits of bike share are recognized by people and lead to a much stronger recovery after the COVID-19 pandemic. This short-term and long-term motivation for adopting the bike share brings a huge potential for the expansion of bike share systems in urban areas in the near future. Therefore, there is a critical need for developing new tools to understand the dynamics of spatial interactions from this new form of transportation. To achieve this goal, three studies are conducted that build on the theoretical basis of spatial interaction models. Specifically, the unconstrained gravity model (Wilson, 1971) is used as the core spatial interaction model across the three studies. Methodological frameworks that build from and incorporate spatial interaction models are introduced in each of the three main

chapters to accomplish the research objectives whose motivation and background are summarized below.

Table 1. Bike share total trip count, mean trip duration, and mean trips per day in the NYC system from 2019 to 2021.

Year	2019	2020	2021
Total trips	20,551,517	19,506,857	27,551,166
Mean trip duration	16:18	21:50	16:30
Mean trips per day	56,306	53,297	75,483

The first study in the dissertation is motivated by the aforementioned challenges from new stations as the system evolves. Among different transportation modes, bike share can be analyzed with models proposed for other transportation modes but it has unique features that require special treatments and make recent cutting-edge trip prediction methods not applicable: individual bike-sharing programs are often piloted for a limited number of zones within an urban area that are known to have relatively high overall activity and transport demand and then systems are expanded and updated according to the evolution of demand over time and across space. Previous flows across stations are essential input in almost all cutting-edge spatial interaction prediction methods. However, the dynamic development of bike-sharing systems brings in a large amount of new bike

stations into the system without any historical flows. This feature prevents a straightforward deployment of the majority of cutting-edge models for flow prediction. A new methodology is hence needed to avoid the issue of missing previous flows when using cutting-edge prediction methods. Therefore, study 1 investigates a methodology for predicting OD flows of bike share systems given that the system evolves over time and demand is constantly changing. More specifically, this work focuses on predicting demand for a new station where there may be no knowledge of previous flows, also known as a 'cold start' station, which occurs when the system is progressively updated in order to maintain efficiency and grow the ridership of bike share systems.

Flow prediction using spatial interaction models and flow interpolation methods are two directions that can be used to compute flows at a new station. On one hand, spatial interaction models are calibrated from the system-wide flow generation processes, so predictions are made based on the general relationships between the independent variables and all spatial interactions between all origins and destinations. On the other hand, interpolation methods may incorporate data borrowed from nearby locations and incorporate local information that is not captured in a spatial interaction model. However, flow interpolation techniques are under-discussed with little literature on either their implementation or application. For example, only an areal natural neighbor method has been introduced for flow interpolation so far (Jang & Yao, 2011; Šimbera & Aasa, 2019). In study 1, a new Kriging-based interpolation method is proposed by adopting Ordinary Kriging and Regression Kriging in the flow domain. Along with the areal-based kriging method proposed in previous work, these interpolation methods are compared to spatial interaction models. Of note is that Regression Kriging also incorporates a spatial interaction model as the regression step before "kriging" the residual of the regression output. This array of potential methods is tested within the NYC system,

which is the longest and largest bike share system in the US, to get an initial result for the effectiveness of the newly proposed flow interpolation method against each alternative. As a result, a hybrid strategy is suggested that uses a different method for different station classifications based on the location of a new station in comparison to existing stations.

Human mobility in major US cities was heavily impacted during the COVID-19 pandemic and the consequential lockdown period, resulting in significant changes in general mobility metrics (Kang et al., 2020; Y. Pan et al., 2020; Sevtsuk et al., 2021), metro ridership (H. Wang & Noland, 2021), bike share systems (Padmanabhan et al., 2021), and micro-transit (Y. Zhou et al., 2021). As will be seen in this research, changes in the coefficients in the spatial interaction models indicate that the COVID-19 pandemic affects the trip generation processes of cycling. Recent studies on bike share usage also revealed changes in the bike share trip duration during the COVID-19 pandemic. For example, in NYC there was a nearly 40% increase in the average trip duration in March 2020 compared to the month before COVID (Teixeira & Lopes, 2020). Similar increases were also observed in other US cities like Boston and Chicago (Padmanabhan et al., 2021) as well as in some European cities such as London, UK (Heydari et al., 2021), Zurich, Switzerland (Li et al., 2021) and Kosice, Slovakia (Kubaľák et al., 2021). However, beyond changes in ridership volume, there is a lack of evidence regarding the processes driving changes in human behavior, such as the effects of distance and attraction factors at different locations. The motivation of the second study is therefore to use spatial interaction models calibrated over different periods of time to investigate how behavior related to bike share spatial interaction processes evolve before, during, and after the COVID-19 lockdown.

As a result, the second study presents a disaggregated comparative modeling framework using two different time scales, yearly and weekly, to capture the dynamics of the determinants in the bike

share usage. A similar framework was proposed to split taxi trips by monthly and hourly subsets (Oshan, 2020), but it has never been applied to a bike-sharing dataset. NYC Citi Bike is selected again as it has the largest usage of bike share systems in the US and is the most frequently discussed in the related literature (Chai et al., 2018; P.-C. Chen et al., 2020; X. Chen & Jiang, 2022; Faghih-Imani, Anowar, et al., 2017; Kong et al., 2020; Liu et al., 2016; Teixeira & Lopes, 2020; Wang & Noland, 2021). In order to get a parsimonious interpretation of determinants from the model calibration procedure, model selection is first performed to obtain a subset of the most important variables. Model selection with the LASSO (Least Absolute Shrinkage and Selection Operator) regression assigns penalties to the covariates by shrinking the associated coefficients until they converge to zero. The path of coefficients toward zero reflects the relative strength of each variable in explaining the observations of the dataset. Yearly modeling and weekly modeling of spatial interaction from the bike share provide a mechanism to observe the dynamics of determinants as a time series. An intellectual significance of the study is that further contextualization of the dynamics was carried out by relating trends from the coefficient time series to features of the COVID-19 pandemic timeline to help interpret the results.

The third study in the dissertation builds on the findings of study 2, which showed that there were behavioral changes in bike share usage during the COVID-19 pandemic, particularly during the lockdown. Behavioral changes associated with trip volume have already been discussed by (X. Chen & Jiang, 2022). This study aims to go beyond this by investigating what other events can cause changes in the spatial interaction processes generating bike share trips and how these events can be detected. Detecting such events that may alter the spatial interaction process is important for the application of study 1 as it highlights the importance of the temporal dependency towards the prediction and understanding of spatial interaction. Event detection is another area where the

temporal subset comparison framework proposed in study 2 can be adopted for events that are less obvious than the COVID-19 pandemic and may have a smaller impact. Unlike the ubiquitous impacts of COVID-19, other events, such as weather, that are critical to the decision to cycle (Bean et al., 2021), can significantly influence bike-sharing over much shorter time horizons. However, these events may be more difficult to isolate, and their ephemeral nature means that the behavioral changes may occur more quickly without lasting very long. As a result, incorporating a finer time scale may enhance event detection.

The problem of event or anomaly detection has a large literature due to the availability of time series data in a wide range of domains, including security and surveillance (Karbalaie et al., 2022), traffic and crowd monitoring (Djenouri et al., 2019), business intelligence (Ranco et al., 2015), social media analysis (T. Cheng & Wicks, 2014; Vioulès et al., 2018), environmental studies (Meyer et al., 2019), medical diagnosis (Ukil et al., 2016), and manufacturing (Pittino et al., 2020). Various methods of event detection have been implemented for analyzing data streams from transportation systems, such as likelihood ratio tests (Pang et al., 2011) and k-nearest neighbor (Dang et al., 2015). However, many of these methods focus on processing events from individual locations (i.e., origins or destinations), while origin-destination events related to spatial interaction have received less attention. As a result, a novel method is explored to detect events in spatial interaction processes by adapting the martingale framework for data streams (Cherubin et al., 2018; Ho, 2005; Ho & Wechsler, 2010) in combination with spatial interaction models. The martingale framework has several advantages, including compatibility with regression-based data-generating processes, potential for "on-line" streaming deployment, and ease of tuning. These benefits increase the significance of introducing such a framework into spatial interaction models that are typically time agnostic. To evaluate this new method, simulated spatial interaction flows are first

used to validate the ability of the method to detect known parameter changes that represent data generating processes (i.e., conditional associations). Then, the framework is tested on empirical data from three US cities, including NYC, which has one of the highest bike share usage rates in the country, as well as Washington, DC and San Francisco as two other major urban areas that are not as densely populated. The results demonstrate the framework's ability to extract different types of events from the data.

1.2 Research objectives

Overall, this dissertation aims to develop a comprehensive framework for understanding and predicting dynamically evolving spatial interaction demand in a bike share system, as shown in Figure 2. By doing so it addresses several research questions that were not adequately explored in previous studies. The framework proposed in this study addresses three critical challenges related to spatiotemporal dynamics in a bike share system. The first challenge is related to the expansion of system infrastructure causing limitations at newly added stations for models like LSTM that require historical flows. The second challenge comes from a gap in the knowledge about the changes in the processes generating bike trips. Although bike share trips after the lockdown due to the initial outbreak of the COVID-19 pandemic recovered to the pre-pandemic level quickly, the mean trip duration significantly increased in 2020 compared to 2019 suggesting behavioral changes from the public in making the decision to cycle during and after the lockdown. Such behavioral changes associated with COVID-19 are not fully addressed in the previous studies by analyzing changes in trip numbers. The last challenge comes from anomalies or events that cause smaller impacts on the trip generation process and are too subtle to be explained by weekly spatial

interaction models. To address this research gap, the third study employs an event detection framework that combines the martingale test and spatial interaction model to detect the events associated with bike share behavior (i.e., changes in coefficients over time). Study 2 directly uses coefficients from spatial interaction models while the regression kriging method in study 1 and the martingale test in study 3 both use the residual of the spatial interaction model as the input, making the spatial interaction model a common thread that connects the three studies and updates this classic spatial analysis framework to better accommodate spatiotemporal data in the era of big data.

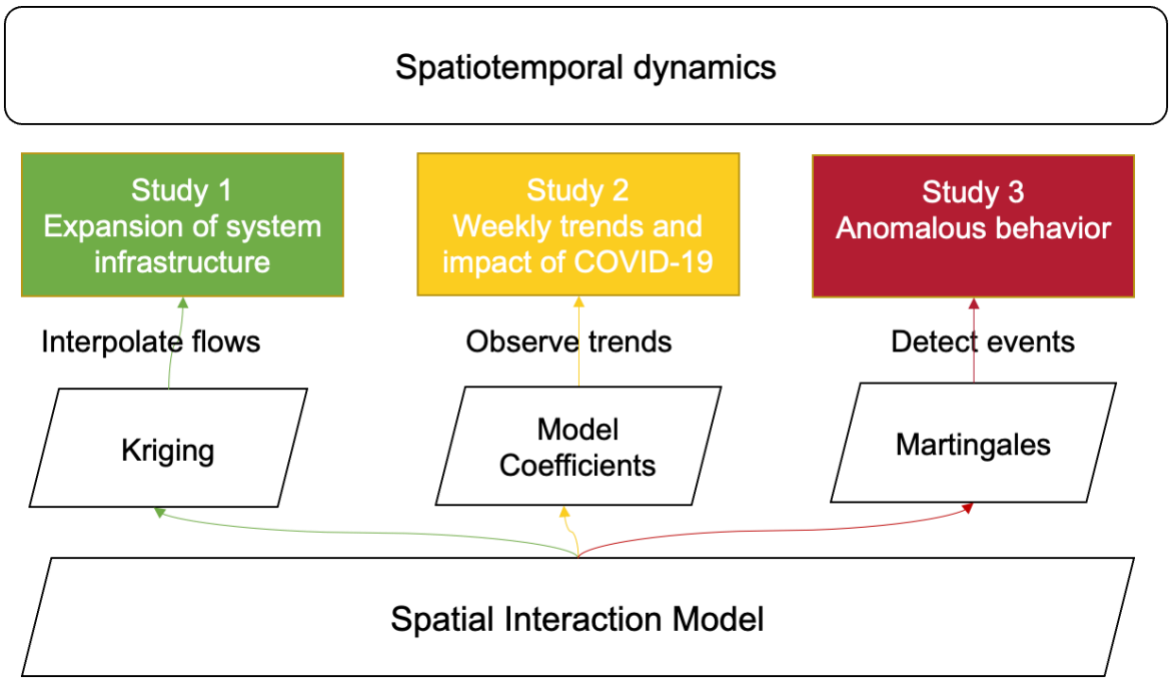

Figure 2. Conceptual framework of the dissertation.

The objectives of each research topic and associated research questions are as follows:

Research objective of study 1. Infrastructure expansion in a bike share system will present a challenge for demand prediction at the station level as most prevailing modeling methods (i.e., LSTM models) rely on historical flows at each station. The absence of historical data for newly

added stations makes such models unavailable and thus requires a novel solution for predicting ‘cold start’ trips at the new stations, either from direct data borrowing interpolation or from indirect model-based interpolation. The first study compares methods and proposes a hybrid strategy taking advantage of both aspects by answering the following research questions.

> *Research question 1a.* How do interpolation methods, including areal natural neighbor, Ordinary Kriging, and Regression Kriging, compare to spatial interaction models for predicting the 'cold start' bike trips?
>
> *Research question 1b*. What is the best strategy for 'cold start' bike trip prediction at different locations?

Research objective of study 2. Bike share usage during the COVID-19 pandemic changed on a much larger scale than the pre-pandemic routine, implying changes in the driving factors of bike trips. Dynamics of determinants of bike share trips during routine activities as well as during and after the COVID-19 lockdown were analyzed through a disaggregate comparative framework and by addressing the related questions below.

> *Research question 2a*. From a long-term perspective, what are the changes in the generating factors of bike trips before COVID-19 in 2019 and across different phases of COVID-19 in 2020 and 2021?
>
> *Research question 2b*. From a short-term view, how did the weekly determinants of bike trips change with the evolution of COVID-19?

Research objective of study 3. Short-term changes in the spatial interaction that are not explained using the approach from study 2 are considered potential events associated with trend breaks in

the spatial interaction processes over a long time period. The third study explores a method to detect the events that can lead to behavioral changes in the spatial interaction processes related to bike share trips. The proposed method is developed using a martingale framework, which is evaluated to answer the research questions below.

Research question 3a. To what extent can events be detected using model-based proxies for changes in human behavior?

Research question 3b. How to effectively combine the spatial interaction model and the martingale framework to detect events?

Research question 3c. What types of events can be reliably detected within different US cities from a multiyear observation from 2018 to 2021?

1.3 Dissertation outline

The dissertation is organized into five chapters. The overall goal of the dissertation is to develop methods to help understand and predict high-frequency spatial interactions produced by bike share systems. Chapter 1 describes the essential background and motivations for three research objectives. Chapter 2 presents a hybrid approach to predict 'cold start' bike trips at newly added stations in a docked bike share system. Chapter 3 introduces a disaggregated comparative framework for capturing and understanding changes over time in the determinants of spatial interactions associated with the COVID-19 pandemic. Chapter 4 continues the focus on changes in spatial interaction processes by adapting and evaluating an event detection framework based on the martingale test. The utility of the event detection method is tested using simulated data and by

applying it to three different US cities. Chapter 5 concludes the dissertation by reviewing the key findings from the three studies, summarizing significant contributions from this research, and discussing the limitations and potential areas of future work.

Chapter 2: Comparing spatial interaction models and flow interpolation techniques for predicting 'cold start' bike share trip demand

2.1 Abstract

Bike-sharing systems are expanding rapidly in metropolitan areas all over the world and individual systems are updated frequently over space and time to dynamically meet demand. Usage trends are important for understanding bike demand, but an overlooked issue is that of ‘cold starts’ or the prediction of demand at a new station with no previous usage history. This chapter explores a methodology for predicting bike trips from and to a 'cold start' station in the NYC Citi Bike system. Specifically, gravity-type spatial interaction models and spatial interpolation models, including natural neighbor interpolation and kriging, are employed. The overall results from experiments of a real-world bike-sharing system in NYC indicate that the regression kriging model outperforms the other models by taking advantage of the robustness and interpretability of gravity-type spatial interaction regression models and the capability of ordinary kriging to capture spatial dependence.

2.2 Introduction

The past century has witnessed a significant increase in urbanization with more than half of the world's population currently living in urban areas (United Nations, Department of Economic and Social Affairs, Population Division, 2019). As a result, it has become increasingly important to understand and anticipate human mobility within and across cities. In particular, public transportation systems, historically composed of buses, trains, and taxicabs, form the backbone of cities, facilitating interaction and providing an affordable and reliable alternative to carry out routine activities compared to private transportation. The development and optimization of public

transportation infrastructure have therefore remained an important aspect of urban planning and community development.

A more recent trend is the emergence of bike-sharing as an alternative means of transportation and the establishment of bike-sharing systems in cities around the world. Compared to other modes of mobility, cycling provides health and environmental benefits in addition to offering a more efficient means of navigating the urban environment (Oja et al., 2011; Otero et al., 2018; M. Wang & Zhou, 2017; Y. Zhang & Mi, 2018). For example, the New York City (NYC) Mobility Report indicates that trips made using the NYC Citi bike share system are over a minute faster than taxi trips across all distance categories within the Midtown area of Manhattan, and cost less than 25% for taxi trips for all trip length categories except those less than half a mile (NYC Department of Transportation, 2019). Such advantages are further highlighted during rush hour (Faghih-Imani, Hampshire, et al., 2017). This has led to the proliferation of bike-sharing systems, with nearly 2000 bike-sharing systems now in operation around the world[1].

Individual bike-sharing programs are often piloted for a limited number of zones within an urban area that are known to have relatively high overall activity and transport demand. Systems are then expanded and updated according to the evolution of demand over time and across space. This dynamic development of bike-sharing systems requires a strong understanding of mobility behavior and flexible methods for predicting spatial-temporal demand. In particular, travel demand

[1] According to bikesharingworldmap.com and including both docked and dockless systems (last accessed on 07/30/2021).

models may focus on predicting overall system demand, the total demand at each location or station within a system, or demand between individual locations. It is this latter scenario that is the primary focus of this research as it typically receives less attention (e.g., Li & Shuai, 2020; Y. Zhou et al., 2019). This is perhaps because it is more challenging to model individual origin-destination (OD) flows due to a lack of detailed data and because they usually contain more noise and higher levels of variability compared to the overall system usage or the total inflows or outflows for a set of locations. However, models of OD flows, often referred to as spatial interaction models, are becoming increasingly possible as detailed data are generated by GPS-enabled sensors and the internet of things (Shaw & Sui, 2018). For example, Calafiore et al. (2021) leveraged user OD flows based on social media check-ins to study the characteristics of cities' neighborhoods. Furthermore, recent machine learning methods for incorporating various dimensions of spatial and temporal dependence hold promise for building models with enhanced predictive capabilities (Chu et al., 2020; Ke et al., 2019; L. Liu et al., 2019; Y. Wang et al., 2019). Consequently, this work investigates a methodology for predicting OD flows of bike share systems given that the system evolves over time and demand is constantly changing. More specifically, this work focuses on predicting demand for a new station where there may be no knowledge of previous flows, also known as a 'cold start', which is necessary when the goal is to progressively update transport infrastructure in order to maintain efficiency and grow the ridership of bike share systems.

Previous work has not examined in detail the task of predicting spatial interaction demand for new stations, likely because more traditional public transportation infrastructure evolves much more slowly compared to the relatively inexpensive and flexible bike share infrastructure. That is, much

of the related state-of-the-art research assumes that the infrastructure is persistent across time and there is prior knowledge of station activity, which is not always the case for bike share systems. Therefore, section 2.3 of this chapter provides some additional background and formalizes the challenges that need to be overcome. Then, section 2.4 presents a novel methodological approach for predicting the spatial interaction demand associated with new bike share stations, and section 2.5 briefs the data used in the case study and experiment settings. Section 2.6 describes the experimental results used to benchmark the proposed approaches. Overall, the results indicate that regression kriging models are slightly more performant than the other techniques considered. Finally, section 2.7 concludes with a discussion of the contributions of this research, the limitations of the proposed approach, and suggestions for future work in this area.

2.3 Background

The widespread adoption of information and communication technology has produced massive amounts of transportation and mobility data, sparking a wave of research into how to best model human movement. Meanwhile, the popularity of bike-sharing systems has inspired much recent research. Si et al. (2019) provide a review of bike-sharing papers published from 2010 to 2018 and group them based on the following categories: demand factors, rider behavior, system optimization, and impact on other modes. The factors associated with variation in bike-sharing ridership demand can largely be summarized as being related to the weather, built environment, sociodemographic, or temporal dimensions (Barbour et al., 2019; El-Assi et al., 2017; Eren & Uz, 2020; Guo et al., 2017; H. Yang et al., 2020). Knowledge of the distribution of trips is useful for developing strategies to optimize systems through bike rebalancing or station repositioning, allowing the system to satisfy higher demand (P.-C. Chen et al., 2020; Faghih-Imani, Hampshire, et al., 2017;

Pan et al., 2019; R. Zhu et al., 2020). The introduction of a bike share system may impact other transport modes, leading researchers to compare bike share usage to taxi and bus ridership (Campbell & Brakewood, 2017; X. Zhou, Wang, & Li, 2019). Another trend focuses on bike share trip prediction using travel demand models and OD flow models, the latter of which is the focus of this study and will be used to consider a range of factors influencing bike share trip demand to predict OD flows.

Trip demand at 'cold start' stations, however, catches less attention and is only explicitly discussed in Noland et al. (2016) and Y. Zhang et al. (2017). And both papers used linear regression models on station-level demand to examine the generalization of the models. Research by X. Wang et al. (2021) discussed the use of a regression model for making predictions at new stations but only performed out-of-sample predictions by randomly selecting stations as a test set, which is not an exhaustive validation for trip demand at potential new stations. Furthermore, there is a lack of effort dedicated to *OD flow* predictions for new stations.

Spatial interaction (SI) describes aggregate movements of individuals, commodities, capital, or information over geographic space, resulting from some requisite decision-making process (Farmer & Oshan, 2017). A typical quantitative representation of SI is the origin-destination (OD) matrix:

$$\mathbf{T} = \begin{bmatrix} T_{11} & \cdots & T_{1j} & \cdots & T_{1m} \\ \vdots & & \vdots & & \vdots \\ T_{i1} & \cdots & T_{ij} & \cdots & T_{im} \\ \vdots & & \vdots & & \vdots \\ T_{n1} & \cdots & T_{nj} & \cdots & T_{nm} \end{bmatrix} \begin{matrix} O_1 \\ \vdots \\ O_i \\ \vdots \\ O_n \end{matrix}$$
$$\begin{matrix} D_1 & \ldots & D_j & \ldots & D_m & T \end{matrix}$$

Equation 2.1

Where T is the OD flows matrix from a set of origins $(O_1, O_2, \ldots, O_n)$ to a set of destinations $(D_1, D_2, \ldots, D_m)$, and T_{ij} is the magnitude of flows from origin i to destination j. Inspired by Newton's law of gravity, early models of spatial interaction theorized OD flows to be proportional to the product of potential at origins and destinations and inversely proportional to the squared distance between them, yielding the following formulation,

$$T_{ij} = k\frac{P_i P_j}{d_{ij}^2}$$

Equation 2.2

where T_{ij} still denotes the flows between origin i and destination j, and represent the potential at i and j, d_{ij} describes the distance between i and j, and k is a scaling factor that ensures the number of flows predicted by the model matches the number of observed flows. In this context, the potential is often defined as the location population or the number of job opportunities (Gao et al., 2013; Krings et al., 2009; Lenormand et al., 2016), but can be expanded to consider a series of origin and destination attributes that may contribute towards the flow generation, each with their own parameter (Fotheringham & O'Kelly, 1989; Oshan, 2020). According to Kar et al. (2021), two groups of variables can be identified besides population or jobs: socio-economic attributes and built environment attributes. The former group usually explains trip generation, such as labor force

(Pourebrahim et al., 2018; Signorino et al., 2011); GDP (L. Zhang et al., 2019); human activity density (Marrocu & Paci, 2013). The latter group includes common destination determinants of travel demand, such as amenities (e.g., schools, hospitals, markets) (Botella et al., 2021; Kar et al., 2021), tourism attractions (e.g., hotel rooms) (Khadaroo & Seetanah, 2008), and land use types (X. Liu et al., 2016).

Recent work seeks to exploit temporal dependence within SI flows to increase predictive performance. The simplest instance involves taking the average of historical observations, which can yield accurate predictions for future flows when there is limited variation in the historical observations. Typical methods using temporal dependence include historical averaging; autoregressive integrated moving average (ARIMA); Deep neural network structures including recurrent neural networks (RNN) and long short-term memory (LSTM) architectures (Cheng, Trepanier, & Sun, 2021; Chu et al., 2020; Ke et al., 2019). The common factor amongst all these methods is that they require sufficient previous OD flows and become invalid to predict future flows when there are no historical observations to draw upon.

Meanwhile, bike share systems are also spatially dynamic in that stations are frequently updated or perhaps more importantly that new stations are added to extend the system, though this is often overlooked in related work. One exception is Lu et al. (2018) who explored the extension of system infrastructure by deploying agent-based methods to simulate the result of adding new stations towards the usage of different transportation modes. In contrast, most previous research focuses on predicting bike-sharing trip flows at existing locations (i.e., in-sample spatial prediction), often using historical data as an important input feature. This is problematic when the focus is instead

on predicting flows associated with a new station that is being added to the system (i.e., out-of-sample spatial prediction) because there is no historical flow data that can be used to learn temporal dependencies. A similar issue often occurs in recommender systems where new users or new items will have no historical record to be used for preference analysis (Su & Khoshgoftaar, 2009; Volkovs et al., 2017) and is often called the 'cold start' issue. This term is also used in the literature associated with detecting stops and trips from GPS trajectories (Schuessler & Axhausen, 2009; Stopher et al., 2005). Overcoming this limitation is the primary contribution of this research in order to develop a robust methodology for predicting historical OD flows at a new bike share station.

It is reasonable to leverage spatial dependence to predict values at unobserved locations based on values from nearby observed locations. The First Law of Geography states that things that are closer together are typically more similar (Tobler, 1970) and is the basis for popular spatial statistics, such as Moran's I measure of spatial autocorrelation and spatial interpolation methods, including natural neighbor interpolation, inverse distance weighting, Kriging, and more (Mitas & Mitasova, 1999). In particular, kriging has become a core spatial interpolation tool and is now used in many topic areas such as air quality analysis (Bayraktar & Turalioglu, 2005), natural resource analysis (Emery, 2005), water studies (Zimmerman et al., 1998) and traffic (Eom et al., 2006; X. Wang & Kockelman, 2009). Recently, spatial interpolation tasks have been adapted into a lattice or graph structure and integrated into generative adversarial networks (D. Zhu et al., 2020) or graph neural networks (Wu et al., 2020), but these extensions do not yet apply to the case of OD flows. For the interpolation of OD flows, Jang and Yao (2011) proposed an areal weighting method, which was further employed by Šimbera and Aasa (2019). As far as the authors are aware there

are no studies extending interpolation methods to SI flows. However, the spatial dependence between SI flows has previously been leveraged for community detection (Gao et al., 2013; Yao et al., 2018) and land use identification (X. Liu et al., 2016), indicating that kriging, which also relies on the presence of spatial dependence, may be promising for flow interpolation. Therefore, this research explores flow-based kriging and compares it to natural neighbor interpolation and gravity-type spatial interaction models.

2.4 Methodology

2.4.1 Problem statement

For a station-based bike share system, S_n, there are n docking stations serving as both origins S_i and destinations S_j and information is available for each trip in the system regarding its origin station, destination station, start time, and end time. Trips are also sorted into discrete temporal subsets, t, based on their starting time (e.g., hour, day, week, etc.). Therefore, each trip in the system can be denoted using a 3-tuple (t, s_i, s_j) and the corresponding OD flow matrix T is comprised of entries denoting aggregated trips between stations at the time t (i.e., $T_{t,i,j}$). The diagonal elements of T (i.e., $i = j$) are filtered out and set to zero to remove their undue influence on any subsequent modeling procedures. A 'cold start' station refers to a scenario where there is no information available about previous flows for a newly added station S_x and the goal is to predict future outflows $T_{t+1,x,j}$ and/or future inflows $T_{t+1,i,x}$. The primary issue that arises is that there are no previous flows to use in any of the methods that leverage historical data. A methodology is proposed below to overcome this limitation by classifying stations and using a combination of regression modeling and interpolation techniques depending on the station class.

2.4.2 Station classification

Predicting the flows associated with the addition of new stations is the primary task of this research. However, depending on the location of the new station and its proximity to currently existing stations, different techniques and information are available to carry out the predictions. At least three different scenarios can be distinguished. The first is referred to here as interpolation, which entails borrowing information directly from the existing stations. Interpolation typically only applies in the situation where the newly added station is sufficiently proximal to existing stations (i.e., within current system coverage). The second scenario is referred to here as margin interpolation and is the case where a new station is added on the margin of the current system. As such, there are some nearby stations with previous flow information that can be borrowed. The final scenario is referred to here as extrapolation and is concerned with the addition of stations that are essentially outside the coverage of the current system. Predictions for this scenario are hypothesized to be only possible through the extrapolation of modeled relationships, since there are no existing nearby stations to borrow information from. A method for identifying empirical instances of system expansion and classifying new candidate stations across the three scenarios is proposed below and then subsequently deployed and evaluated.

Newly added stations are identified by examining the time series of trip data for the bike share system. For each station present in the system before July 2020, an array of station inflows (or station outflows) for each temporal subset (weekly in this case study) is used to track its operation status. Intuitively, the first non-zero entry of the array, $t_{in} > 0$, is recorded as a preliminary inferred date that a station was initially put into operation. However, these preliminary dates are

then refined by manually checking for consistent station service as in practice there sometimes are test trips prior to the official launch of a new station. In addition, the system record indicates that all new stations added after the initial system rollout in 2013 did not occur until 2015. Therefore, the original stations existing before 2015 (Table 2) are not included in the set of classified stations nor are they used for prediction validation.

Table 2. Numbers of stations added over time by month and year.

Month and Year	2013	2015	2016	2017	2018	2019	2020
January	-	-	2	2	9	6	8
February	-	-	2	8	2	3	5
March	-	-	2	4	6	6	1
April	-	-	2	4	3	17	2
May	-	-	3	5	7	11	36
June	336	-	5	4	5	5	35
July	1	1	8	4	4	3	-
August	-	85	98	4	5	4	-
September	-	39	43	64	1	15	-
October	-	16	2	74	3	38	-
November	-	5	2	6	3	34	-
December	-	2	2	4	4	15	-

Next, these new stations, S_x, are classified between interpolation, margin, and extrapolation. This is done based on their relationship to the existing system coverage, which is represented here by computing the convex hull of all the stations in operation at the time when S_x is introduced. The convex hull of all the station points provides a simplified representation of the system service area

in continuous Euclidean space, though the urban environment does not exist separately from the natural environment (i.e., rivers). To ensure these restricted areas are not included in the representation of system coverage, a few extra steps were taken to prepare a modified convex hull for the bike share system. First, stations on Governor's Island and a single isolated station in the southern part of Brooklyn were removed from the analysis because these stations are essentially disconnected from the larger system. Then, multiple convex hulls were created separately for stations in Manhattan and stations in Brooklyn/Queens, ensuring that neither of the convex hulls cross into major waterways.

For every temporal subset t, only the system coverage associated with stations running at time $t - 3$ is used to classify the new station S_x initialized at time t where each temporal subset pertains to a week within the period from January 2015 through July 2020. This time lag of up to three weeks ensures that stations rolled out consecutively over a relatively short time period are not considered as previously existing to each other and is necessary because there is usually a short period of time before a new station becomes fully integrated within the system. If S_x falls outside this current system coverage, it will be regarded as an extrapolation case. In contrast, if S_x is within this current system coverage, it will be regarded as an interpolation case. It is then necessary to further distinguish the partial interpolation cases, which correspond to stations added to the margin of the current system coverage. The three cases are formally classified by the percentage of overlap between their Voronoi tessellation cell and the current system coverage. Stations overlapping < 5% are classified as an extrapolation station while those overlapping > 95% are classified as an interpolation station. The remaining stations are classified as margin stations.

Applying the above classification to all newly added stations identified in the previous step. Using these three different categories, it is possible to apply and evaluate unique mechanisms to borrow flow information based on data and/or modeled relationships for each category. The hypothesis employed here is that different mechanisms will be more efficient for each category because different types and levels of information are available. In particular, it is anticipated that better predictive performance will be attained for stations classified as extrapolation cases using a SI modeling approach because borrowing information for data from relatively far stations could introduce a disproportionately large amount of misinformation. In contrast, the interpolation and margin cases are anticipated to achieve higher predictive performance using methods that incorporate data-borrowing through interpolation techniques. That is, flows for stations classified as interpolation and margin are expected to be best predicted using interpolation methods whereas those that are not must rely on extrapolation through modeled relationships (i.e., SI model). However, it is less clear whether or not the same method will be the most effective for both interpolation and margin stations, since different levels of information are available. To investigate these issues, several interpolation methods are explored in the following sections and then subsequently compared to each other and to predictions from SI models.

2.4.3 Modeling strategies

Gravity-type spatial interaction model

The unconstrained gravity-type spatial interaction model (Gravity SI) described in section 2.3 is perhaps the most widely used model for diverse types of aggregate transport flows (for several recent examples see Kar et al., 2021; Lenormand et al., 2016; Oshan, 2020; T. Zhou et al., 2020). It is calibrated here using a log-linear Poisson regression with a power distance-decay function and a set of origin/destination attributes using the *spint* module of the Python Spatial Analysis

Library (PySAL) (Oshan, 2016). Following Eren and Uz (2020), these attributes include points of interest (POI) for urban amenities and services, transportation infrastructure, and socio-demographic factors. For transportation infrastructure, accessibility to other bike stations is computed based on a distance-weighted sum (i.e., spatial lag) of nearby bike station capacity[2]. POI data was obtained from SafeGraph (2020) and contains a hierarchical schema. Eleven categories were formed to aggregate POIs from this schema and include *care*, *education*, *finance*, *food*, *housing*, *recreation*, *religion*, *shopping*, *travel*, *professional*, and *other services*. Further descriptions of data sources and variables are summarized in Table 3. The selection process of distance parameters for station accessibility and POIs is based on trial and error, however, sensitivity results show there are no significant differences in gravity SI results when using other distance bands (e.g., 500 meters or 1000 meters) to compute these variables.

[2] Since capacity values from the most recent station information are representative of all previous system states, capacity values were based on system snapshots of the station information from Sep 2018, May 2019, and Feb 2020. Of the 1103 stations that existed from 2015-2020 this provided valid capacity information for all but 135 stations, which either were not running during the snapshots or had zero capacity values. These 135 stations were not included in the computation of the accessibility metric used here.

Table 3. Attributes used in the spatial interaction models in Chapter 2.

Attributes	Source	Features description
Population	Cenpy Census.gov	Population (2017 ACS5) of each census tract
Employment	Longitudinal Employer-Household Dynamics (LEHD)[3]	Workplace Area Characteristics by census block
Station accessibility	Station Info[4]	Weighted sum of nearby station capacity with inverse distance weights
Access to subway	NYC Open Data[5]	Euclidean distance to nearest subway station.
Points of Interest	SafeGraph[6]	Place count weighted by spatial lag within 1500 meters of station

Natural neighbor interpolation

Spatial interpolation methods predict unknown values for an unsampled point in space based on its relationship to a set of sampled points. Given values of a random field $Z(\cdot)$ measured at locations $s_1, \ldots, s_n$ yielding $Z(s_i)$ for any station s_i, the objective is to estimate the value $Z(s_x)$ for one or more unmeasured locations s_x. One well-established spatial interpolation method is the natural neighbor technique that finds the closest subset of input samples to a query point and weights them proportionally based on areal overlap to estimate a value (Sibson, 1981). Based on

[3] https://lehd.ces.census.gov/data/

[4] https://gbfs.citibikenyc.com/gbfs/en/station_information.json

[5] https://data.cityofnewyork.us/Transportation/Subway-Stations/arq3-7z49

[6] https://www.safegraph.com/covid-19-data-consortium

the assumption that nearby stations typically experience similar levels of demand, it is possible to borrow data for a new station from neighboring stations using this method. The natural neighbor interpolation method for points/polygons was extended to spatial interaction flows by applying a modified areal-based weighting scheme (Jang & Yao, 2011). Equations 3.1-3.2 present the natural neighbor formula for calculating the flow T_{xj} between a new station S_x and a destination station S_j. First, Voronoi tessellations are computed for $\boldsymbol{S_n}$ with and without S_x, denoted as V_{n+x} and V_n, respectively, with each individual Voronoi polygon approximating the service area for each station. In equation 3.1, m is the number of stations overlapping with S_x, p_k is the proportion of the overlapping area between Voronoi shape of S_x in V_{n+x} and S_k in V_n in relation to the total area of the Voronoi shape of S_x in V_{n+x} (Equation 3). The resulting $[T_{x1}, T_{x2}, \ldots, T_{xn}]^{\top}$ are the 'borrowed' outflows of S_x. Thus, natural neighbor interpolation provides an areal-based method that can be used on flow data and will be one of the interpolation methods applied here.

$$T_{xj} = \sum_{k=1}^{m} [p_k \times T_{kj}] \qquad \textit{Equation 2.3.1}$$

$$p_k = \frac{A^{V_{n+x} \cap V_n}{}_{kx}}{A^{V_{n+x}}{}_x} \qquad \textit{Equation 2.3.2}$$

Kriging

While natural neighbor interpolation derives weights based only on location, kriging techniques derive weights based on both the location S_x and value of each sample point $Z(s_i)$ with $i \in (1,2,\ldots,n)$. It is an optimal linear estimator of the form

$$Z(s_x) = \sum_{i=1}^{n} \alpha_i Z(s_i) \qquad \textit{Equation 2.4}$$

where the weights α_i are chosen to make the estimator unbiased and of minimal prediction error. Kriging is a two-step process. First, the spatial covariance structure of the sampled points is

determined by fitting a variogram (a spherical model is used here) that captures the variability between all data points as a function of distance. Then, weights derived from this covariance structure are used to interpolate values for unsampled observations across the spatial field. Ordinary kriging assumes the random field $Z(\cdot)$is intrinsically stationary; that is for any location s:

$$E[Z(s)] = \mu \qquad \textit{Equation 2.5.1}$$

$$Var[Z(s) - Z(s+h)] = 2\gamma(|h|) \qquad \textit{Equation 2.5.2}$$

where $\gamma(|h|)$ is the semi-variogram and a function of distance h that separates two locations. Further mathematical details are available in (Cressie, 1993).

Ordinary kriging typically uses a k-dimension (usuallyk <= 3) point as an input location and a 1-dimension target value Z. However, a spatial interaction flow between stations is a spatial process involving two points in a 2-dimension Euclidean space (k = 4). To accommodate this higher dimensionality, a flow-based extension inspired by (Y. Zhou et al., 2019) is proposed that aggregates all the outflows to the m possible destination stations or inflows from m stations to the single origin station s_i as $Z(s_i)$ and the definition of T_{ij} remains the same as in Equation 2.1. The coordinates of the origin station remain in 2-D space, but the target value Z_i is an m-length vector representing the flows to each destination. According to (X. Liu et al., 2016), this station-centric view, which aggregates the OD flows into vectors describing flows coming in and going out from one single station, is also referred to as the OD flow signature of a station. In this station-centric view, the adoption of the vectorized Z is needed for handling higher-dimensional Z within kriging

techniques. The inflow predictions $Z_{in}$and outflow predictions Z_{out} are carried out separately and then concatenated as the overall OD predictions for a target station.

Alternatively, regression kriging leverages information from exogenous variables in addition to the spatial dependence in a sample by first fitting a regression model and then kriging the residuals of the regression model. Therefore, a Gravity SI model is first fit and then a flow-based ordinary kriging (OK) model as described above is used to interpolate the residuals of the gravity-type SI model. Specifically, when using the station-centric view in the regression kriging model (RK), the kriging step uses 2-dim input with k-dim targets, while the regression step uses location data in OD flow form with 4-dim features.

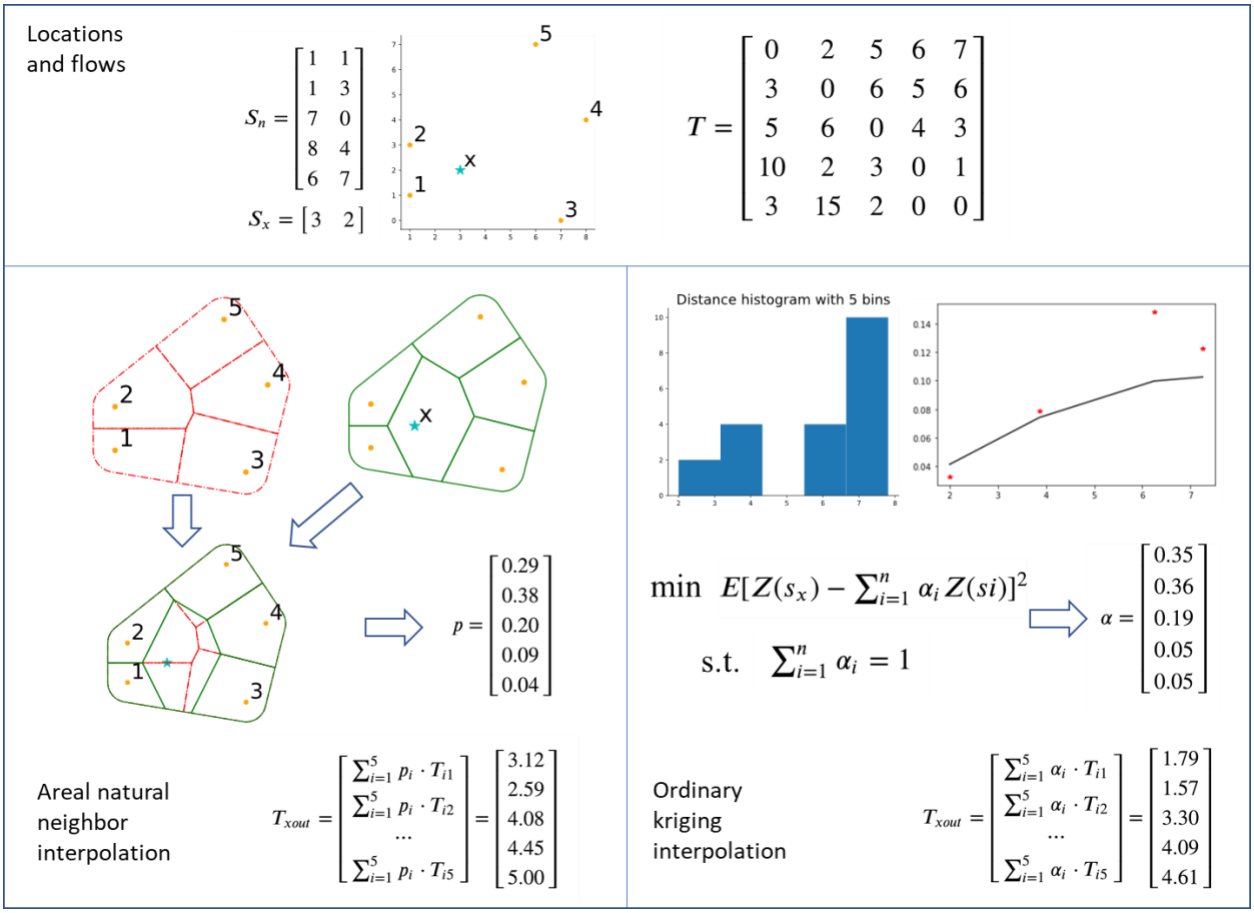

Figure 3. Illustration of areal natural neighbor interpolation and ordinary kriging interpolation with toy data.

To better highlight the difference between the kriging interpolation and natural neighbor interpolation, an illustration with pseudo data is attached to demonstrate the two interpolation processes step by step in Figure 3. Both methods take identical data structure as input data, e.g., existing locations S_n, a 'cold start' location S_x, and flow matrix among existing stations T. The bottom-left section shows the steps of areal-based natural neighbor interpolation. First, the service area of each station defined by the Voronoi shapes is calculated before and after a 'cold start' station is added. Then the overlapped area over the 'cold start' station is calculated at each existing station, consisting of the portion (p) of new stations which is the final proportional weight to calculate the interpolated outflows and inflows at the new station shown in the last row. In contrast to the natural neighbor that exploits locations only, ordinary kriging interpolation leverages both locations and flow similarity. Under the assumption of ordinary kriging, variations between stations at a fixed range of distance is only decided by the distance h. Thus, distances between each pair of origin and destination are grouped into bins (Right-bottom section, Figure 3 left) and the variance in each group is calculated and plotted (Right-bottom section, Figure 3 right). It is proved that the optimization equation can be solved using the semivariogram only. Details can be found in geostatistical textbooks such as Le & Zidek (2006). So, it is essential to interpolate the flow variance between new stations and any existing stations by fitting a covariance function (black solid line in Right-bottom section, Figure 3 right). Finally, the optimized alpha that minimizes the prediction error is calculated and used for the flow interpolation results just as the natural neighbor interpolation method.

2.5 Data

2.5.1 Study area

The Citi Bike system in New York City started operation in 2013 and now becomes the biggest bike share system in the US. Among the 809 stations added to the system since 2015, 55 of them had too few trips to produce reliable output in any one of the methods, specifically producing a null or negative correlation index value. Thus, the following results come from the remaining sample of stations ($n = 754$) with 313 interpolation stations, 123 margin stations, and 318 extrapolation stations using the (0.05,0.95) classification threshold. The spatial distribution of the stations is mapped in Figure 4 along with the original (pre-2015) set of stations. All the trips are aggregated into unique spatial and time tuples by their original stations, destination stations, and the week of the trips starting from Jan 1st, 2015. In the regression-based models, the following expression is used: *"flows ~ cost + origin attributes (15) + destination attributes (15)"* Origin and destination attributes including 15 variables each listed in Table 3 where POI includes 11 categories, e.g., *care*, *education*, *finance*, *food*, *housing*, *recreation*, *religious*, *shopping*, *travel*, *professional*, and *other services*. In the interpolation-based models, OD-matrices are formatted as the demonstration in Figure 3.

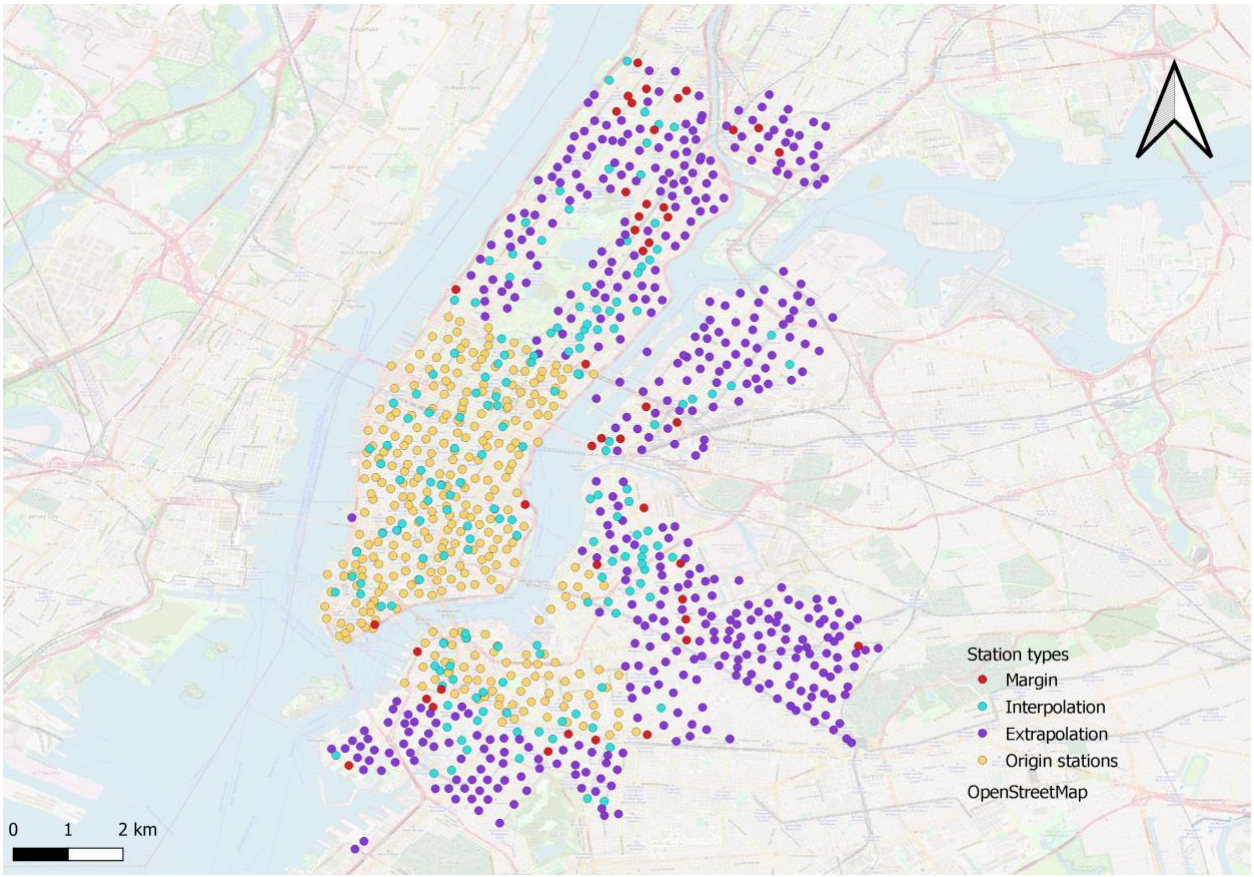

Figure 4. Spatial distribution of bike stations color-coordinated by the three derived classes for newly added stations and the original stations.

2.5.2 Study design

Each new station is associated with a unique time frame for training and testing. So iterating station-wise, SI models were trained for each added station S_x, with a training set including all the OD flows available in the time period before S_x is added, and with prediction test set from the time period after S_x is rolled out. Training data consisted of flows one week before a new station was added at time t, (i.e., $t-1$) while the evaluation data was set to flows from one week after the roll out of a new station (i.e., $t+2$). This one-unit period provides a chance for demand to stabilize after a new station is added to the system for a complete week. Bike trips with duration more than

3 hours are excluded as abnormal trips. To evaluate the performance of each prediction method for all S_x, Pearson's R correlation coefficient is employed[7].

2.6 Results

2.6.1 Gravity-type spatial interaction model calibration

Before producing the prediction results, it is necessary to calibrate the gravity-type SI models. An advantage of the SI model over the interpolation methods is the ability to elucidate how independent variables affect bike trip flows based on the parameter coefficients. To highlight the weight of each independent variable, the top of Figure 5 shows the average parameter magnitude and 95% confidence intervals based on the models for each station. The bottom of Figure 5 captures the top 11 most important features over time.

[7] Zero flows were not included when calculating the performance metrics.

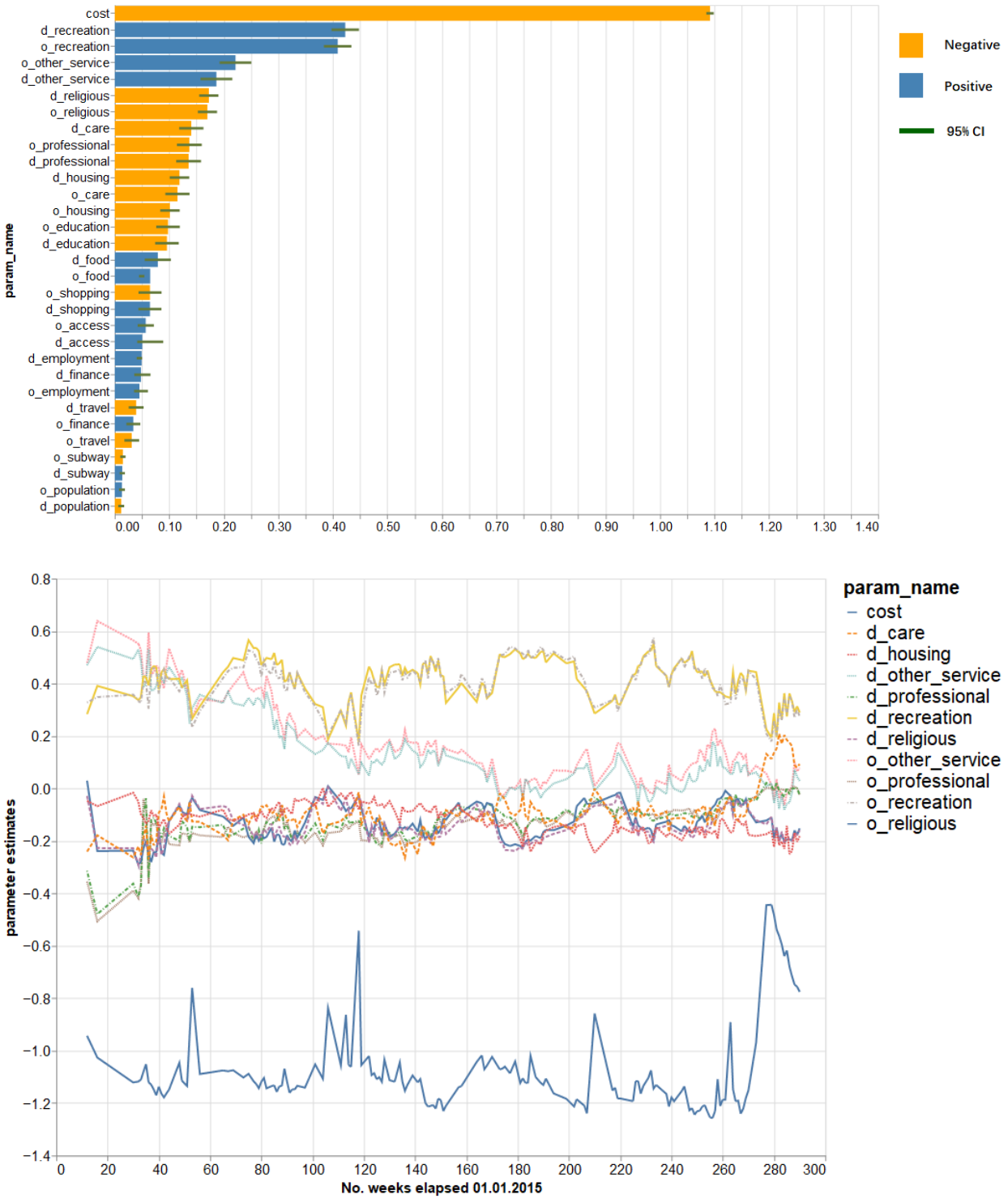

Figure 5. Top: Feature weight from the SI model results averaged over the time periods. The X-axis represents the absolute value of the parameter estimates and the color represents the sign of the average magnitude. The dark green strip shows the average range. Bottom: Time series of top 11 largest feature weights. The X axis is the number of weeks elapsed since 01/01/2015.

Generally, parameter estimates associated with a variable have the same direction, either negative or positive, and similar magnitudes for the origin stations and the destination stations. The cost factor, which is the average trip completion time of the OD pair and is typically called the distance-decay effect, is the most important factor, attesting to the First Law of Geography. The next most important factors included *recreation* and *other services* POIs. The former POI group suggested the purpose of the bike share trips for leisure activities. The latter group, *other services*, includes many parking facilities. It could be interpreted as a potential common commuting pattern: people park their cars and then take bike trips. Surprisingly, population was not a top factor, suggesting the residential population around stations is not necessarily a strong indicator of the size of the potential bike share user base. In terms of the parameter estimate stability over time, the top 11 important factors typically have consistently positive or negative signs. Some general trends can also be observed over time. First, the distance-decay factor associated with trip duration became more negative (i.e., stronger) over time as the system expanded. There is also a periodic fluctuation that captures the seasonal trend where distance-decay is less negative in the winter (the spikes around 50th, 110th, 210th weeks). Second, the impact of the COVID-19 lockdown was a decrease in the magnitude for the parameter estimates of most factors, likely because the regular trips of the public were essentially halted during this time and the alternative behavior was either less associated with these factors or generally more random. Besides, the gravity SI model also showed robustness in the parameter importance when changing the distance band from 1500m to 1000m to compute spatially lagged explanatory variables (i.e., POIs and accessibility), providing that the direction and magnitude of coefficients remain the same over the two distances.

2.6.2 Prediction results

Table 4. A summary of the prediction results based on Pearson's R for each method using data for each classification category and using all data. Standard deviations are in parentheses after the mean values.

Pearson's R (Standard deviation)	**Interpolation**	**Margin**	**Extrapolation**	**All**
Natural neighbor	0.53 (0.22)	0.47 (0.22)	-	-
Ordinary Kriging	0.52 (0.20)	0.45 (0.22)	0.41 (0.20)	0.46 (0.21)
Gravity SI (Poisson)	0.44 (0.19)	0.41 (0.24)	0.40 (0.24)	0.42 (0.22)
Gravity SI (NegBin)	0.42 (0.18)	0.37 (0.22)	0.39 (0.22)	0.40 (0.20)
Regression Kriging (Poisson)	0.54 (0.21)	0.49 (0.24)	0.41 (0.22)	0.47 (0.23)

The prediction results based on the correlation index Pearson's R between predicted and actual trip counts were recorded in Table 4 for the five methods (natural neighbor, ordinary kriging, regression kriging, gravity-type SI model, and negative binomial model) using data for each classification category (interpolation, margin, extrapolation), as well as the entire dataset. Overall, the results demonstrate that regression kriging is probably the most well-rounded model to capture the correlation in all three station types. The results also provide evidence in support of the primary hypothesis that different mechanisms in spatial interaction and spatial interpolation will be different depending on the location and the regression kriging can outperform the single methods of ordinary kriging or SI model. Meanwhile, the standard deviations around 0.2 indicate the

correlation varies much across stations. It is hard to say regression kriging can always outperform other methods.

2.6.3 Spatial trends

The relative comparison of the candidate methods within one location is more meaningful than the quantitative comparison of metrics across stations. Figure 6 reveals the spatial distribution of 'cold start' stations rendered with the best method in the individual station. Warm colors are associated with interpolation methods (Red: Natural Neighbor; Orange: Ordinary Kriging) and cold colors stand for regression methods (Cyan: Gravity SI; Blue: Negative Binomial). Green dots represent the compound model: regression kriging method. Overall, there is a substantial portion (518 out of 754) of interpolation methods topped as the best methods over the two regression-only methods, which supports flow interpolation as flow prediction tools. Then focusing on the lower Manhattan Island where stations are mostly added as interpolation types. Interpolation methods are commonly rated as the best methods there which comply with the intuition that nearby flow patterns facilitate interpolation methods. Two regression methods as best methods could hardly be spotted in lower Manhattan, but located in North Manhattan, Queens, and Brooklyn (north, east, and south of the system, respectively).

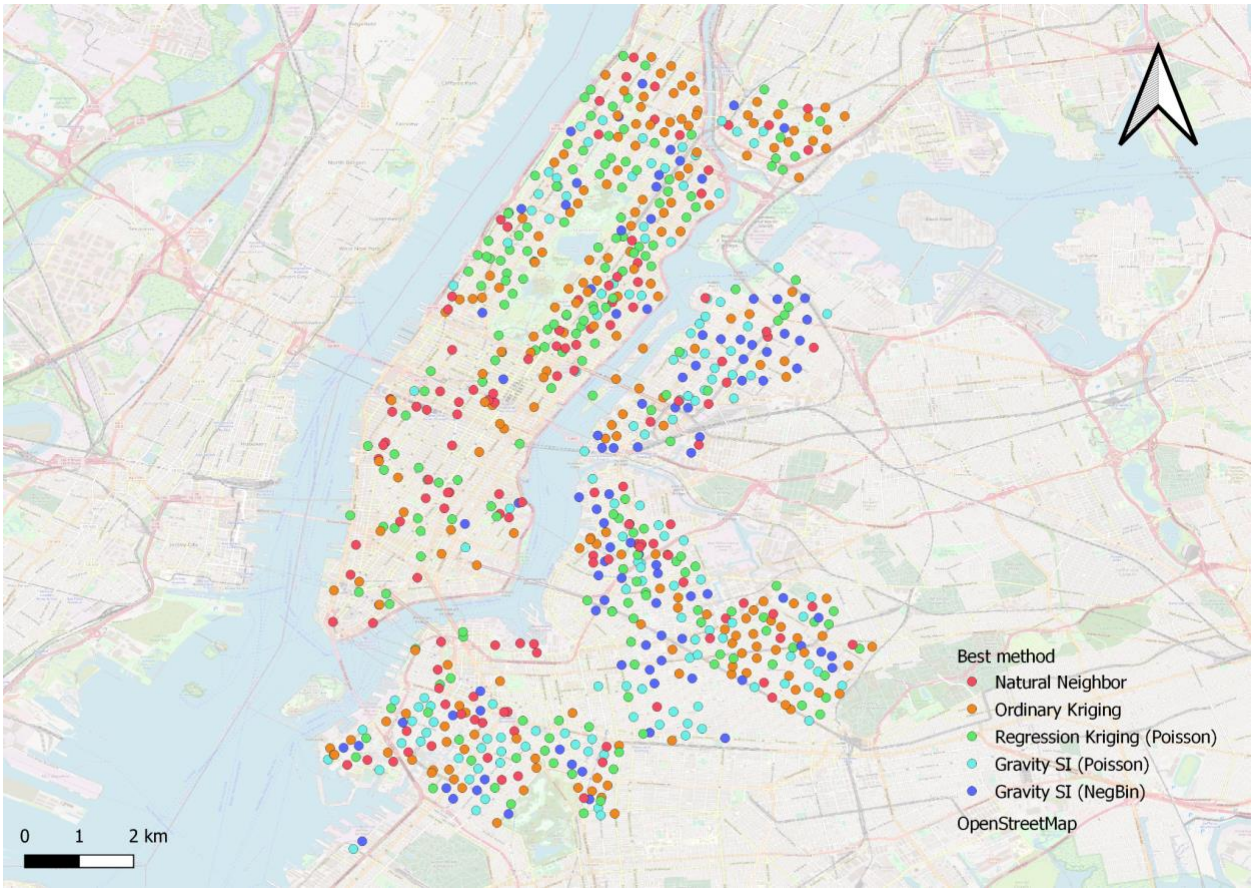

Figure 6. Spatial distribution of the best method for flow prediction at each 'cold start' station.

On the edge of the bike share system, where added stations are usually of the extrapolation type, a mixture of best methods can be seen. Even though extrapolation stations are out of the coverage of the existing system with limited nearby spatial dependence, regression models are not necessarily superior to interpolation methods in all cases, which is unexpected. It implies the necessity of considering the spatial dependence or spatial structure of the bike share system at all times regardless of when locations are added. Another explanation could be that fewer trips at extrapolation stations introduce more noise than signal, having a negative impact on all methods. When comparing two gravity models, the Negative Binomial (NegBin) model seems to do better

in the outskirts of the system where there are probably more stations with a few numbers of rides and therefore more overdispersion.

2.7 Discussion

Spatial interaction demand for bike-sharing trips has caught the attention of many researchers in recent years as new bike share systems are installed at an astonishing speed around the world. Yet the prediction of demand at 'cold start' stations is an overlooked issue. Previous studies work around the issue either by filtering out the new stations or using a different spatial aggregation, such as grids. This chapter leveraged spatial interaction models and flow interpolation techniques to propose an approach to compare different models through a case study using the NYC Citi Bike system. Specifically, the proposed approach attempts to predict OD flows of newly added stations after the system infrastructure changes.

After comparing all candidate methods on each identified 'cold start' station, results show that the gravity SI model comes with the advantage of the interpretability of the parameter estimates. For example, the interpretation of gravity SI models shows that the leading trip generation factor is the number of recreation sites nearby, which provides useful additional information to advise the planning of bike share systems. Alternatively, interpolation methods, including natural neighbor and ordinary kriging, show better predictability for stations classified as interpolation but are less performant for stations classified as extrapolation. Regression kriging combines both gravity SI and ordinary kriging and yields the best performance. Finally, spatial trends reveal some heterogeneity in the prediction performance of different methods. Specifically, the downtown Manhattan region shows higher predictability for interpolation methods, but stations added in

Brooklyn are less performant for regression methods only. Interpolation methods unexpectedly outperform regression models in many extrapolation cases, implying the presence of long-range spatial dependence and suggesting the use of spatial interaction models that incorporate spatial dependence (Oshan, 2021) in future work.

One significance of this work is that it begins to fill the gap of the missing historical data that is needed for many popular methods. For example, the methodology could be used to generate pseudo historical flows so that methods dependent upon them can be used to make predictions over time even for 'cold start' stations. Therefore, the proposed approach facilitates a more robust demand modeling framework.

However, trip prediction for stations classified as extrapolation is still limited using the proposed approach because neither the gravity-type spatial interaction model nor the interpolation techniques work as well as they do for the interpolation stations. For future work, the idea of geostatistical transfer learning may help overcome the issue (Hoffimann et al., 2021). Meanwhile, the evolving techniques of graph convolutional neural networks (such as Pareja et al., 2020) may be adapted as an alternative of flow interpolation method to be compared with the proposed Kriging methods in future work. Another limitation that needs to be more fully explored is the weak predictability of 2020 stations, which is possibly due to the low trip counts or drastic behavioral changes during the pandemic, or both. When there are low trip counts, the methods used here tend to underestimate the few stations with higher activity and more effort is needed to develop methods that can handle this scenario.

The methods included here only provide an initial investigation of the 'cold start' issue. Future work may unfold differences in the performance of methods at station level to show the magnitude of the differences and further investigate differences in spatial dependence at a finer spatial scale. Future studies could also further investigate and leverage the temporal dependencies of the OD flows. In this work, a weekly time interval was used, though other intervals could also be explored, as well as the temporal windows used to characterize demand before and after stations are added to the system. Future work could therefore explore different time parameters or even combine them to increase predictive accuracy. These are just a few suggestions that could be on the line of inquiry initiated here to grapple with the issues caused by 'cold start' stations in dynamic transportation systems.

2.8 Conclusion

This chapter focuses on the overlooked 'cold start' issue as historical flows are available at newly added stations. Instead, flow interpolation methods based on Kriging are proposed in the flow domain. Specifically, Ordinary Kriging and Regression Kriging with the adaptations in the flow domain are investigated and compared with existing flow interpolation of areal natural neighbor, as well as spatial interaction models that calibrate relationships between independent variables and spatial interaction flows. Based on experiments conducted on a bike-sharing system in NYC, the regression kriging model exhibits superior performance compared to other models regardless of the locations of 'cold start' stations by leveraging the strengths of both gravity-type spatial interaction regression models, which are robust and interpretable, and ordinary kriging, which is capable of capturing spatial dependence. The distribution of best methods at each station also

suggests a hybrid strategy to use interpolation-based methods at stations added within the system coverage and regression-based methods at stations added at the new areas of the system.

Chapter 3: Modeling the temporal dynamics of bike share trip determinants and the impact of the COVID-19 pandemic

3.1 Abstract

Spatial interaction modeling of trip demand can help identify the key determinants of trip generation and inform the planning and development of transportation systems. However, such models are often based on data aggregated across long periods of time (i.e., months, years, decades), which produce a single set of results that summarize the entire period of time. This aggregate perspective is essentially static and is unable to indicate the temporal dynamics of trip determinants. At the same time, recent studies highlight the massive impact of the COVID-19 pandemic on human mobility and suggest substantive changes to the determinants of trip-making behavior over time. Therefore, this work explores the temporal dynamics of trip demand determinants before, during, and after the pandemic lockdown in New York City and uses the bike-sharing system as the case study. This is done by calibrating spatial interaction models for weekly subsets of bike share trips and examining the dynamics of the parameter estimates associated with each determinant over time. Results indicate detailed shifts in the relationships between trip demand and factors such as trip distance, bike station capacity, and various types of nearby amenities. Through this disaggregate comparative modeling framework, it is possible to uncover both routine fluctuations and pandemic disruptions in terms of the determinants of bike share trips. These dynamics contribute to a better understanding of human mobility behavior and the use of transportation infrastructures, which can be useful for system maintenance, planning expansions, and anticipating vulnerabilities.

3.2 Introduction

Spatial interaction modeling of trip demand may identify the key determinants of trip generation and further inform the planning and development of transportation systems. However, such modeling practices are often deployed with data aggregated over a period of time and result in one set of coefficients of determinants of bike share trips. This static perspective cannot capture the dynamics of trip determinants. An alternative dynamic perspective is lacking for two primary reasons: 1) spatial interaction data were historically limited to being collected intermittently before the widespread availability of location-enabled sensors, and 2) traditional transportation infrastructure and the associated urban environment usually changed slowly so that spatial interaction models representing multi-year periods were sufficient. Now, neither of these scenarios holds as there is an abundance of data about rapidly changing urban systems. Consequently, there is an increasing demand to be able to understand these dynamics and a methodological framework is proposed here within the context of bike share systems.

Spatial interaction flows of transportation, such as commuting data, used to be captured from surveys, which were usually sampled discretely over time, such as the American Community Survey by the US Census that is compiled over several years. However, the use of geolocation technologies in transportation systems has enabled individual trips to be recorded with precise timestamps, such as those used in the bike share systems that emerged in the last decade. The detailed time information allows temporal dynamics of the bike trip usage with resolution up to an hour to be investigated through different studies (Noland et al., 2019; Shen et al., 2018; Y. Yang et al., 2019).

Urban transportation systems are becoming increasingly complex as micro-mobility modes, such as, docked or dockless bike share systems and e-scooters are introduced to address the first- and last-mile problem. There is an increasing demand for the dynamic planning of transportation, as infrastructures of such micro-mobility systems are versatile and can be added or moved at lower costs than the expansion of traditional public transportation infrastructure, such as a metro station (Liu & Oshan, 2022). Additionally, studies on the impact of short-term public transit disruptions on bike share usage (Saberi et al., 2018; Y. Yang et al., 2022; Younes et al., 2019) have not only underscored the capability of micro-mobility as a complement to public transportation but also posed new dynamic modeling challenges in response to disruption-driven trip demand. This therefore presents a practical challenge as more dynamic modeling can guide the deployment and rearrangement of a bike fleet to meet changing travel demand.

Another driving factor for the need for dynamic modeling arises from the COVID-19 pandemic starting in 2020, which changed short-term travel behavior and resulted in changes to different spatial and temporal distributions of general mobility (Kang et al., 2020; Pan et al., 2020; Sevtsuk et al., 2021), metro ridership (H. Wang & Noland, 2021), bike share systems usage (Padmanabhan et al., 2021), and e-scooter rides (Y. Zhou et al., 2021). Furthermore, these changes in travel behaviors may imply the possible long-term social effects of COVID-19 (van Wee & Witlox, 2021).

Hence, modeling spatial interaction flows within a transportation system can help us understand changes to human mobility. The detailed and publicly available trip history records make a bike share system a good target to study the temporal dynamics of system usage, which serve as a proxy for human mobility dynamics. Previous studies on bike trip determinants explore bike trip

generation (Noland et al., 2016), but very little work so far has addressed the dynamics of trip demand determinants with a refined temporal resolution to understand bike share behavior in the context of a massive societal stressor, like the COVID-19 pandemic. To fill the gap in understanding the dynamics of bike share trip determinants, this study proposes an analytical framework for exploring the temporal dynamics of determinants in spatial interaction flows. Bike share system data from before, during, and after the COVID-19 pandemic lockdown are exploited as a case study to demonstrate the framework's effectiveness in finding changing determinants of bike share trips. This research uses a disaggregate comparative framework to explore the dynamic determinants of bike-sharing trips. By understanding these determinants, it becomes possible to better respond to different types of stimulators.

The remainder of this chapter will first describe the data and methodology that are used for the study. In the results, variable selection is discussed. After that, the results of yearly and weekly dynamics from the NYC CitiBike case study are described. The final section summarizes the findings and concludes the chapter with some implications and limitations.

3.3 Data and methods

3.3.1 Independent variables

Data preparation consisted of collecting various independent variables that may contribute towards explaining the generation of bike trips. In Table 5, a set of sociodemographic variables and POIs features are collected and aggregated by each dock station which serves as both origin and destination features of spatial interactions. These features include population, employment, station capacity, subway accessibility, and points of interest with classification from Foursquare. The table also lists the methodology, data source, and the year of data acquisition for each feature, and it is

worth noting that each element in the POI categories is a separate variable. The median bike trip duration for each origin–destination pair is used as the distance cost factor. Many of the origin or destination variables here are overlapping with those used in the spatial interaction models in the first study but the nearby capacity variable has been substituted with the capacity directly available at each station. This is because the capacity information can only be accessed from the General Bikeshare Feed Specification (GBFS) service which is a live feed with no official historical data cached. Trip data in study 1 traces back to 2015 with a certain number of stations no longer in service at the time of data collection in 2020. However, for collection after 2020 when this study is performed, most stations in 2019 remain in the system for continuous operation so more than 95% of stations and 98% of the trips have valid capacity information in the recent GBFS cache, which allows this study to use direct capacity as a feature.

Table 5. Variables for model selection in Chapter 3.

Variable name	Feature description	Data source – year
Distance cost	Mean trip time in seconds	Citibike trip records – 2019 to 2021
Population	Population by census tract	Census ACS 5-year - 2018
Employment	Total employment by census block	LEHD Origin-Destination Employment Statistics - 2018
Station capacity	Number of total docks at a station	Citibike GBFS – 2019 to 2021
Subway access	Euclidean distance to nearest subway station	NYC Open Data - 2021
Point of interests	Weighted sum of nearby POIs with inverse distance weights with a distance band of 1500 m. Categories: (1) healthcare, (2) education, (3) finance, (4) food, (5) housing, (6) recreation, (7) religious, (8) shopping, (9) travel, (10) professional, and (11) other services	SafeGraph - 2020

3.3.2 COVID-19 pandemic semantics

Daily confirmation number of COVID-19 cases is accessed from the GitHub repository of NYC Health Department[8], which is available for the study period of 2020 and 2021. According to vaccination data from the NYC Health Department[9], the mass vaccination campaign against Coronavirus in NYC commenced in early 2021 and experienced the most noteworthy increase between March and June, before slowing down after August (See Figure A.1 in Appendix A).

[8] https://github.com/nychealth/coronavirus-data
[9] https://github.com/nychealth/covid-vaccine-data

3.3.3 Spatial interaction model

A subset of variables is used in the final spatial interaction model based on the previously introduced unconstrained gravity model (Equation 3.1) for different years and weeks. Model calibration was carried out using the Python package *spint*.

$$T_{ij} = k\frac{V_i^{\mu} W_j^{\alpha}}{a_{ij}^{\beta}} \qquad \textit{Equation 3.1}$$

3.3.4 Variable selection

Not all the variables are equally important in the model fitting. To simplify the model, the variables whose coefficients are around zero will not be used in the model calibration. On one hand, when the confidence interval of a coefficient estimate overlaps with the value of zero, the interpretation of the variable becomes less informative. On the other hand, insignificant variables may bring in collinearity to the significant variables. LASSO (Least Absolute Shrinkage and Selection Operator) is a regression technique that helps to identify and select the most important features (or variables) that contribute to the model. Variable selection with LASSO applies a penalty to the regression coefficients, which causes some of them to be shrunk to zero, effectively removing those variables that are not relevant to the outcome (Equation 3.2). Final variable selection started with LASSO but also considered additional factors that are theorized to be associated with changes during COVID-19 as well as considering collinearity.

$$\min_{\beta_0,\beta} \frac{1}{N}\sum_{i=1}^{N} w_i l_i(y_i, \beta_0 + \beta^T x_i) + \lambda\left[\frac{1-\alpha}{2}\|\beta\|_2^2 + \alpha\|\beta\|_1\right] \qquad \textit{Equation 3.2}$$

3.4 Results

3.4.1 Bike trip overview

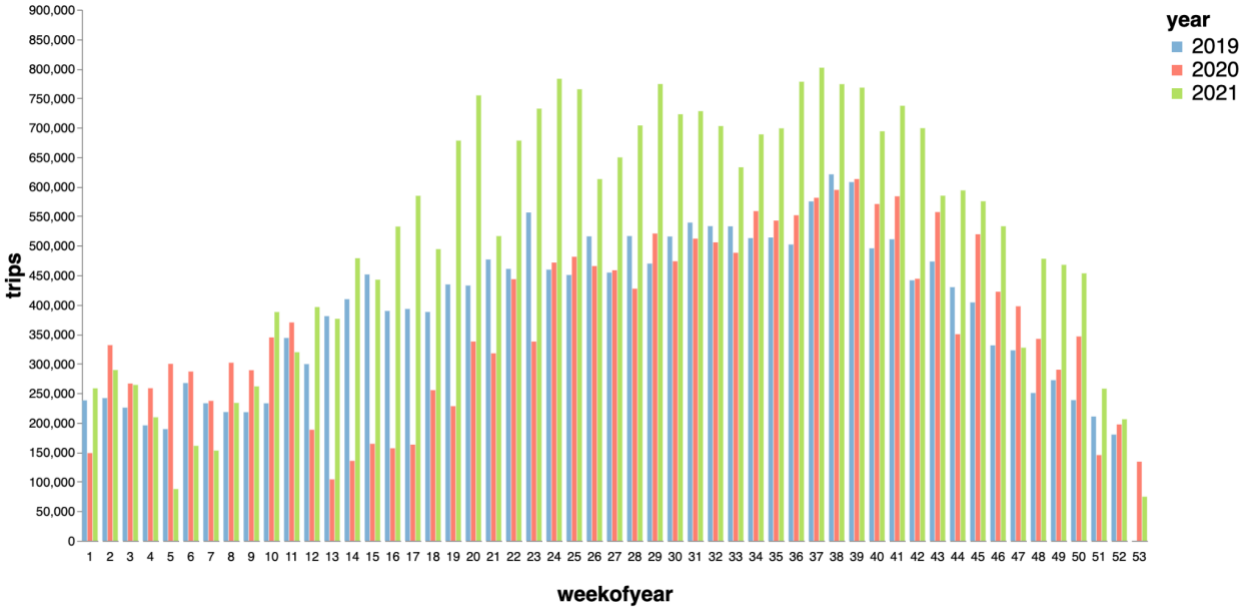

Figure 7. Weekly trip numbers in the NYC bike share system from 2019 to 2021.

Figure 7 demonstrates the total number of trips from CitiBike for each week from 2019 (blue), 2020 (red), and 2021 in (green). A side-by-side comparison of weekly trips across the three years highlights the impact of the COVID-19 pandemic, as well as the associated lockdown order. Specifically, weekly usage in 2020 started to drop in week 12. The Monday of the first week to drop is Mar 16, 2020, which is the first day that all schools in NYC closed. Usage resumed to normal levels by week 22 (May 25 - May 31, 2020), which is ten weeks after the initial outbreak of COVID-19 and right before the Reopening Phase 1 starting June 8. Weekly trips for the rest of 2020 almost follow a similar pattern for 2019 and even exceed 2019 usage in the last several weeks of 2020. Weekly usage in 2021 exceeds 2019 in most of the weeks except for the start of 2021. From the total trip counts in Table 1, the total trip number in 2021 exceeded 2019 by 34%. The

weekly trip numbers over three years show that the system usage recovered and thrived beyond 2019 levels right after the lockdown. However, trip numbers convey limited information on the change of determinants in different stages of the pandemic. The average trip time has increased from 16 minutes in 2019 to nearly 22 minutes in 2020 also indicates behavioral changes between years.

3.4.2 Variable selection

The regularization paths from the LASSO result give helpful information on the importance rank of variables as shown in Figure 8. Specifically, a more important variable doesn't reach the X-axis (y=0) until larger values of lambda. The cost factor representing the distance decay has the most powerful effect because: first, it has the absolute value among all the variables before the LASSO penalty applied to the regression; and second, it is the last variable to reach 0 on the X-axis. Both support the notion that the cost factor can account for most deviance (variation) of the dependent variable within the model. Except for the cost, other variables at origin or destination locations seem to share a similar regularization path. With variable selection starting from right to left on the X-axis, the two most important variables are recreation and station capacity. The employment factor is the final factor that can be discerned, while the remaining factors are mixed with each other and cannot be distinguished based on their regularization paths.

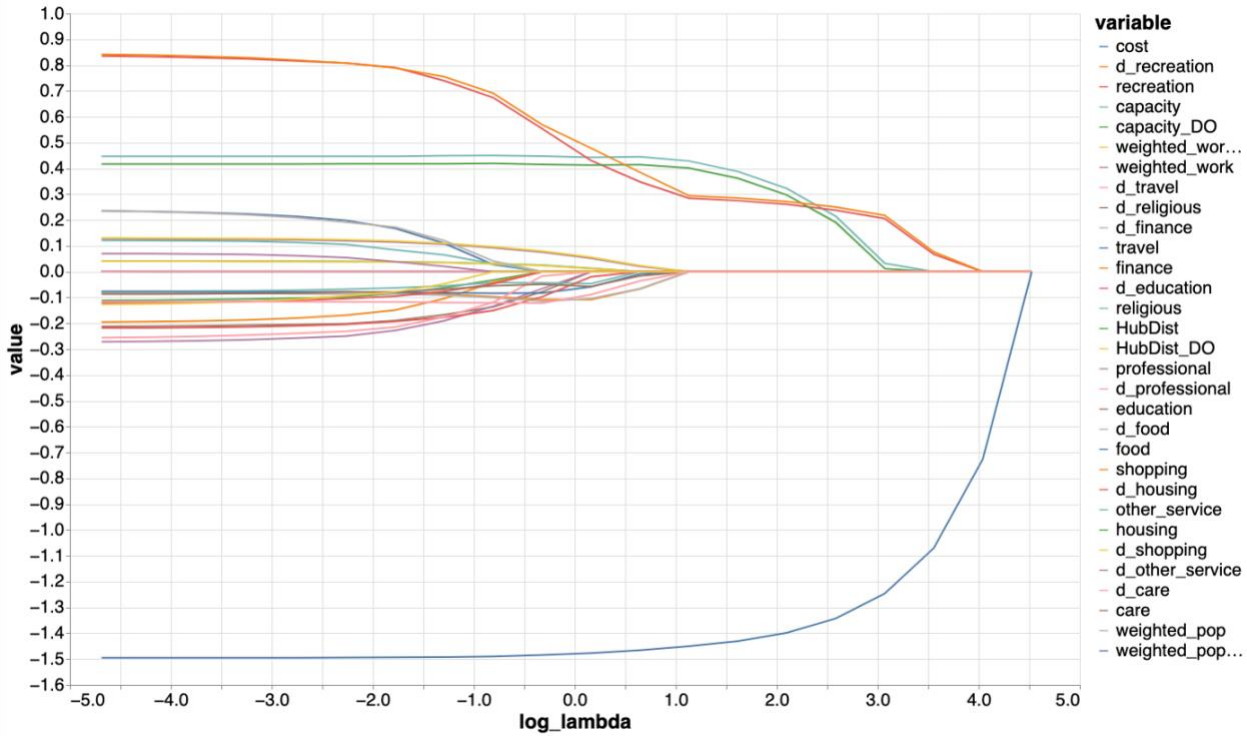

Figure 8. Regularization paths for the LASSO results. A more important variable ends in y=0 with a larger lambda.

Even if some variables are not listed amongst the top factors from the lasso results, they may still be interesting in regard to the COVID-19 pandemic. Here, we examined two possible examples, healthcare facilities and restaurants. It is noteworthy that restaurants at origins and destinations are also showing the third largest intensity when lambda takes the minimum value in Figure 8. However, adding the extra variables might result in collinearity issues during model fitting. Collinearity refers to the situation when two or more predictor variables in a regression model are highly correlated with each other, which can lead to unstable estimates of the regression coefficients and make it difficult to interpret the effects of individual predictors on the outcome variable. The variance inflation factor (VIF) is a measure used to detect collinearity among the covariates in a multiple regression model. A VIF score measures the extent to which the variance of the estimated regression coefficient for a particular predictor variable is inflated due to

collinearity with other predictor variables in the model. This measure is calculated by regressing each predictor on all others being used in the regression.

$$VIF(\beta_j) = \frac{1}{1-R^2{}_j} \qquad \textit{Equation 3.3}$$

where $R^2{}_j$ is the R-squared value generated by regressing predictor X_j on all other predictors. Multicollinearity is thought to be a problem if VIF > 10 for any given predictor (Dormann et al. 2013).

Potential collinearity among independent variables was analyzed by visualizing their correlation at each origin location, as shown in Figure 9, and calculating the VIFs of the variables, as listed in Table 6. The three-step selection process is named after "full", "partial", and "final" in terms of the status of variables. The scatter plot between recreation places and restaurants suggests a linear relationship, indicating collinearity between these two variables. This observation is confirmed by the VIF scores, which exceed 20 for both restaurant and recreation, indicating a strong collinearity between them (column *VIF full* in Table 6). However, since the recreation factor is stronger than the restaurant factor in the LASSO result, the recreation variable is chosen over the restaurant variable. Even after dropping the origin and destination factors of the restaurant, the recreation factor still shows a VIF value slightly above 10, which is the threshold for a strong collinearity. The VIF of healthcare factor is close to 10, indicating a collinearity with the recreation factor in the "partial" status of the variables (column *VIF partial* in Table 6). To avoid the collinearity between recreation and healthcare, a decision is made to drop the healthcare factor from the spatial interaction model.

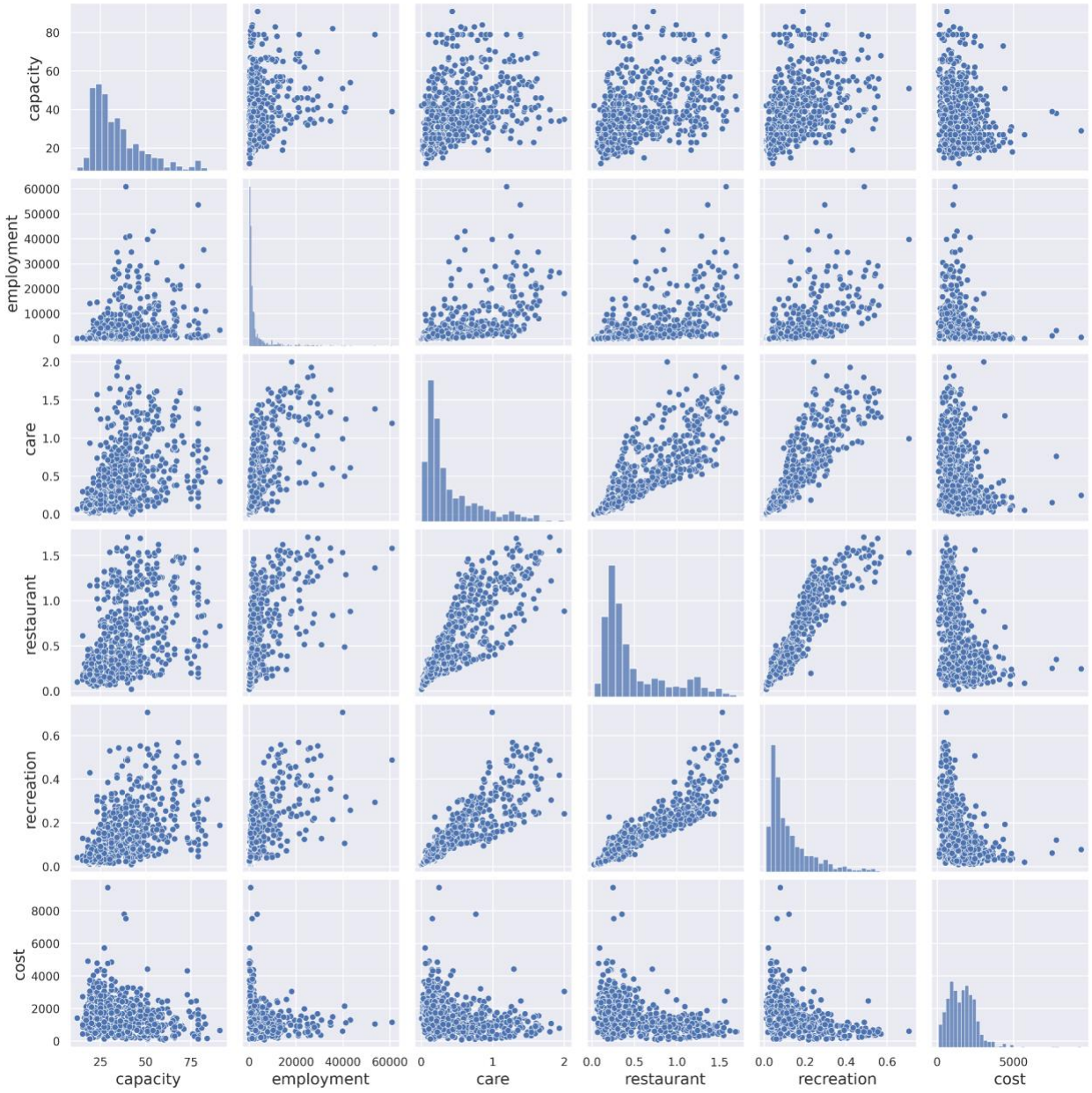

Figure 9. Pairwise scatter plot for selected variables in the spatial interaction design matrix for 2019 model.

Table 6. Variance inflation factor values with different independent variables for the spatial interaction models.

Variable name	Model Term	VIF full	VIF partial	VIF final
Distance decay	OD	3.3315	3.3242	3.3201
Station capacity	Origin	7.1353	6.9679	6.8294
	Destination	7.0818	6.9121	6.7737
Recreation	Origin	20.1928	10.4382	4.9595
	Destination	20.1380	10.4555	4.9336
Employment	Origin	2.4068	2.3996	2.2311
	Destination	2.3982	2.3908	2.2222
Healthcare	Origin	10.7218	9.8345	-
	Destination	10.7309	9.8497	-
Restaurant	Origin	20.6844	-	-
	Destination	20.5502	-	-

The final selection of determinants to explore for dynamic modeling of spatial interactions from NYC bike share data is **distance cost**, **recreation**, **station capacity**, and **employment**, as both origin and destination features. This line-up has all VIFs lower than 10, with the largest VIF values of 6.82 (column *VIF final* in Table 6).

3.4.3 Yearly trends

The yearly models are calibrated using aggregated bike share trips data from 2019, 2020, and 2021 for each origin-destination pair. Table 7 displays the coefficient estimates and 95% confidence intervals for the cost (distance decay) and origin/destination variables. Results from comparing the

variable coefficients in 2020 and 2021 to those in 2019 can provide insight into how the behaviors have changed from the pre-pandemic level.

Table 7. Yearly spatial interaction model coefficients and 95% confidence intervals.

Year		**2019**	**2020**	**2021**
Variables	**Model Term**	**Estimates CI**	**Estimates CI**	**Estimates CI**
Cost (distance decay)	OD	-1.443 +/- 0.009	-1.446 +/- 0.007	-1.429 +/- 0.005
Station capacity	Origin	0.373 +/- 0.024	0.513+/- 0.019	0.460 +/- 0.015
	Destination	0.341 +/- 0.024	0.479 +/- 0.019	0.435 +/- 0.015
Recreation	Origin	0.258 +/- 0.018	0.221 +/- 0.014	0.313 +/- 0.010
	Destination	0.286 +/- 0.018	0.241 +/- 0.014	0.324 +/- 0.010
Employment	Origin	0.033 +/- 0.008	-0.030 +/- 0.006	-0.032 +/- 0.004
	Destination	0.040 +/- 0.008	-0.033 +/- 0.006	-0.034 +/- 0.004

The distance decay remains relatively stable for the yearly trends, hovering around -1.44. Although there is a slight drop in 2021, the 95% confidence interval overlaps with that of 2019. When comparing the origin and destination coefficients of the same variable type, a general trend is observed, with both coefficients displaying a small shift across all three years. For instance, station capacity has a +0.03 difference from the origin coefficient to the destination in all three years. However, all differences between the origin and destination coefficients fall within the range of confidence intervals, indicating that they are not significantly different. A potential interpretation for the same coefficient of origins and destinations is that most origin-destination pairs have symmetric trip numbers (i.e., trips from A to B are similar to those from B to A). Therefore, only

destination trends are discussed between years to avoid redundancy. The station capacity shows a significant increase in 2020 (from 0.40 to 0.51) before dropping slightly to 0.47 in 2021, reflecting a stronger association between capacity and the number of trips during the COVID-19 pandemic. The association between destinations with more recreation opportunities drops in 2020 compared to 2019 (0.49 to 0.37) but increases (0.51) in 2021. The relationship between trips and destinations nearby to many jobs changes from a positive coefficient before the pandemic to a negative one in 2020, potentially reflecting fewer commuting trips. In 2021, it remains negative, possibly due to the continued availability of work-from-home opportunities.

In summary, the driving factors behind the rapid recovery and then increase in bike trips exhibit diverging trends. One trend, as displayed by distance decay and station capacity, is that some associations are essentially unchanged during COVID-19. Another trend, represented by factors such as recreation opportunities, shows a decrease in association before returning to pre-pandemic levels. The final trend, exemplified by factors such as employment opportunities, is that its association with bike trips changes since the outbreak of COVID-19 and remains a long-term change that doesn't recover to pre-pandemic levels as did recreation opportunities. These long-term trends highlight the importance of also investigating more short-term trends in the determinants to gain a more comprehensive understanding of the dynamic and static drivers of trip demand.

3.4.4 Weekly trends

For each factor, the figures below display the weekly trends of each determinant by year, with dashed lines indicating the 95% confidence interval. The plots also feature COVID-19 case trends at the top as a reference for the various stages of the pandemic. It is worth noting that the confirmed

cases in NYC at the end of 2021 were alarmingly high, with a daily average of over 25,000. To facilitate easy comparison of the COVID-19 waves from March 2020 to November 2021, the cases from week 50 to 52 in the end of 2021 have been omitted from the plots.

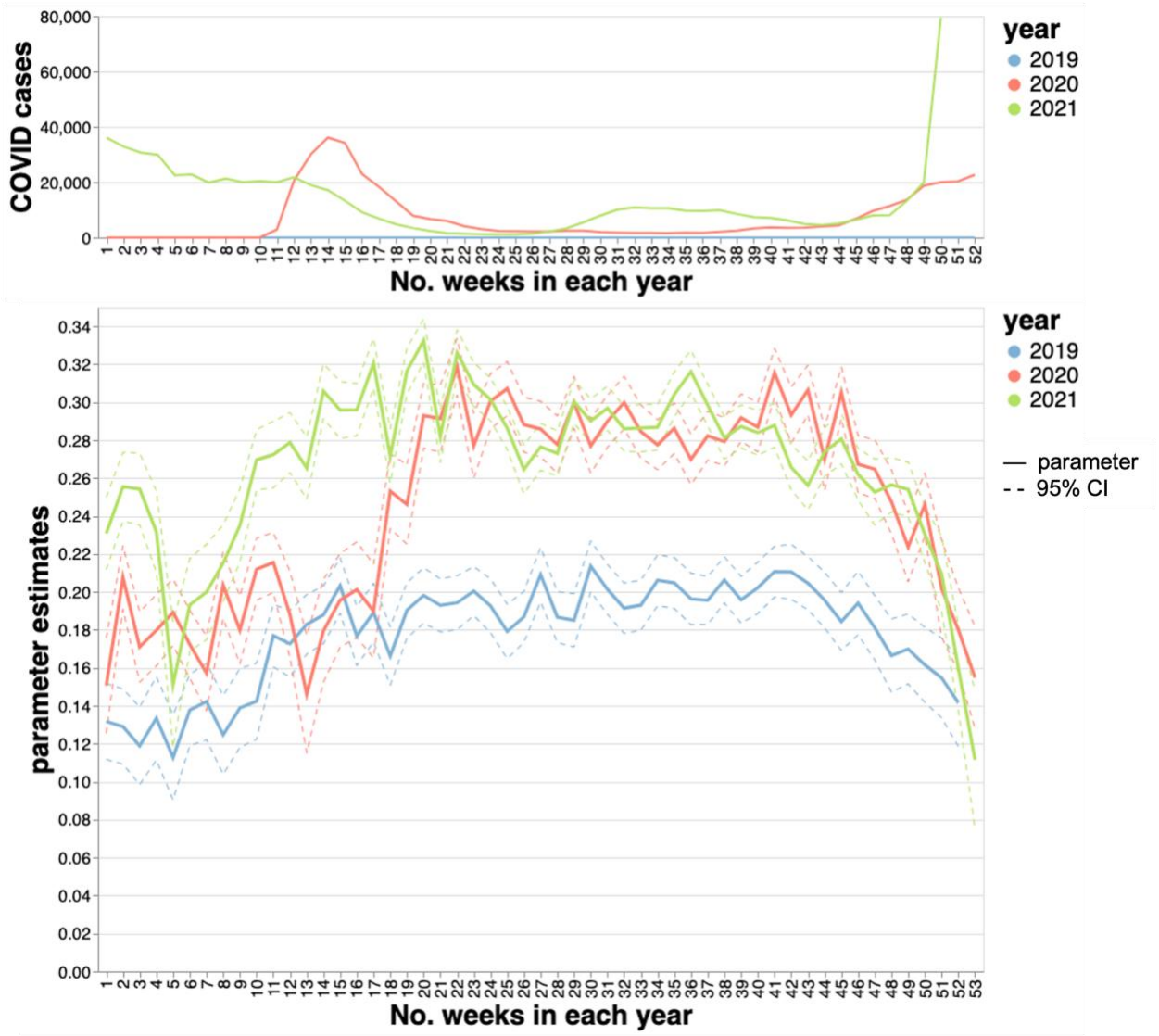

Figure 10. Top: COVID cases by week. Bottom: Destination capacity coefficient estimates and 95% confidence interval by week.

In 2019, the association between trips and the capacity factor (represented by the blue line in Figure 10) exhibited a typical arc with an increase during the summer months, indicating routine dynamics.

In 2020, the association initially decreased during the lockdown period but quickly rebounded to pre-pandemic levels after the reopening order in June. The remainder of 2020 followed the same path as 2019, but at a higher level. In 2021, the dynamics were interrupted by a drop at the beginning of the year, but then almost followed the routine of 2019 at a higher level similar to 2020. However, different waves of COVID-19 cases all had an 'undermining' effect on the association with the capacity factor. A stronger coefficient estimate here means trips are more likely to terminate at a dock with more capacity, suggesting the desire to be able to efficiently find a parking spot was stronger during periods with fewer COVID-19 cases.

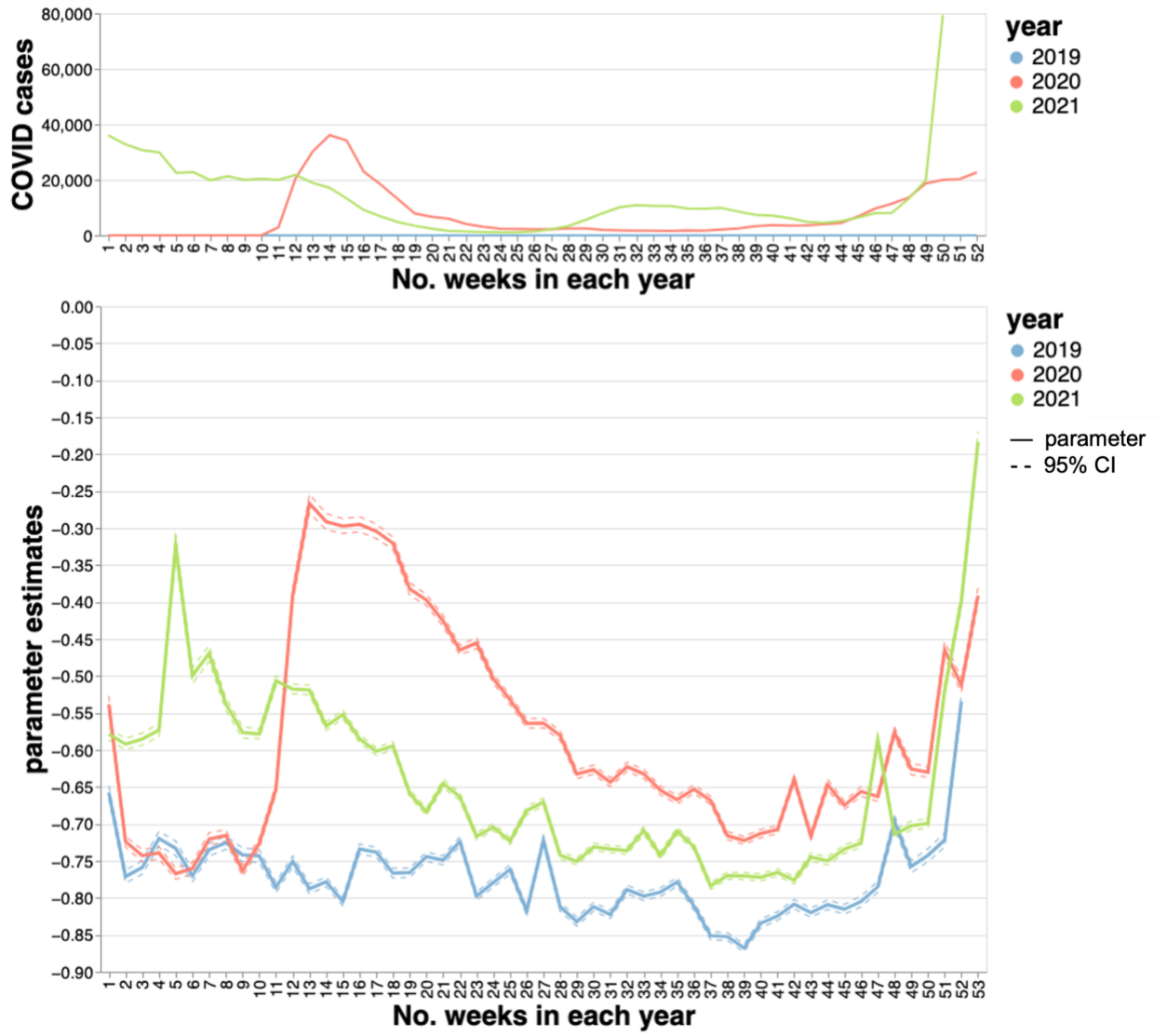

Figure 11. Top: COVID cases by week. Bottom: Distance decay coefficient estimates and 95% confidence interval by week.

In 2019, the routine dynamics of the association between trips and distance decay, as depicted by the blue line in Figure 11, remained relatively stable over the year, with a slight upswing in the latter half. However, with the onset of lockdown measures in late March 2020, there was a reduction in the negative association of distance decay and bike trips. This suggests that people were traveling longer distances and were less concerned about the distance they were traveling. While there was a recovery in the relationship shortly afterward, the trend declined again towards

the end of 2020 and the beginning of 2021. Upon comparing the changes in distance decay coefficients with the COVID-19 waves, it is evident that changes in distance decay coincided with increases in COVID-19 cases before widespread vaccination became available in mid-2021. Interestingly, despite the peak in COVID-19 cases in mid-2021, there was no apparent impact on the association between distance and bike trips, unlike the two preceding waves. Following mid-2021, the association increased and became more similar to the routine dynamics observed in 2019 while still remaining weaker than pre-pandemic levels.

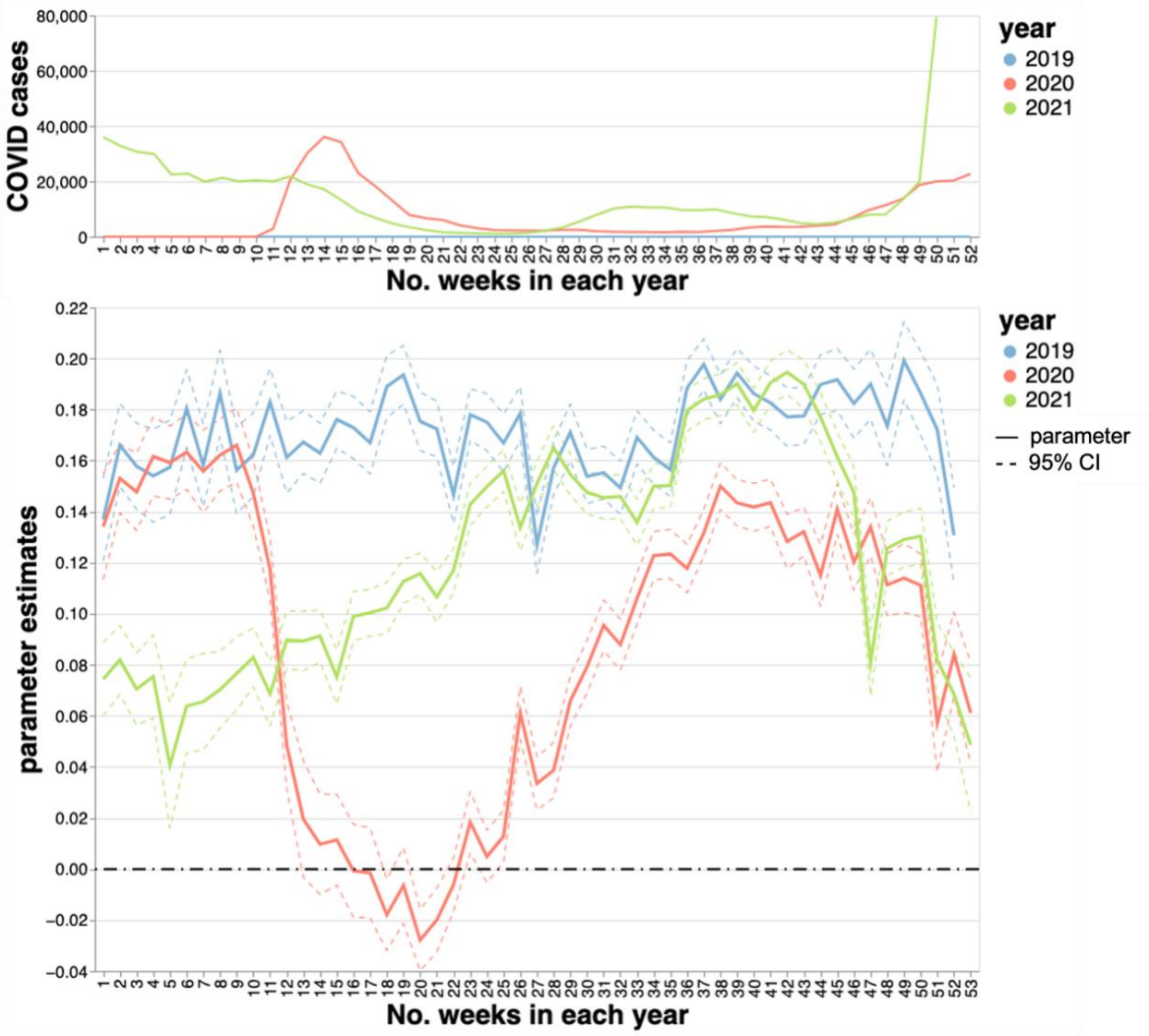

Figure 12. Top: COVID cases by week. Bottom: Destination recreation opportunities coefficient estimates and 95% confidence interval by week

The association between trips and recreation opportunities at destinations was relatively stable over time by August in 2019 but became slightly stronger during the last three months of the year (Figure 12). In 2020, the onset of the pandemic caused a decline to almost no association between destination recreation levels and bike trips during the lockdown period, but it gradually recovered to pre-pandemic levels after August 2020. However, when COVID-19 cases increased during the

end of 2020 and the start of 2021, the relationship weakened again before eventually recovering to the 2019 levels. In terms of COVID-19 impacts on the association of recreation opportunities and bike trips, it is notable that the pandemic had a significant impact during the peak of cases in contrast to the one during the summer season. This was due to the fact that destination recreation opportunities include indoor venues such as museums, which experienced a decrease in visitors during peak COVID-19 cases. However, during summers, the association dynamics quickly resumed to pre-pandemic levels due to the availability of outdoor activity options.

Figure 13. Top: COVID cases by week: Bottom. Destination employment coefficient estimates and 95% confidence interval by week.

Unlike the previous relationships, the association between trips and destinations nearby to many jobs have significantly changed since the onset of the pandemic in March 2020, as shown in Figure 13. In normal times, destinations with many jobs are strong attractors of bike trips, but the relationship became weakly negative during the pandemic. In 2021, the relationship gradually recovered to zero and remained uncorrelated throughout the year until the end of 2021, potentially

due to the prolonged work-from-home opportunities offered by various employers during the pandemic, which has reduced the number of people commuting to workplaces and, consequently, the demand for bike trips to and from work.

3.5 Discussion

This study investigates the changes in bike share trips as one potential proxy for human mobility during the COVID-19 pandemic, with a focus on the processes associated with bike trip generation and post-pandemic recovery status. Previous studies have mostly examined the spatiotemporal changes of bike trips during the lockdown but neglected the bike trip generating processes and did not extend as far in time towards a post-pandemic period. The study addresses this gap by modeling high frequency spatial interactions and revealing the behavioral changes beyond the changes in trip numbers.

The study uses yearly and weekly aggregation to analyze long-term and short-term trends in bike trips, respectively. Long-term trends pertain to aggregation of data and results by calendar year from 2019 to 2021 and highlight the potential long-term changes in the coefficient estimates. At this temporal scale, the association of the distance decay factor with bike trips remained essentially unchanged during the three years. In contrast, the association between trips and destinations with more jobs seems to suffer from a long-term impact of COVID-19. Destinations with more jobs used to have a positive relationship with bike trip volume before COVID-19. But such relationships turned negative in both 2020 and 2021, reflecting a long-term change in the trip purpose, namely that individuals took less commuting bike trips after the pandemic. This decrease is likely related to the prolonged work-from-home opportunities. However, bike trips still thrived

in 2021 with total usage exceeding that of 2019. This can be explained by the stronger association between trip volume and higher recreation opportunities in 2021, which indicates an increasing number of trips with recreation purposes. The decrease in the employment factor and the increase in the recreation factor suggests a change in the functional role of bike trips after the pandemic and contributes to the understanding of how human mobility changed after the initial lockdown. Previous studies on the impact of the COVID-19 pandemic on bike share trips modeled the drop and recovery of bike trip volume with lockdown policy and reopening orders (Wang and Noland, 2021) but lacked insights in the association between trips and destination opportunities. Aggregating trips by year removes variation about several significant changes related to the pandemic but nevertheless there is still some evidence of changing processes, which supports the need for further modeling at a more disaggregate temporal resolution.

Weekly subsets of the data resulted in coefficient trends that show more dynamic relationships between bike trips and different factors than the yearly aggregations. Coefficients from the weekly models in 2019 may be considered as an example of routine dynamics. Previous work (Oshan, 2020) showed a seasonal trend in the distance decay factor using weekly subsets across several years for taxi data from NYC around 2015, with colder months having a stronger distance decay. Converse seasonal trends show in the distance decay as the weekly trends of distance decay in Figure 11 seems to show weaker relationships in the colder months, implying that individuals prefer shorter trips during the warmer months especially in September 2019. A seasonal trend can also be seen in the capacity factor where it is stronger during the warmer months than the colder months. Increased association between trips and station capacity during warmer months suggests a stronger desire to find a parking spot upon trip arrival. This decision preference might arise when

the system is under heavy usage and more frequently riders may be under more competition with each other to find an empty dock. Under this scenario, this means more trips might end at a larger station rather than smaller stations that are harder to find a parking spot during the rush hours.

The comparison of weekly trends in 2020 and 2021 with the routine levels in 2019 provides insights on how COVID-19 disrupted the bike share system. The yearly trends showed that distance decay did not change in 2020 compared to 2019 and hovered around -1.44. However, the relationship between trips and distance decay from the weekly trends became weak during the peaks of COVID case incidences, indicating the travel behavior changed as people tended to take longer trips and become less sensitive to distance during periods that may have been perceived as higher risk to use other modes. Potential reasons why the annual 2020 model did not show a different relationship between trips and distance decay factor than the relationship in 2019 may be include: 1) the first two and half months in 2020 didn't experience the impact of COVID-19; and 2) the annual relationship may have remained the same if the distribution of trip distances across a year was similar, even the distribution changed for shorter periods of time. The weekly results confirm that the recovery of some of bike trip behaviors after the lockdown were quick and therefore might be less likely to appear in the yearly model. Between peaks of COVID-19 cases, the distance decay quickly recovered to a similar relationship from the pre-pandemic period. Even though distance decay largely recovered, the relationship never reached the same level as in 2019, indicating some longer lasting changes. The capacity factor also showed changes associated with COVID-19 such that during the peak of COVID-19 cases, the relationship became stronger than the pre-pandemic levels. Considering the persistent decrease in distance-decay after the pandemic, another possible explanation for the stronger relationship with the capacity factor could be that an

individual may spend more effort planning a longer trip and could become more likely to select a larger station that will optimize the trip by reducing the time needed to look for a parking spot. Another relationship that changed with the peak in COVID is recreation opportunities. The relationship coefficient estimate dropped to zero during the lockdown period, overlapping the time that almost all recreational activities paused. The relationship also recovered between the infection peaks of COVID-19, but one interesting finding is that it fully recovered to the pre-pandemic level during the summer of 2021 despite the existence of another peak of COVID cases. As the mass vaccination in NYC starting in early 2021 decreased risk, it helped stimulate demand for recreation trips. This finding also demonstrates that not all the infection peaks of COVID-19 induced the same impact on bike trips as similar behavioral changes were largely mitigated for the peak in mid-2021 by the mass vaccination.

Thus, the COVID-19 pandemic introduced additional complexity to human mobility behavior. As the changes brought about by the pandemic are long- and short-lasting and multi-phase, it is crucial to carefully consider the time period used for modeling dynamic behavior. Additionally, the relationship between trips and origin-destination factors may exhibit subtle changes when the event scale is shorter than the time horizon used for modeling. Therefore, it is necessary to conduct spatial interaction modeling at a more disaggregate temporal resolution, as this approach allows for a more detailed analysis of dynamics and can help the development of more nuanced and contextualized interpretations of results.

Limitations

This study uses spatial lags of Points of Interest (POIs) as features to better understand the relationship between bike trips and geolocated factors, in contrast to traditional land use data (Noland et al., 2016). POIs offer a greater number of location types (Table 5) than land uses, which are typically limited to fixed spatial partition and a limited number of categories (e.g., recreational, residential, mixed-use, etc.). However, the results of collinearity tests showed that the full range of POIs with weights from a fixed spatial lag was not fully leveraged due to their collinear spatial distribution. For instance, within a 200-meter range of a bike station in a Manhattan business district, the presence of pharmacies (healthcare) is not significantly different from the presence of restaurants since both types of places are common in the area. The presence of both types of POI could possibly introduce collinearity between the two POI types. In the future, additional information about individual trips and their purposes may be able to help alleviate the issue of collinearity between different types of POIs by only using certain POIs for certain types of trips. A different way to construct the place of interest attributes may also improve the data issue that causes collinearity.

Another pitfall sourced by the data quality is the absence of dynamics in the origin and destination variables. Due to the lack of dynamic demographics and POI data, all the independent variables are static. In this case, determinants might generate different values than using dynamic features as independent variables. Coefficients from dynamic input variables may reveal slightly different stories in the behavioral changes.

It is important to note that there are differences in the magnitude of the same factor between the yearly and weekly models. Additionally, sudden changes in the weekly determinants at the beginning and end of each year are due to the missing days in the weeks on the edge of a year. These differences in coefficient estimates between different modeling time periods may be attributed to the modifiable areal unit problem (MAUP), a topic commonly discussed in spatial statistics. Furthermore, the bike share data has unbalanced training data as zeros are excluded, resulting in a different number of aggregated flows in the weekly aggregations compared to the yearly model. Therefore, to further explore this issue, methods for unbalanced model training could be explored in the future (Y. Yang et al., 2021). Furthermore, interpretation from the results depends on the model coefficients from the gravity-type spatial interaction models, which may be different from another type of spatial interaction model. Future work could compare multiple spatial interaction models to validate the robustness of results.

3.6 Conclusion

The COVID-19 pandemic has had a significant impact on human mobility behavior, underscoring the need to study high-frequency spatial interaction to comprehend these changes and how people have adapted to the "new normal". In study 2, a disaggregated comparative modeling framework was used with both long-term and short-term aggregations of data, leading to two key conclusions. First, factors of bike share trips show different evolutionary paths after the pandemic. Specifically, the association between trips and destination features, such as station capacity and recreation opportunities, experienced similar changes due to increased cases of COVID-19 but quickly returned to pre-pandemic levels between peaks of cases. However, at the end of 2021, not all behaviors have fully recovered, and associations between trips and factors of distance decay and

employment remain different from pre-pandemic levels. Second, different insights from the long-term and short-term changes in bike trip determinants highlight the significance of examining pandemic disruptions and routine fluctuations using disaggregated comparative modeling to understand human mobility behavior and the use of transportation infrastructure. This modeling framework can be extended to further years to gain a deeper understanding of the behavioral changes brought about by the pandemic and contribute to a better understanding of the "new normal" as part of future planning decisions. Overall, this research can help inform policies and decision-making processes that affect human mobility behavior and transportation infrastructure in the context of the ongoing pandemic and future public health crises.

Chapter 4: Event detection in bike share trip behaviors with spatial interaction models and martingales

4.1 Abstract

Event detection has become increasingly important in various domains, including security, traffic planning, social media, and environmental science, and at the same time it has become increasingly possible thanks to the technological advancements in video surveillance, sensors, and the web. In particular, event detection with spatial interaction processes is important for understanding human mobility behaviors and socio-economic activities that cause behavioral changes in human mobility. This study proposes a framework that combines the martingale test with the spatial interaction data to detect events from human behaviors using spatial interaction models as a proxy for the processes related to human behavior. The framework's performance is evaluated with simulated data in experiments to detect events in artificial changes of spatial interaction processes. Empirical work is also conducted using bike share data from three different US cities to gain insights into real-world events, such as extreme weather changes, seasonal activities, holiday breaks, and COVID-19 pandemics, that can be detected using the proposed framework. This study develops a novel method for event detection from the perspective of spatial interaction processes and provides guidance on how to effectively combine spatial interaction models and martingale tests to detect events. Lastly, the study discusses model-tuning and limitations to guide future work in implementing a more versatile event detection framework based on spatial interaction data and models.

4.2 Introduction

In recent years, event detection has gained significant attention in various application domains, including security and surveillance (Karbalaie et al., 2022), traffic and crowd monitoring (Djenouri

et al., 2019), business intelligence (Ranco et al., 2015), social media (Vioulès et al., 2018), environment (Meyer et al., 2019), medical diagnosis (Ukil et al., 2016), and manufacturing (Pittino et al., 2020). The increasing adoption of event detection can be attributed to the remarkable advancements in technology, particularly in video surveillance, sensors, and the web. These developments have made it possible to extract real-time data in the form of visual and text information, which can reveal valuable insights into anomalous behaviors. In the realm of security and surveillance, event detection has proven useful in identifying intrusions and suspicious activities, thereby enhancing safety and preventing criminal activity. Similarly, in traffic and crowd monitoring, event detection is used to monitor traffic patterns and identify incidents such as accidents or road closures. Social media analysis also benefits from event detection, which can be employed to monitor public opinion and track the dissemination of information, thus facilitating informed decision-making for businesses. Additionally, event detection can aid in crisis management by swiftly identifying and responding to emergency situations, particularly those resulting from natural hazards.

Among the event detection scenarios, event detection with spatiotemporal data from urban environments is imperative to understand the factors that may change human mobility behaviors, such as disruption in the metro services caused by construction (Younes et al., 2019) and by strikes (Y. Yang et al., 2022). This practice garners increased attention, particularly with the abundance of data stemming from transportation systems like sensor or surveillance data, as well as social media check-in with geospatial tags (Miranda et al., 2017). With the recent advances in geolocation technologies, trips with detailed information are collected for high-frequency trip records. For example, trip records from taxi and bike share services are used in event detection to better

understand human mobility dynamics and improve event management and city planning (Chen et al., 2017; Doraiswamy et al., 2014).

There are multiple techniques available for event detection on spatiotemporal data, and the choice of technique depends on the data format and intended purpose. Djenouri et al. (2019) classify traffic flow outlier detection methods into three categories: statistical, similarity, and pattern mining. Statistical methods treat data as a statistical process (Kingan & Westhuis, 2006) and utilize statistical tests to identify outliers. Similarity methods, such as K-nearest neighbor, use distance measures to identify outliers in the input data (Dang et al., 2015). Pattern mining methods extract key data structures as patterns to distinguish anomalies, including trend decomposition (Zhu & Guo, 2017) and principal component analysis (Chawla et al., 2012). Event detection on a vector of spatial or temporal data can be generalized as an interesting subpath problem, such as locating an ecotone for ecological zones, with techniques such as changing point detection using CUSUM (Alippi & Roveri, 2006) and interesting subpath detection with statistical significance (Xie et al., 2020). The various techniques of event detection on spatiotemporal datasets have improved our understanding of how events evolve over time and space.

However, spatial interaction processes have not been adequately explored in the previous research in the domain of OD flows, especially in the relatively new mode of bike share systems. Meanwhile, flow processes that cannot be explained by the current spatial interaction model will produce larger model residuals and decrease the performance of a spatial interaction model. For example, COVID-19 has altered spatial interaction behaviors and caused a trend break during the lockdown period in NYC (Figure 14). To address this issue, this chapter proposes an event detection framework that can detect outliers based on these types of model-based changes. Such a technique

has not been previously explored in the spatial interaction domain and needs to be evaluated for its ability to detect anomalies in OD flows.

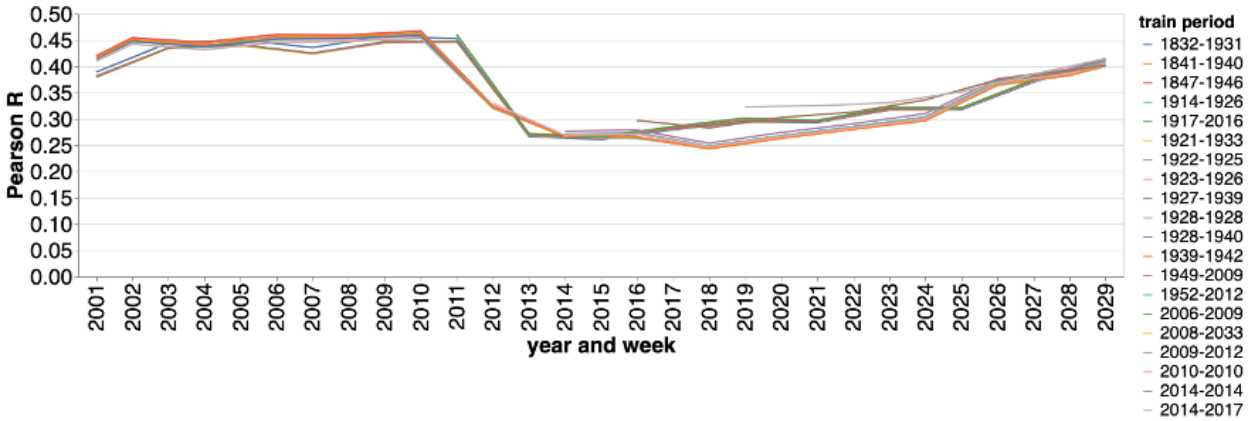

Figure 14. Demonstration of trend breaks from April to June 2020 in model performance (Pearson's R) from spatial interaction models trained with different periods of data.

The martingale framework for event detection is a statistical method that can fit classification, clustering, and regression-based event detection problems (Ho & Wechsler, 2010). The framework utilizes the martingale test that examines exchangeability within a sequence of data (Ho, 2005) and processes one sample at a time. Its 'online' feature makes it an ideal tool for real-time detection with applications in various fields, including video streams (F. Cai & Koutsoukos, 2020), social media (Vioulès et al., 2018), and flight behaviors (Ho et al., 2019). However, the martingale framework has not been widely applied in human mobility and transportation studies and requires evaluation in the spatiotemporal domain.

Spatial interaction models are used to understand human behaviors by explaining the origin-destination trip generating processes. Event detection using a model-based proxy can yield different insights from those using raw data distributions. For example, the second study of the

dissertation revealed behavioral changes from the dynamics of distance decay, which cannot be achieved by merely analyzing the total trip numbers. However, current event detection for bike share trips mostly relies on spatiotemporal data distributions (Doraiswamy et al., 2014; Lam et al., 2019), resulting in a research gap in event detection from the view of spatial interaction processes. Thus, this study raises the first research question: *Can we detect events from human behaviors using model-based proxies?* To further explore the martingale framework, the second question is *How can we effectively combine spatial interaction models and the martingale test to detect events?*

In order to answer both research questions, the study adapts the martingale framework with spatial interaction models to detect events in high-frequency OD flows from bike share trips. In the experiments, the study first evaluates the framework with simulated data to evaluate its performance on event detection with controlled simulations. Empirical work is then conducted with bike share data from multiple US cities to answer the third research question "*What types of events can be reliably detected across time and different US cities?"* Additionally, the study provides a discussion of model tuning and limitations to assist future applications of the martingale framework using spatial interaction process.

4.3 Methods

This section provides a detailed description of the proposed martingale framework for event detection using spatial interactions models. The initial steps introduce essential concepts and explain the working of the martingale test for event detection. The subsequent steps describe the necessary adaptations made from the original framework to tailor it to spatial interaction processes.

4.3.1 Exchangeability and martingales

The first step is to introduce the definition of exchangeability. Given a sequence of random variables $(Z_1, Z_2, \ldots, Z_n)$ that all take values in the same example space. The sequence is exchangeable if the joint distribution $P(Z_1, Z_2, \ldots, Z_n)$ of a finite number of the random variables is invariant under any permutation from the sequence, i.e, $p(Z_1, Z_2, \ldots, Z_n) = p(Z_{\pi(1)}, Z_{\pi(2)}, \ldots, Z_{\pi(n)})$, for all permutations π defined on the set $\{1, \ldots, n\}$.

The concept of martingale, originally used in gambling, refers to a fair game of chance where the outcome of each round is independent of previous rounds. For instance, consider Alice playing a sequence of coin toss games where heads earn her one dollar and tails lose her one dollar. Let Z_i represent the amount Alice earns or loses in the ith game, where a negative Z_i indicates a loss. The gambler's total winnings at the end of the i th game are denoted by M_i. The independence of Z_i from previous individual game earnings $(Z_1, Z_2, \ldots, Z_{i-1})$ implies that the conditional expectation of Z_i given these previous earnings is equal to the unconditional expectation of Z_i, which is zero. Moreover, the expectation M_{n+1} of the gambler's winnings at the end of the $(n+1)\ th$ game, given all previous outcomes, is equal to the winnings at the end of the nth game. Thus, the conditional expectation of the random variable M_{n+1} is simply the value of the current random variable M_n. Such relation ensures a martingale, as a sequence of random variables, remains stable in value with some fluctuation if the process of Z_i is random.

A formal definition of martingales is as follows. A sequence of random variables $\{M_i: 0 <= u < \infty\}$ is a martingale with respect to the sequence of random variables $\{Z_i: 0 <= i < \infty\}$, if, for all $i >= 0$, the following conditions hold (Ho et al., 2019):

- M_i is a measurable function of $Z_1, Z_2, \ldots, Z_i$,
- The expectation of the absolute value of M_i is finite, i.e., $E(|M_i|) < \infty$,
- Given $Z_1, Z_2, \ldots, Z_n$, the conditional expectation of M_{n+1} is the previous martingale value M_n, i.e., $E(M_{n+1}|Z_1, \ldots, Z_n) = M_n$

4.3.2 Martingale test

Event detection based on martingales performs a martingale test that examines the null hypothesis that "exchangeability holds" when every new data point is observed (Vovk et al., 2003). Unlike the gambling example, a martingale value within event detection provides evidence to reject the null hypothesis. Thus, the term *strangeness measure* is introduced to score the difference from a new value compared to the other previous values. Strangeness is defined on the type of event and input data, so a variety of possible strangeness measures related to classification, clustering, and regression could be used. A specific definition of regression-based strangeness for spatial interaction processes is elaborated in the session 4.3.3.

A martingale test over a sequence of input is a loop-like algorithm as shown in Figure 15. Specifically, strangeness is calculated from the residual of the spatial interaction model as the deviance from the current input to the known regression model. The current strangeness value is added to a list of previous strangeness values and then a *p-value* is computed for the current state using this list. The *p-value* plays the role of a random variable Z_i in the definition of martingale is calculated from strangeness for all the available strangeness in the training set as

$$p_i(\{(x_1, y_1), \ldots, (x_i, y_i)\}, \theta_i) = \frac{\#\{j : s_j > s_i\} + \theta_i \{j : s_j = s_i\}}{i} \quad \textit{Equation 4.1}$$

where θ_i is a random number from $[0, 1]$, the symbol # means the cardinality of a set, and s_i is the strangeness of sample i.

Martingale value *M* calculated from existing *p-values* has been proposed in two forms in previous work (Fedorova et al., 2012), e.g., *randomized power martingale* in product form and *simple mixture martingale* in integral form. In the product form, the power martingale for some ϵ, denoted as ${M_n}^{\epsilon}$, is defined as

$$M_n^{\epsilon} = \prod_{i=1}^{n} \epsilon {p_i}^{\epsilon-1} \quad \textit{Equation 4.2}$$

where $\epsilon \in [0,1]$, with empirical choice of 0.92 in one previous example (Ho, 2005). The integral-form simple mixture martingale, denoted as M_n, is the mixture of power martingales over different $\epsilon \in [0,1]$:

$$M_n = \int_0^1 M_n^{\epsilon} d\epsilon \quad \textit{Equation 4.3}$$

This study focuses on the mixture martingale as the default option for its simplicity. The alternative form using power martingales has the capability to adjust the sensitivity of the event detection algorithm. Detailed differences from the two forms of calculation are compared in the result session.

The martingale test will reject the null hypothesis if *M* is larger than a *threshold* λ which is another parameter that influences the algorithm. The last step of a sample processed in the algorithm is either to update the regression model with the new data point or to reset the training set after a change is detected.

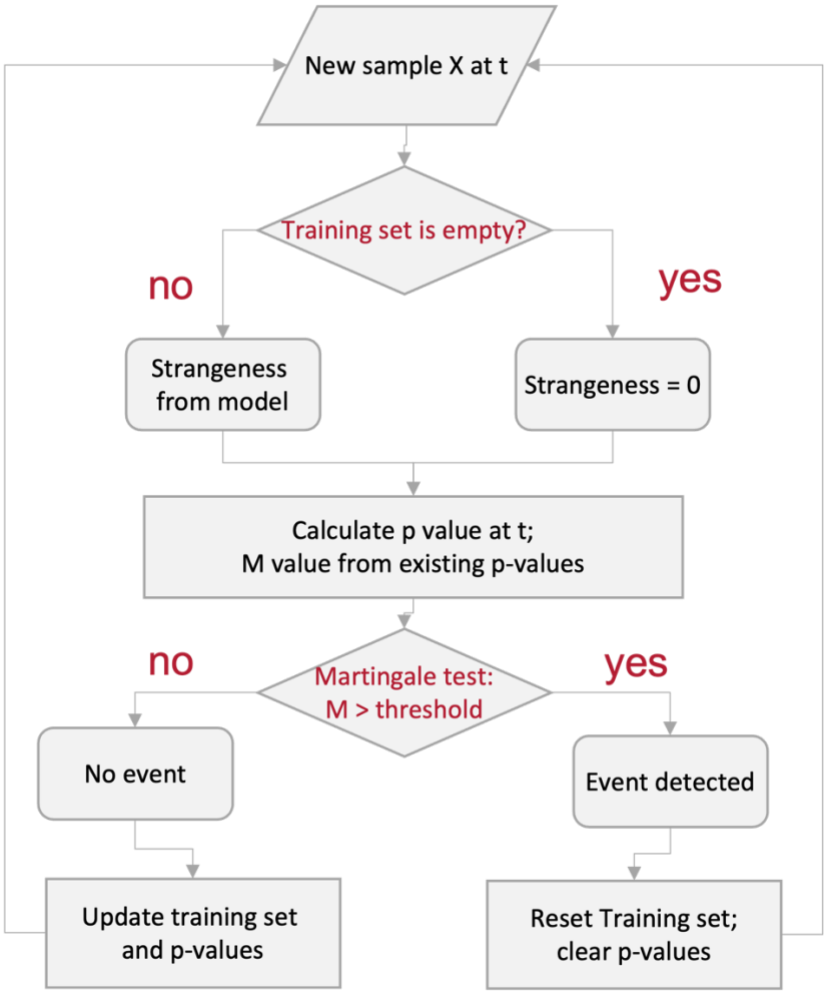

Figure 15. Algorithm of event detection based on martingale test.

4.3.3 Adaptations

Before applying the martingale framework for spatial interaction data streams in event detection, the proposed method must address two crucial adaptations. First is the definition of strangeness for regression-based event detection. Given the training set $T = \{(x_1, y_1), (x_2, y_2), \ldots, (x_n, y_n)\}$, where $y_i \in \mathbb{R}$, the strangeness of an example (x_i, y_i) with respect to a regression model is defined as

$$s(T, (x_i, y_i)) = \frac{|y_i - f(x_i)|}{exp(g(x_i))} \quad \textit{Equation 4.4}$$

where the numerator function f is the fitted regression function. In this study, a spatial interaction model is used here, which is essentially just a particularly structured regression model. The denominator $exp(g(x_i))$ is an estimate of the accuracy of the regression function f on x_i, where function $\boldsymbol{g}$ is the prediction of the value $ln(|y_i - f(x_i)|)$ for the example x_i (Papadopoulos et al., 2002). Both Gaussian regression and Poisson regression have been tested as g and Gaussian regression provided better results in sensitivity experiments.

The second adaptation is the dimension reduction of the origin-destination (OD) network into a single-valued martingale. Imagine a fully connected OD network with n sites, every time t it may generate a matrix of OD flows with the size of n^2 and the same dimension for the strangeness of each OD pair residual. However, the original martingale framework expects one strangeness value to calculate the scalar value of a martingale for the current time t. Thus, a representative strangeness should be extracted from the n^2-dim strangeness. Taking the median value of the strangeness was the most effective solution, outperforming the mean or using the maximum value. This is because the mean and max functions can more easily be influenced by extreme values, whereas the median value better reflects the overall distribution of strangeness values. Therefore, using the median value enables a more accurate representation of the collective strangeness of each OD pair while reducing the dimensionality of the OD network to a scalar-valued martingale.

4.3.4 Simulation design

Before conducting the empirical work, simulated data are used to manipulate changes in the data generating process and validate the framework in detecting artificial changes. The simplest spatial interaction model from Equation 3.1 is used with one variable for origins and destinations that represents population. The choice of total trips is made to approximate the daily statistics observed

in the empirical work in the NYC system. Specifically, a set of 25 sites were randomly generated in the plane $(0,100) \times (0,100)$, with 600 possible OD pairs (Figure 16). The cost factor d_{ij} is calculated from the Euclidean distance between the two points for each OD pair. A random population value from a uniform distribution from the interval $[50000,500000]$ is assigned to each site. A sequential data stream with length of 200 is generated with one or more parameters (i.e., processes) changed in the middle of the stream. Specifically, each time t, using the multinomial distribution, 50000 flows are distributed to each OD pair based on the probability calculated from the spatial interaction model that is obtained by dividing the predicted number of trips for an OD pair by the total number of predicted trips. The data generating process was replicated 100 times ($t = 1,2, \dots ,100$) with the parameters of the spatial interaction model as $k = 1, \mu = 1, \alpha = 1, \beta = 1$, for 'pre-event' data. A similar process was used for another 100 replications for times ($t = 101,102, \dots ,200$) by changing one or more parameters in the spatial interaction for 'post-event' data. This strategy was repeated 50 times using the proposed framework and mean time delay between the true and predicted time of the parameter change (i.e., event) as one benchmark of performance.

Event detection based on martingale test depends on p-value which is a random variable. The uncertainty within p-values means a possibility that event detection practices generate results other than true positives that an event is detected after the changed time, including false negative cases that the artificial change is not detected and false positive cases that are false alarms for non-existing changes. In the event detection applications, recall rate is imperative that is defined as $\frac{\#\ of\ true\ positives}{\#\ of\ true\ positives + \#\ of\ false\ negatives}$. Thus, sensitivity analysis was performed on the relationship of delay time and recall rate with 1) the changed time of the events and 2) the magnitude of changes

as complementary results to gain more insights on how the framework performs with the simulated data.

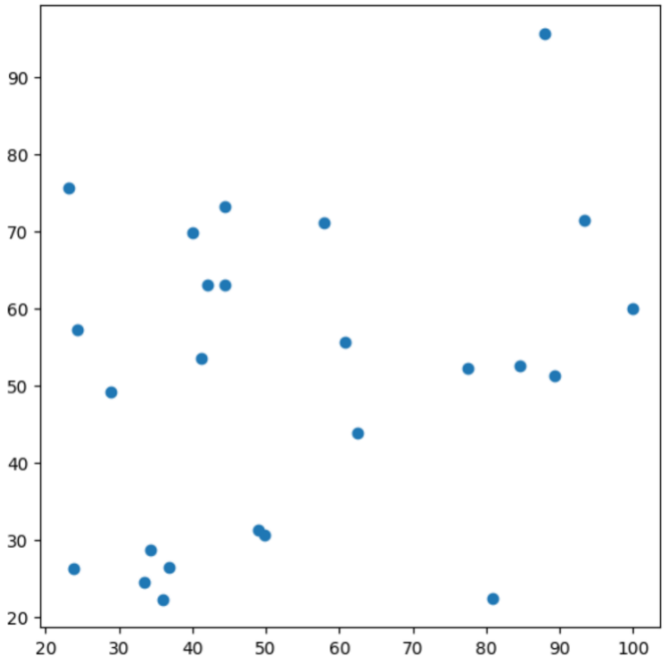

Figure 16. A demonstration of random distribution of 25 simulated sites.

4.3.5 Empirical design

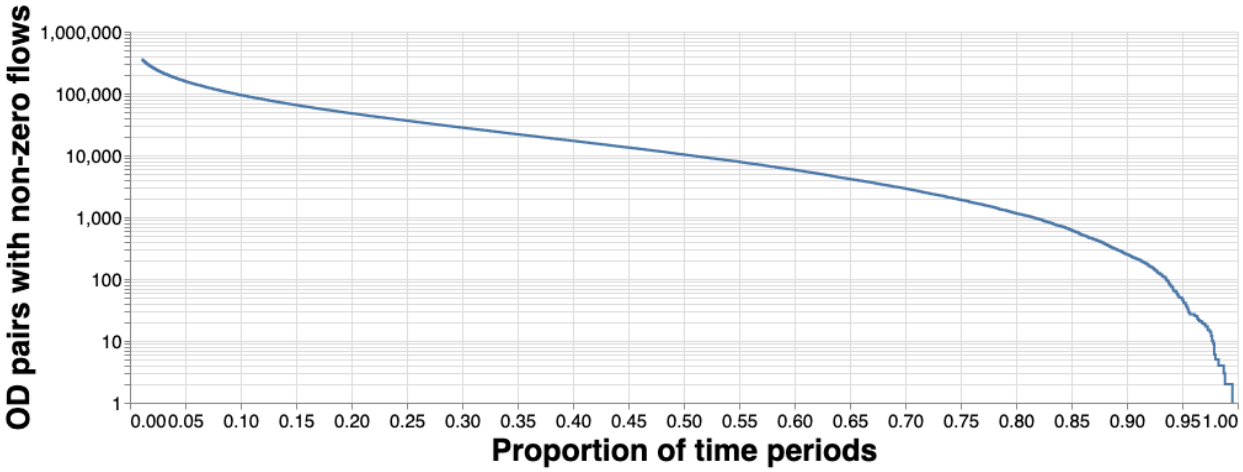

Figure 17. Relationship between OD pairs with non-zero flows and proportion (p) of time periods, e.g., weekdays, in the NYC system.

The empirical work involves utilizing bike trips that are aggregated over a given time period, such as weekly or daily. In the case of NYC, experiments showed that aggregation over a week or a day results in a large proportion of OD pairs with zero flows. Including all the OD pairs in the input often leads to failure in event detection. One explanation is that the unbalanced training set carries large variance at the stations that occasionally have positive flows but most have zero flows. Therefore, the algorithm requires observations that are not consistently zero valued and so it is important to only include OD pairs that are consistently non-zero. However, the definition of consistency is subjective as a consistent OD pair should have M time periods with non-zero flows among total N time periods. Therefore, a threshold proportion p is used to filter the OD pairs, termed "consistent OD pairs" thereafter, meeting the proportion condition that $p >= M/N$. Figure 17 demonstrates such a relationship of the number of OD pairs changing with the proportion p of time periods to help choose the proper threshold. The graph illustrates a logarithmic decreasing pattern when the threshold is below 0.85, followed by a linear decrease. An ideal choice for the consistency threshold is when p is 1.0, but the plot shows no such OD pairs have positive flows every weekday in the NYC system, so the threshold should be set lower than 1.0. For the empirical work in the NYC system, a spatial subset of consistent OD flows that have positive values in 85% of weekday sampling periods (e.g., $p = 0.85$ for NYC data) is used. Figure 18 demonstrates distribution of bike stations (Left) as well as the consistent OD pairs and the flow intensity of the NYC system (Right). The majority of consistent OD pairs are located around Central Park and in lower Manhattan. Strong connections can be seen in the west rim of Manhattan, while some isolated OD pairs are spotted in the west NYC. Different sampling windows, such as weekly, daily, and subsets of weekdays, have been tested from a temporal perspective. Overall, selecting a spatial

subset of consistent OD flows and using appropriate sampling windows is crucial to the reliability and effectiveness of event detection in the context of bike trip flow networks.

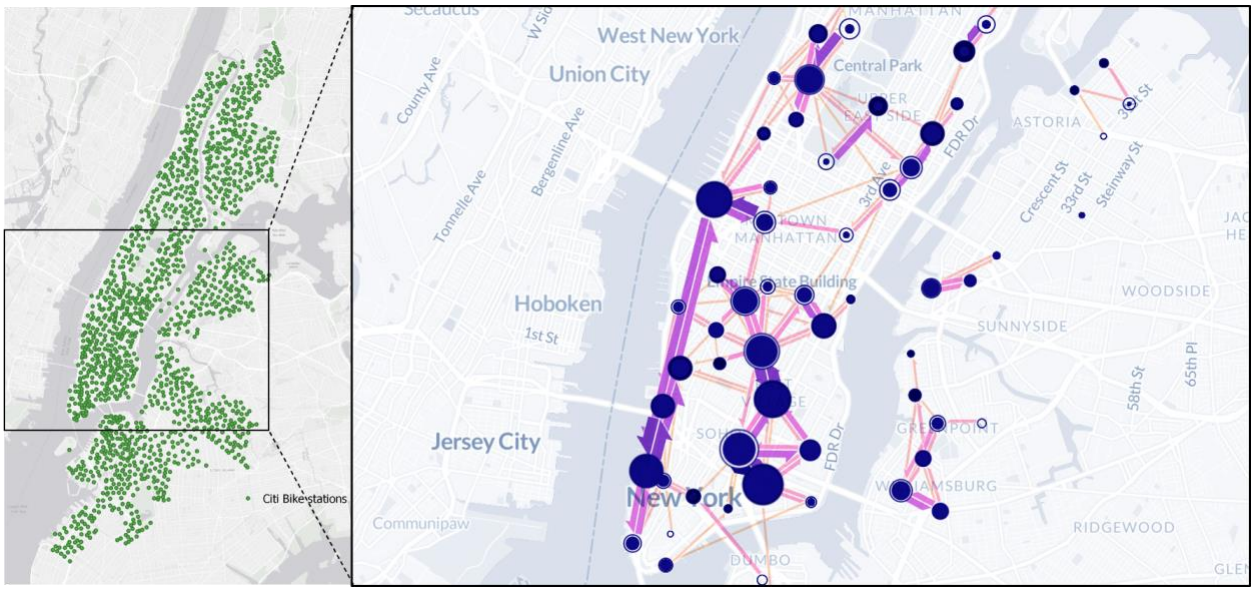

Figure 18. Left: Station distribution in NYC Citi Bike. Right: Illustrations of consistent OD flows in NYC Citi Bike with 85% time periods having positive flows.

To further highlight the significance of the proposed martingale framework, martingale values that are used for event detection are compared with the dynamic determinants that describe the potential behavioral changes in bike trip generating processes. Then they are compared with event detection outcomes for a previous tool that detects events from trip number dynamics. Both comparisons are expected to provide evidence in the capability of the framework to capture the potential behavioral changes which is not obvious from the trip numbers.

4.4 Results

4.4.1 Simulation

Simulated data from a gravity-type spatial interaction models are generated using different controlled settings. Table 8 displays the settings used in the simulations and the mean delay time for each setting. Any single change in the generating process can be reliably detected with a similar delay time. The changing of two parameters (row 3 and 4 in Table 8) theoretically results in larger model residuals, but the mean delay time only has a small improvement, which implies that increasing the magnitude of changes does not improve the delay performance. The right side of Figure 19 shows how martingale values grow with time for one distance cost change test with a red vertical line marking the time of the actual change. The plot illustrates how martingale values change over time before and after a controlled event occurs. Initially, martingale values will decrease and present some fluctuations, which will eventually cease as more data is received. When the event occurs, it requires extra data points to stimulate a peak in the martingale values, but the current model gets retrained after the threshold is exceeded, and the martingale values repeat the pattern observed at the left side of the plot. The distribution of mean delay time in four sets of experiments is shown in the left boxplot of Figure 19. The distribution of the delay times seems to decrease with large changes in the parameters, but the median values are not significantly different from each other.

Table 8. Simulation results for each setting, and mean delay time for detecting the true change event.

Parameter changed	**Changes**	**Mean time delay**
Origin	1 to 2	10.2
Cost	1 to 2	10.0
Origin, Cost (Double)	1 to 2	9.6
Origin, Cost (Double+)	1 to 4	9.2

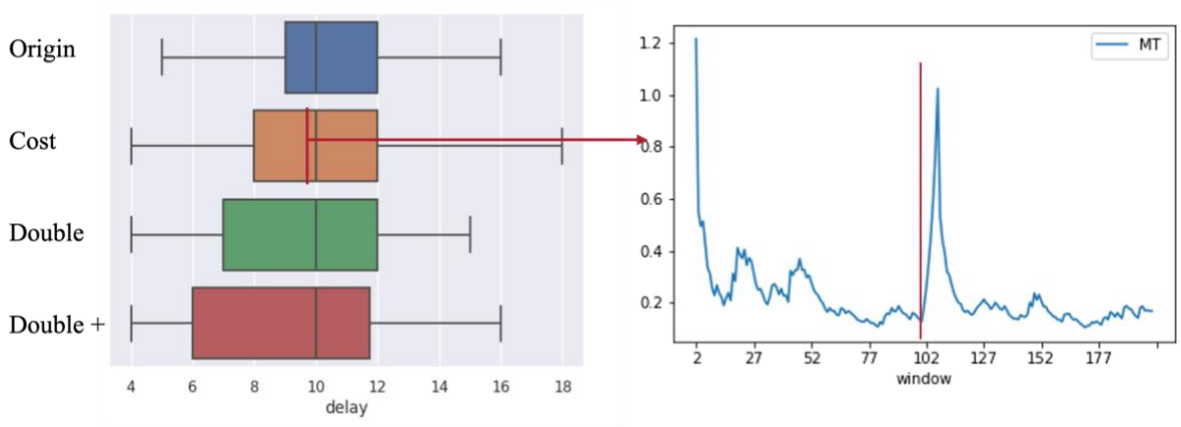

Figure 19. Left: Summary of 50 runs for four simulations. Right: A set of martingale test values by time in one sample experiment of "cost" change, with a red line marking the time of change.

Relationship between change time and delay

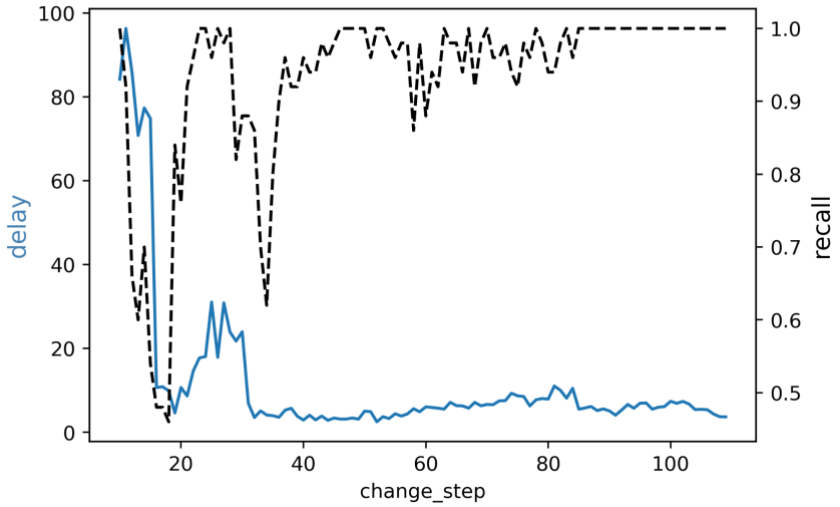

Figure 20. Delay times and recall rates from an experiment on the relationship of the delay time and parameter change.

This subsection describes the results of experiments conducted to investigate the impact of delay time on event detection. Model parameters were changed at different times (from t=10 to t=110), and the results are presented in Figure 20. The mean delay time did not vary significantly with different times of intended changes after t=30, ranging between 5 and 10. However, there were large fluctuations in the delay measured before t=30, possibly due to the regression model in the martingale framework requiring more time to stabilize. As a result, the initial frames may not have sufficiently trained the spatial interaction model before encountering the event. Additionally, the lower recall rate for earlier events indicated that the changes were not successfully recognized in those cases. This simulation suggests that quickly occurring events may be more challenging to detect.

Relationship between change magnitude and recall rate

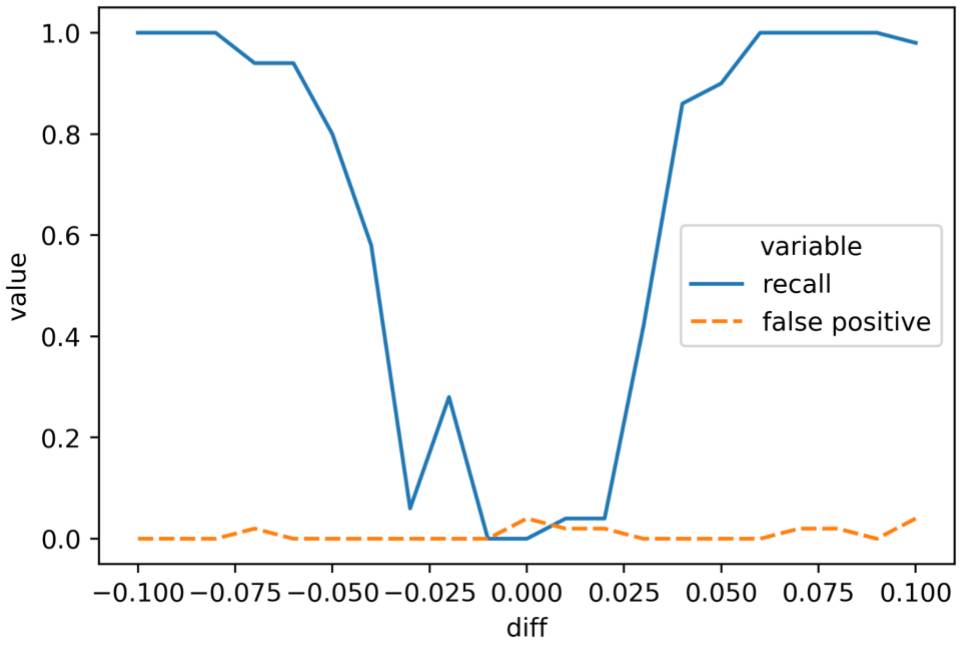

Figure 21. Recall and false positive rate from experiments with magnitude of event using the cost factor.

Figure 21 shows how the recall rate changed events associated with different magnitude changes in the process associated with distance decay (i.e., cost). The recall rate is almost 100% for changes larger than 10%, indicated by the region beyond the scale of the X-axis. For example, when the cost factor changes from -1 to lower than -1.1 or higher than -0.9. However, when the changes are less than 0.05 (5%), the recall rate drops, forming a U-shaped curve. This suggests that event detection is likely to miss an event if the process change is very small. The false positive line (orange) plots the false events triggered during the frames before the true events. These results convey that there is a small chance (0 or 1 out of 50) of false positives in the simulation. So multiple trials are recommended in case of false positives in a single trial. Overall, the examination of the recall rate for weaker events indicates that the strength of an event is important for this method.

The experiments with simulated data demonstrated that an artificial event causing changes in the spatial interaction generating processes can be detected with the proposed framework, despite small defects in the chance of missing an event when the events are weak or occurring quickly. The delay time and a small chance of false positives requires a careful interpretation from the real-world results in order to get robust results. Overall, the method might not be perfectly out-of-box, the simulation results support the fact that the method can detect events from empirical datasets.

4.4.2 Empirical work in NYC

Previous studies (Noland et al., 2019; Oshan, 2020; Shen et al., 2018; Y. Yang et al., 2019) have identified variance in the intra-city bike share usage between weekdays and weekends. To better capture different signals, the analysis focused on daily samples for either *weekdays (Monday, Tuesday, Wednesday, Thursday, Friday),* or *weekends (Saturday, Sunday)*. Figure 22 shows martingale values as well as events of interest from the NYC bike share weekday data. Environmental contexts such as weather, social media of the bike share operator, and COVID-19 cases are examined to understand these events as shown in Table 9. Martingale values reveal that the first event (marker A) corresponds to heavy snow in March 2018 with no delay in detection. Shortly after, an increase in temperature in May 2018 showed a peak (marker B). Another smaller peak (marker C) is related to a thunderstorm that disrupted bike trips heavily on May 15, 2018. Peaks D and E refer to holiday breaks at the end of 2018. The last cluster of peaks (marker F) in the data stream are pandemic-related events in 2020 and 2021. The first peak in this cluster (marker F) is related to trip changes due to lockdown, showing a peak 18 frames after the start of lockdown. Overall, this weekday example demonstrates that a variety of events can be identified in the

martingale values. The causes include extreme weather changes that lead to increases and decreases in trips, holiday breaks, and pandemic lockdowns.

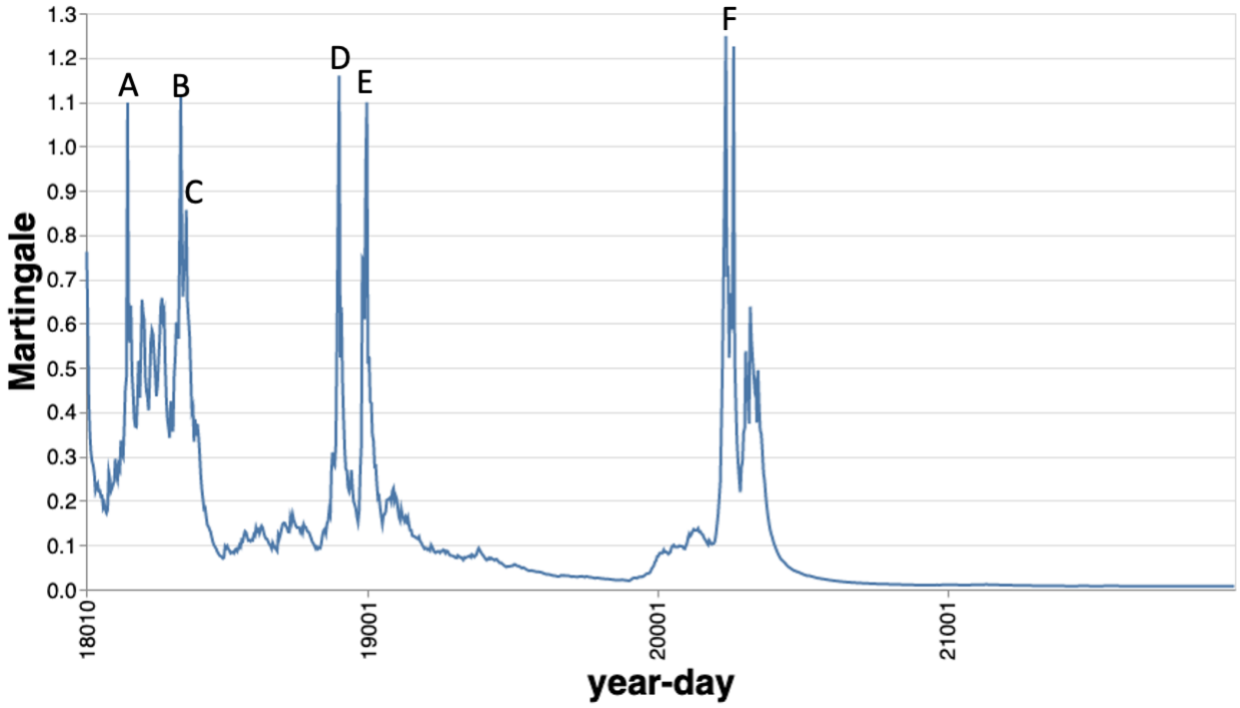

Figure 22. Martingale values and events of interest (marker A-F) from weekday samples in the NYC system.

Table 9. Highlighted markers in the sequence of martingale values from the NYC experiment and associated events, with occurrence time, cause of the event, and the delay compared to the occurrence time (if applicable).

Marker	Date, weekday	Cause of the event(s)	Delay (days)
A	03/02/18, Friday	Heavy snow and rain on March 2nd, 2018.	0
B	05/09/18, Wednesday	Warm weather starting May 2nd, 2018.	5
C	05/15/18, Tuesday	Extreme weather: one single day with high temperature and thunderstorm	0
D	11/26/18, Monday	Holiday break: Thanksgiving	2
E	12/24/18, Monday	Holiday break: Christmas	0
F	04/09/20, Thursday	Covid-19 pandemic: lockdown started	18

Relationship between detected events and potential behavioral changes

To further investigate the relationship between a detected event and potentially associated behavioral changes, the time series of martingale values were aligned with the dynamic determinants (i.e., coefficient estimates) using the same features from study 2 but for the weekday samples used here. Figure 23 shows martingale values for the weekday samples and trends of the distance decay factor from the weekday spatial interaction models. Detected events, including marker A, B, D, E, and F, can be matched with a change in the distance decay as shown in red vertical lines. This means the events in the martingale can be associated with the behavioral changes regarding travel distance for bike trips. However, there are additional spikes in the dynamics of distance decay that exhibit similar changes to the detected events marked in red lines but do not appear as a peak in the martingale values. Furthermore, the trends of the distance decay factor after the initial lockdown shifted back to the pre-pandemic level but did not trigger an event in the martingale values, as it moved away from the pre-pandemic level during the lockdown.

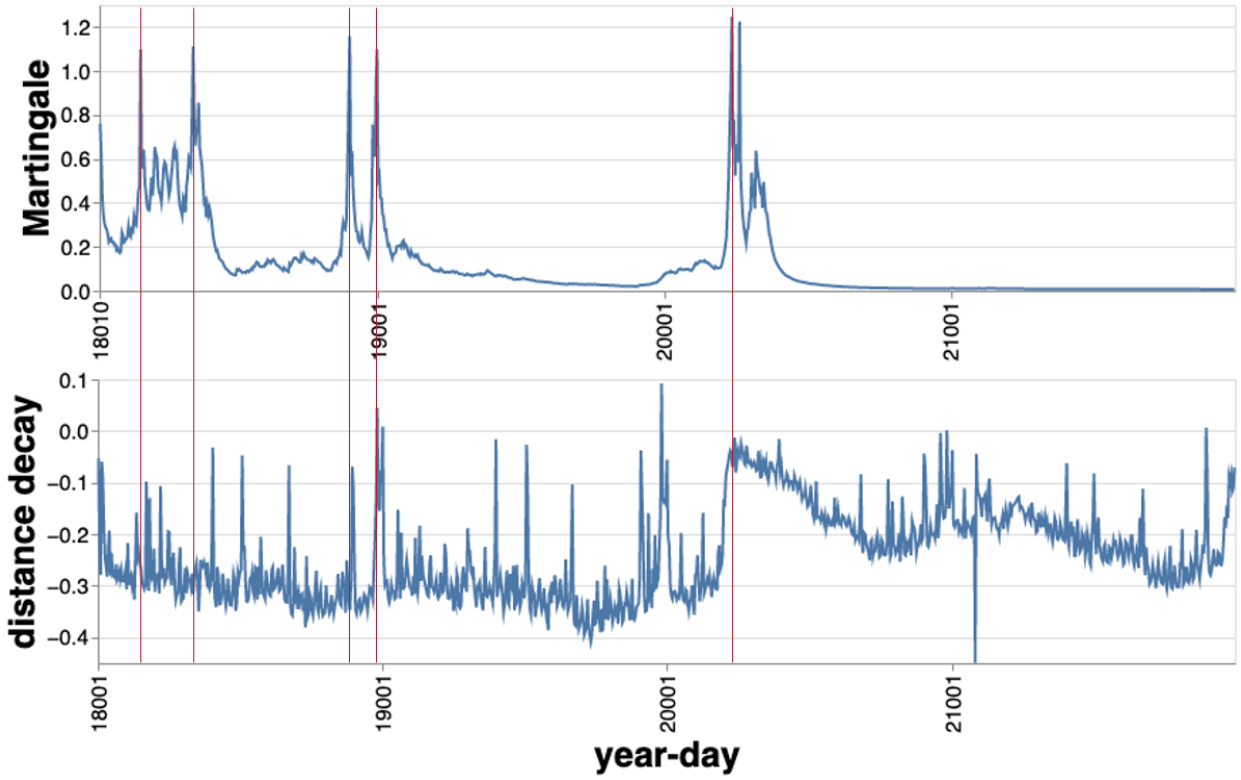

Figure 23. Martingale test value for weekday samples and distance decay from daily spatial interaction models. Red lines mark the events from A to F except for C in Table 9.

Comparing martingale values with trip numbers and Change Scores

A comparison of trip numbers and an event detection algorithm based on trip numbers with martingale values is shown in Figure 24. In the comparison between martingale values and trip numbers, an increasing or decreasing trend in the trip numbers seems to visually match one or more peaks in the martingale values. Events like the COVID-19 pandemic and holiday breaks at the end of a year can be visually identified in the trip number dynamics, but events that did not last a long time due to extreme weather are difficult to identify. The martingale framework seems to work better in detecting an event that didn't change the trip number obviously, such as event B

and C in Table 9. The ChangeFinder[10] algorithm by Takeuchi and Yamanishi (2006) is an online change point detection algorithm that uses a Sequentially Discounting Auto Regressive learning algorithm. The algorithm takes initial frames (such as first 10 frames) of input series as a training set and outputs a scalar value Change Score to indicate the possibility or intensity of change happening at each time. Figure 24 shows how the change score compares with the martingale value from the martingale framework. The zig-zag change score provides limited information towards detecting change scores, probably because daily trip numbers fluctuate so much that the ChangeFinder method highlights every small fluctuation as events. It can be observed that the martingale framework tends to suppress noise and stimulate spikes during periods with notable changes. This comparison showed that the martingale values from the spatial interaction model are better for detecting outstanding events than the Change Scores from the dynamics of trip numbers. For simplicity, this section only applies one of existing change detection method. To get a better insight in the sensitivity of the martingale framework, further comparisons may be performed.

[10] https://pypi.org/project/changefinder/

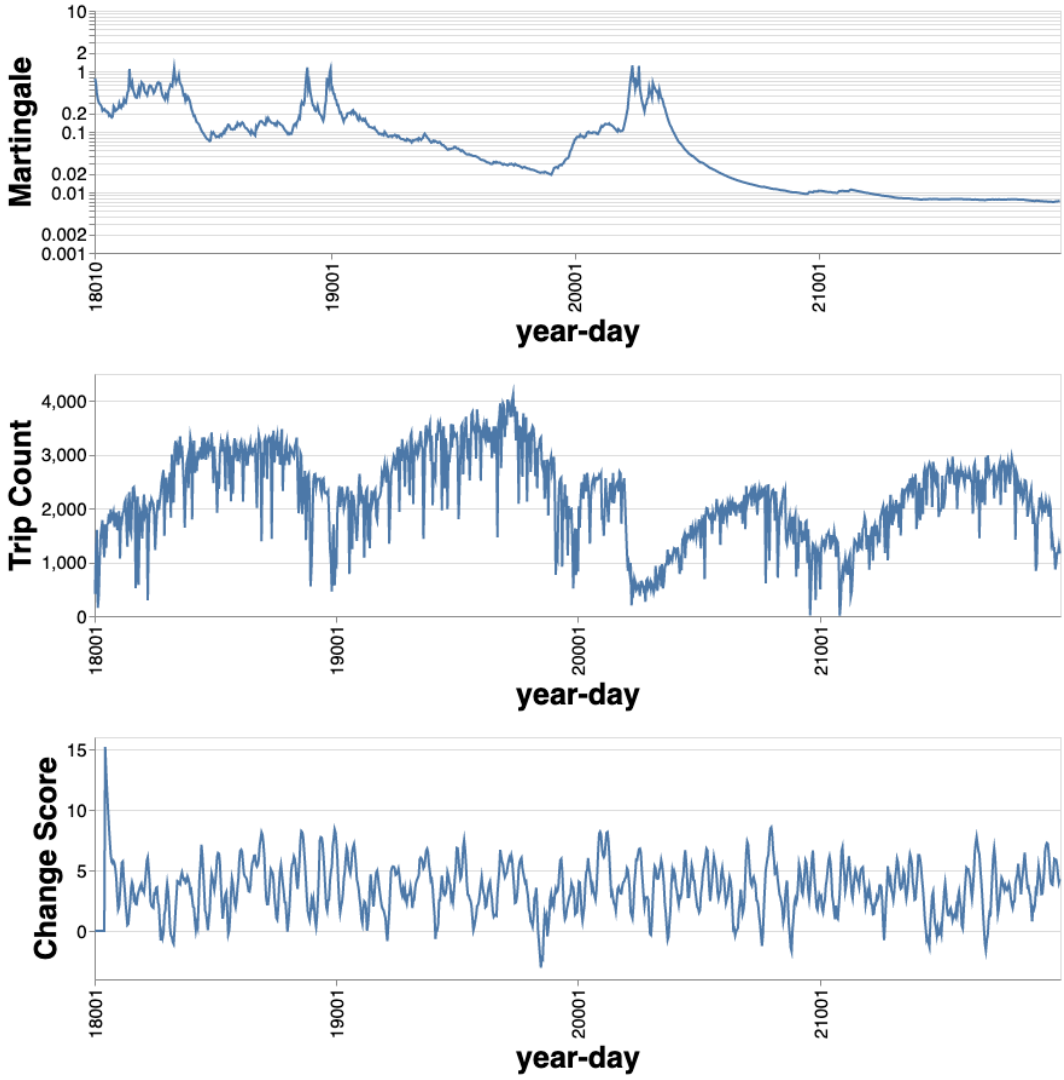

Figure 24. Martingale values (log-scaled) (Top) compared with trip numbers (Middle) and change scores from the changefinder algorithm (Bottom) using the weekday samples.

4.4.3 Comparison with additional US cities - Washington, DC and San Francisco

In order to test the robustness and generalization of the proposed method, more US cities are included in the empirical work in addition to NYC. The largest bike share systems in the US other than NYC include Chicago, DC, and San Francisco. Both Chicago and NYC have substantial seasonal changes that impact bike trips and result in detected events while Washington, DC and

San Francisco have milder winter seasons than Chicago and NYC. Hence, the same procedure was applied to analyze DC and San Francisco data as was used for NYC, and the results are presented below. In all cities, the data sources and variable selection process were replicated with those used in NYC. The selected variables of three datasets are largely overlapping but have slight differences. A full list of variables used in the spatial interaction models of three cities can be found in Table B.1 of Appendix B.

Washington, DC

The Capital Bikes system in DC is the second-largest bike share system in the US, with more than 600 running stations and ten thousand daily trips as of the end of 2021. In comparison, the NYC system has 1000 stations and 50 thousand daily trips. However, bike share trips in DC result in a sparser OD matrix than in NYC with fewer consistent OD pairs. When choosing the same threshold of 0.85 used in NYC for the consistent OD pairs, only about 20 pairs meet the specified number of time periods. Those pairs consist of too few trips to represent the entire system. Therefore, a lower threshold is needed to satisfy two conditions: (1) the number of OD pairs are numerous enough to represent the system; and (2) non-zero flows between the OD pairs are numerous enough to detect events from. Empirically, setting the threshold at 0.7 resulted in more than 100 OD pairs and reasonable results. The distribution of the consistent OD pairs is shown in Figure 25, with consistent bike trips happening around the National Mall and the Tidal Basin, where many tourist sites are located. The remaining consistent OD pairs are located in the east and north parts of DC, which are mainly residential areas. Compared to the NYC system, popular trips in DC are

disconnected from each other, leaving a gap around central DC. This is surprising given the well-planned bike lanes in those areas[11].

The consistent bike trips around tourism destinations suggest the role of bike share for recreational purposes. This observation is further supported by the bike trip distribution by weekdays, which shows Saturday as the day with the most bike trips out of seven weekdays. This pattern is unique to the DC system, as the other two systems have a weekday from Monday to Friday as the busiest day of the week. As a result, the daily spatial interaction data frames for DC consist of weekends only e.g., the subset of $(Saturday, Sunday)$. Figure 26 shows the martingale values for the weekend samples in DC. Compared to the results from NYC, the peaks of the martingales are lower and appear as a cluster of peaks rather than single spikes. Four events are identified and interpreted in Table 10. Despite the possibility of false positive signals generated by early frames (as shown in Figure 21), the first event (A) detected in DC is validated using a training set that starts much earlier in late 2017 to minimize the chances of false positives. Event A involved an abnormal increase in trips on a Saturday and was possibly caused by a promotional event by the bike share operator, which was identified on the social media platform Twitter using the hashtag "bikeinbloom". This event coincided with the yearly cherry blossom season in DC, which attracts many visitors to the Tidal Basin. Subsequent events in DC are similar in type to those identified in the NYC system, such as holiday breaks, extreme weather, and the COVID-19 pandemic.

[11] https://ddot.dc.gov/page/bicycle-maps

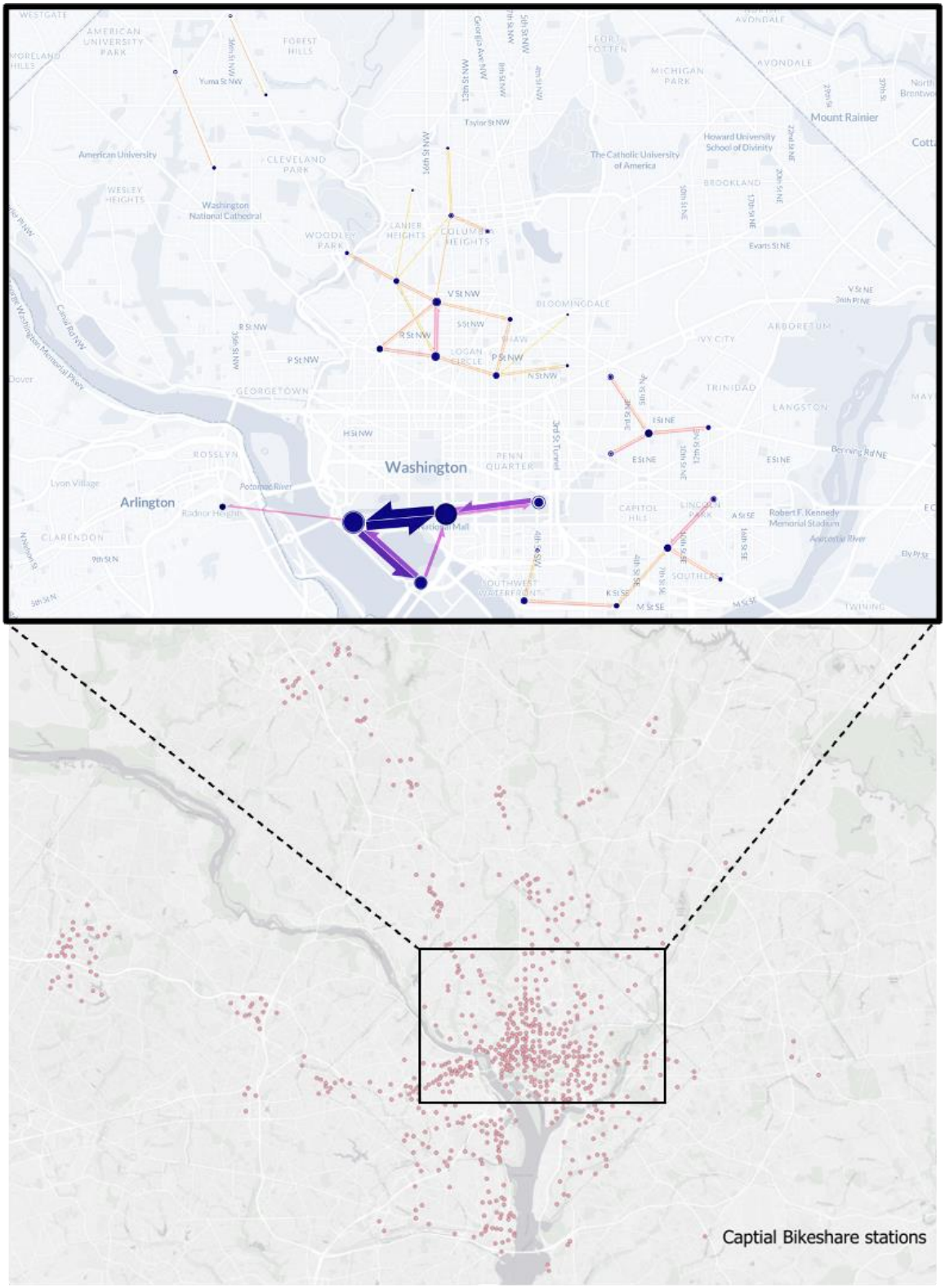

Figure 25. Bottom: Bike station distribution in Washington, DC Capital Bikeshare. Top: Illustrations of consistent OD flows in Washington, DC Capital Bikeshare with 70% time periods having positive flows

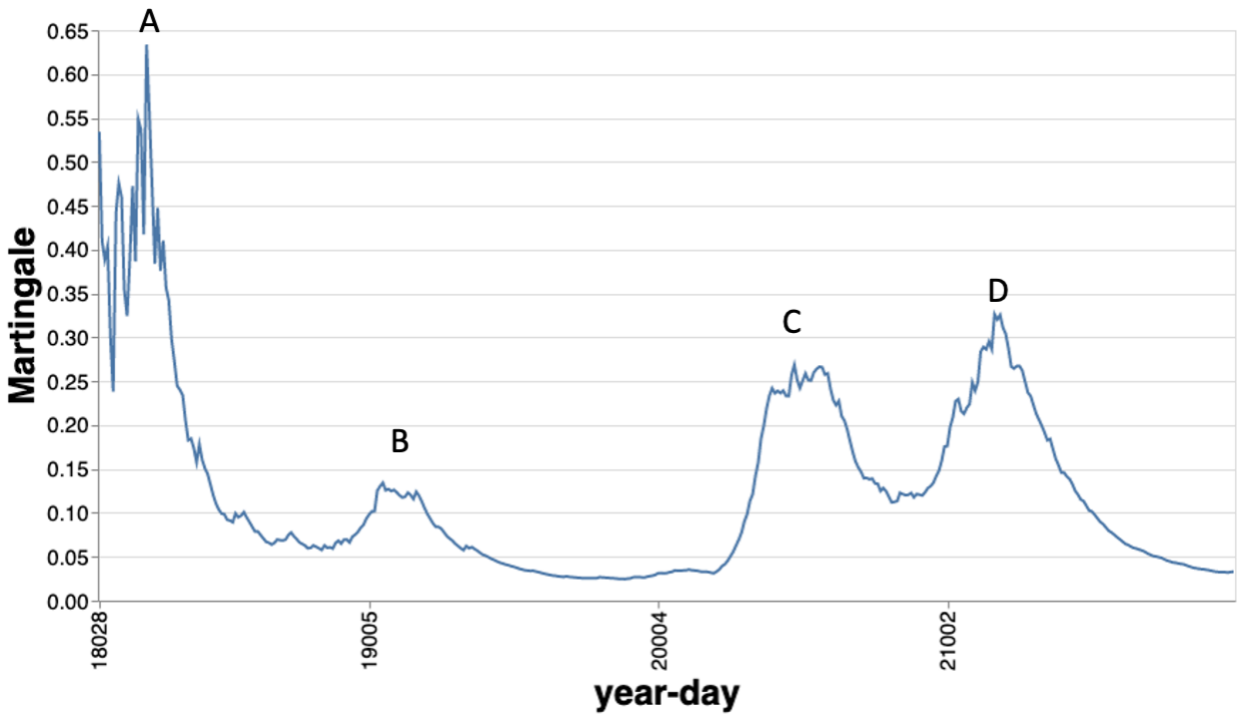

Figure 26. Martingale values and events of interest (marker A-D) from weekday samples in the Washington, DC system.

Table 10. Highlighted markers in the sequence of martingale values from the Washington, DC experiment and associated events, with occurrence time, cause of the event, and the delay compared to the occurrence time (if applicable).

Marker	Date, weekday	Cause of the event(s)	Delay (days)
A	03/31/18, Saturday	Special bike promotion events and cherry blossom	0
B	01/19/19, Saturday	Holiday breaks	16
C	05/17/20, Sunday	Covid-19 pandemic: lockdown started	18
D	02/28/21, Sunday	Holiday break and snow on 01/31/21	NA

San Francisco

The San Francisco Baywheels system operates in the great Bay Area, California, with bike stations distributed across three service areas: San Francisco downtown, East Bay including Berkeley and Oakland, and San Jose. The system has about 500 dock stations in total, with daily bike trips ranging from 4000 to 5000, approximately half of the trips in the DC system. The OD matrix for the San Francisco system is slightly sparser than Capital Bikes in DC, requiring an even lower threshold of 0.60 to collect more than 100 OD pairs with a higher percentage of positive flows. Unlike the systems in NYC and DC, the San Francisco system essentially consists of three separate service areas with very few trips crossing between them. Using a threshold of 0.60, consistent OD pairs (shown in Figure 27) mainly connect transportation hubs and residential areas, indicating that the function of the system is primarily for commuting trips.

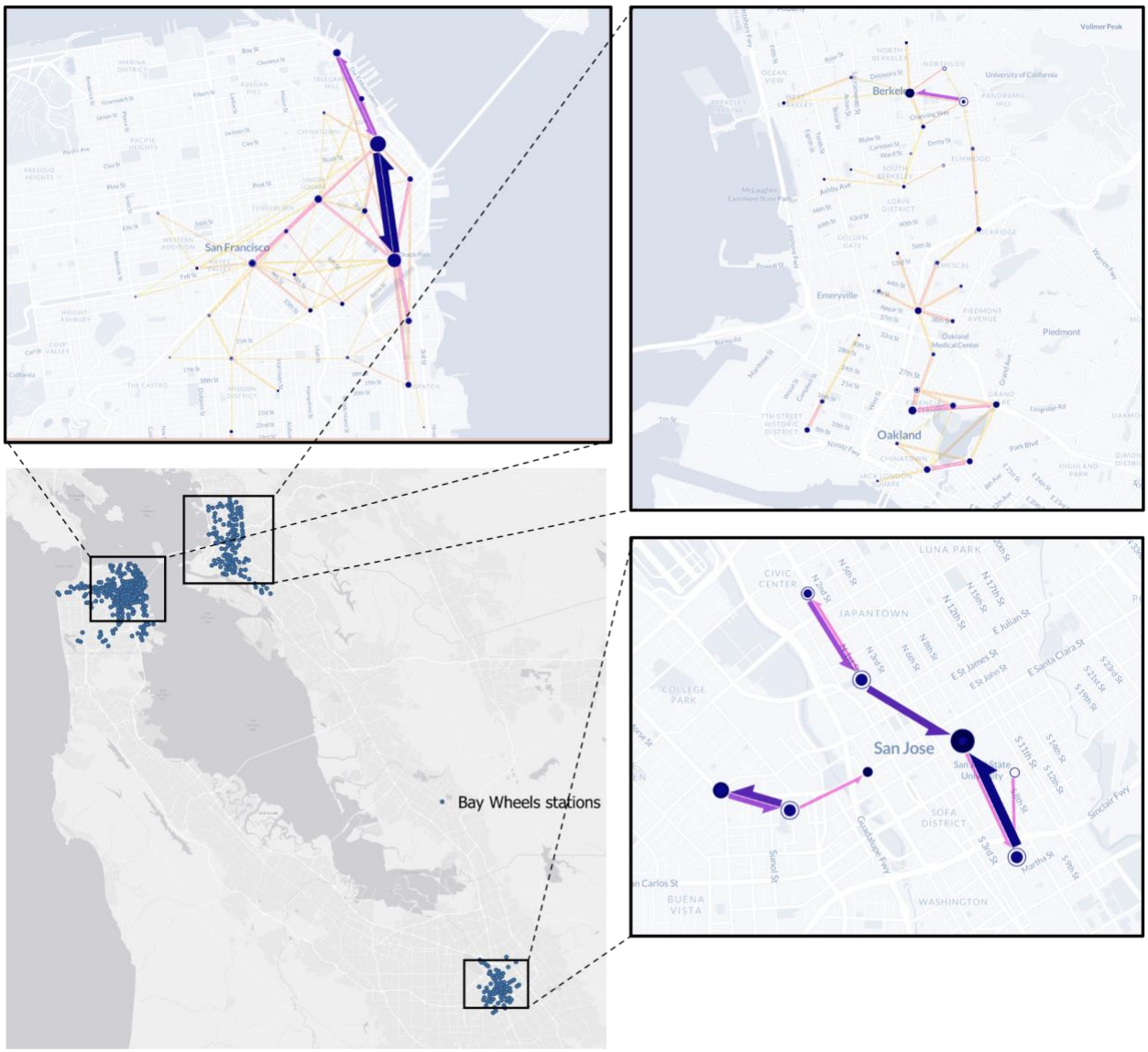

Figure 27. Bike station distribution in San Francisco Baywheels (Bottom-Left) and illustrations of consistent OD flows in the areas of downtown (Top-Left), East Bay (Top-Right), and San Jose (Bottom-Right) with 60% time periods having positive flows.

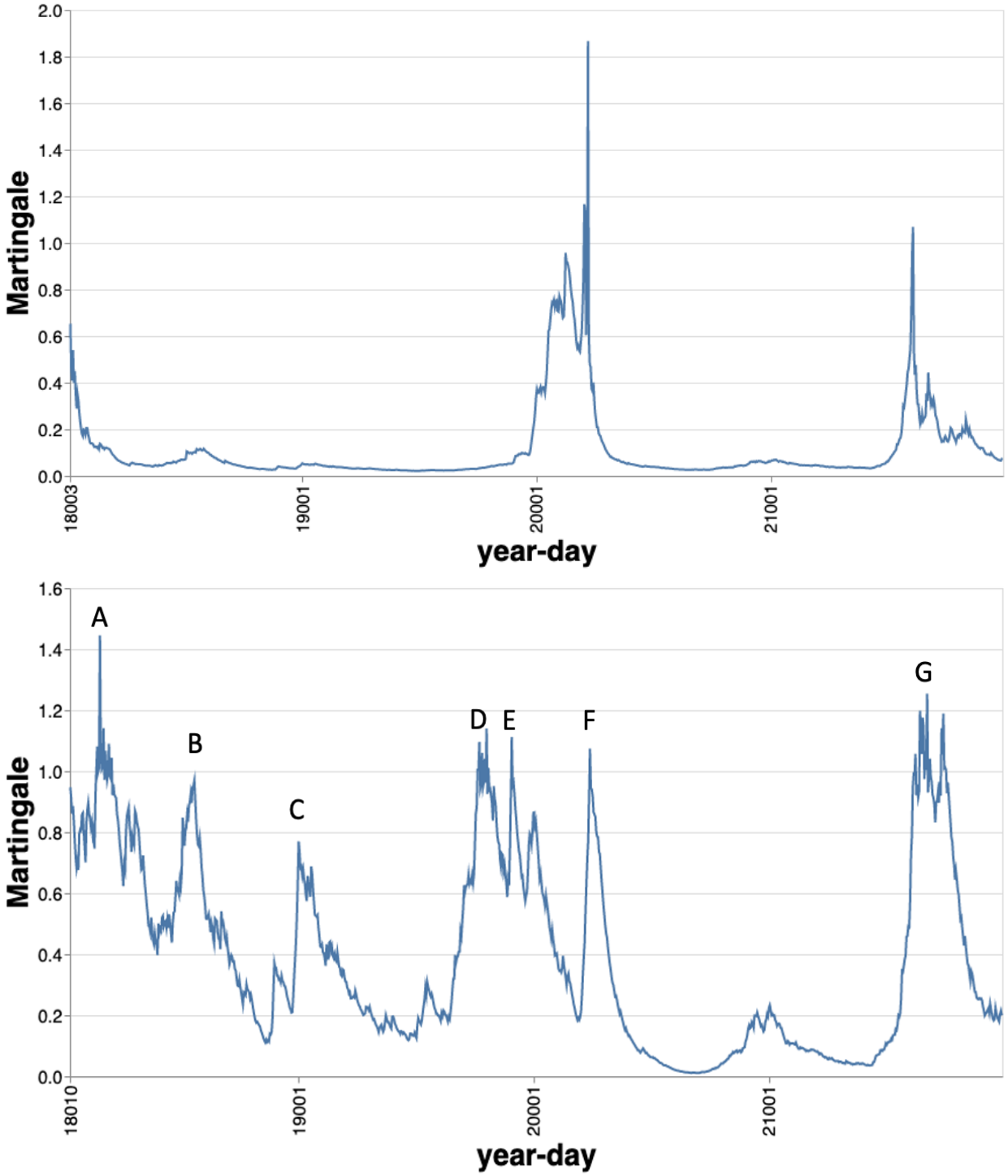

Figure 28. Martingale values and events of interest (marker A-G) from weekday samples in the San Francisco system. Top: values calculated from mixture martingales. Bottom: values calculated from power martingales (ϵ=0.92).

Table 11. Highlighted markers in the sequence of martingale values from the San Francisco experiment and associated events, with occurrence time, cause of the event, and the delay compared to the occurrence time (if applicable).

Marker	Date, weekday	Cause of the event(s)	Delay (days)
A	02/26/18, Friday	Cold day on Feb 19, 2018.	5
B	07/04/18, Wednesday	Decreased trips during July 4th	0
C	01/01/19, Tuesday	Holiday break: Christmas	6
D	09/02/19, Monday	Decreased trips during Labor Day	27
E	11/28/19, Monday	Holiday break: Thanksgiving	0
F	03/30/20, Thursday	Covid-19 pandemic: lockdown started	11
G	08/16/21, Monday	Covid-19 pandemic: increased trips after vaccination	NA

San Francisco's warmer weather results in fewer fluctuations in trip numbers throughout the year compared to the two east coast metropolitan areas. However, the milder weather and lower threshold for consistent origin-destination pairs create another challenge in event detection. When using the default parameter setting from the NYC system, San Francisco generates fewer and smaller peaks in the martingale values, as shown in the top of Figure 28. To address this, the empirical work for San Francisco also explored an alternative method for calculating the martingale values, specifically the randomized power martingales. This approach proves to increase the sensitivity of martingales towards detecting unusual events. The parameter ϵ ranges from 0 to 1 and can be used to adjust the sensitivity of the martingale. Higher values of ϵ tend to trigger higher martingale values and detect more events. Conversely, lower ϵ values generate less sensitive martingale sequences more similar to the mixture martingale. A value of 0.92 was employed, as was previously suggested in an example by Ho and Wechsler (2010), and the results

are shown in the bottom of Figure 28. Table 11 presents the interpretation of events, which includes three spikes in the latter half of 2018 and 2019 (Markers A, B, and C) that are not captured by the mixture martingales. The mid-2018 spike is caused by the break in the trend due to Independence Day on Wednesday, July 4th, which received much fewer trips compared to other weekdays. This event highlights the commuting function of the bike share system, as observed from the consistent OD pairs. Another event (D) was detected that is linked to Labor Day in 2019, showing a delayed effect. Additionally, two events in 2021 (Markers E and G) were observed, with the latter event being related to the increase in bike trips following the massive vaccination campaign during mid-2021. These events demonstrate the usefulness of the power martingales in capturing a wider range of events in the San Francisco bike share system.

4.5 Discussion

The flexibility of bike share systems allows them to update their infrastructures as needed to better accommodate demand and costs. For instance, Capital Bikes in DC deployed bike corrals and pop-up valets to temporarily increase station capacity at certain popular destinations during the Cherry Blossom festival when regular docks quickly filled up[12]. Thus, detecting abnormal bike trip demand is essential to the versatile operation strategy of bike share systems. Events that affect bike trip demand can be as long as the COVID-19 pandemic, or as short as thunderstorms lasting a few hours. Therefore, event detection methods are crucial towards maintaining the resilience of bike share systems. This study aims to explore a new method for event detection in the bike trip

[12] https://twitter.com/bikeshare

generating processes, which can assist bike share operators in managing demand and improving system performance.

This study adapted the martingale framework with spatial interaction data. The process of adaptation provided insights into the calculation and data transformation needed to effectively utilize spatial interaction data. The study also discusses the appropriate regression functions for optimal results while allowing flexibility for more advanced spatial interaction models beyond the gravity-type models used here. However, a major challenge in the adaptation process was the dimension reduction from the origin-destination matrix to a scalar value for the martingale. To address this, various reduction methods were tested, including mean, max, and quantiles, with the median quantile proving to be the most effective. However, the reduction function may undermine the framework's ability to detect local events that only pertain to a portion of the system network. The remaining adaptation process was straightforward, as the default parameter settings were found to work well with both simulated and empirical data from New York City. These insights gained from the adaptation process can be helpful for future applications and provide guidance for overcoming potential challenges.

To gain a better understanding of the methodology, a wide range of simulations were conducted using controlled spatial interaction data streams. Specifically, spatial interaction data frames generated from two sets of parameters were concatenated to simulate a stream containing an event that is associated with a model-based proxy for changing processes. The simulated spatial interaction data frames had the same total volumes, so no changes could be inferred from the number of trips. The results showed that for a single parameter change in magnitude larger than 10% were likely to trigger events using the proposed framework. The simulated data also revealed

a delay time after the actual changes. While the calculation of the p-value included some degree of randomness, empirical work has demonstrated that this randomness only resulted in subtle variations in the martingale values across different trials. These variations did not significantly impact the detection of events. Lastly, the magnitude and timing of changes seemed to have little correlation with the delay time with only minor improvements for increasingly larger parameter changes. However, this may have been due to the simulation design as in practice there was not typically a delay between detected events and potential ground truth events. Overall, these simulation results validated the adaptation of the martingale framework with spatial interaction data and highlighted features that are essential in the interpretation process, such as the extent of changes that can be reliably detected, recall rate, and delay time. However, it also highlighted that the framework has a potential limitation in detecting rapid events.

Experiments with spatial interaction data from the NYC system supported two purposes: (1) the effectiveness of the framework to detect real-world events; and (2) the types of events to be captured. Using the p-values definition that includes a random component within the calculation of martingale values means there is randomness in the event detection process as the algorithm produces slightly different martingale value sequences using the same input. Nevertheless, multiple trials of the method highlighted some events leading to system-wide impact on the travel behavior, including extreme weather, holiday breaks, and the COVID-19 pandemic. The martingale values were then compared with dynamic determinants and trip numbers from the same scale of time periods. A number of behavioral changes (Figure 23) or trip number drops (Figure 24) are captured as peaks in the martingale values. The former results showed that the proposed framework can detect events that are associated with model-based behavioral changes. And the latter results showed the framework can detect events that are not obvious in the trip number

fluctuation. Upon comparison between the proposed framework and an alternative event detection algorithm that uses trip numbers, it can be inferred that the latter method is more prone to generating false positive events by marking all fluctuations as highlighted events, while failing to detect actual events. All of these results support the need for the proposed method. However, some events may be missed by the martingale framework due to the aforementioned feature of the framework: a cluster of multiple rapid events and may be detected as a single peak (event). Evaluation with data from NYC also showed the complexity of real-world events that may vary widely in the length of time and the intensity of changes in the trip generation processes.

Event detection results with real-world data were also compared for three US cities with substantial bike share usage. Commonly detected events are caused by extreme weather, which results in both decreases and increases in trip numbers, holiday breaks during Thanksgiving, Christmas, and New Year, and the COVID-19 pandemic. Due to different social and geographical contexts among New York City, Washington DC, and San Francisco, this comparison identified unique sets of events for each city. For example, New York City is often affected by the extreme weather from snow, while DC has the seasonal cherry blossom festival. With less extreme weather, bike share usage from San Francisco is depicted as commuting-centered so that holidays happening within the weekdays can be detected as events. Differences in the trip number of the three systems also drives differences amongst the results. With fewer trip numbers, San Francisco data requires a more sensitive setting for the algorithm by using the power-form martingales, as previous literature on model tuning gives options for changing the way a martingale is calculated to adjust the sensitivity of event detection. Results here demonstrated the difference in the impact factors that may experience abnormal usage in a bike share system. Detected events may guide system operators in short-term operations and long-term planning. For example, during the start of the warmer months,

increased rebalancing operations may be needed to meet the sudden increasing trip demand in the NYC system. While in the San Francisco system, system expansion planning could involve infrastructure in recreation areas to increase its usage during the holiday breaks. However, the empirical work is still at an early stage as only a subset of peaks in the martingale values are identified and interpreted. In future work, more events may be identified and interpreted after further tuning the sensitivity of the framework.

Limitation

Real-world data are more complex than simulated data and the events often come with changes in different magnitudes and lengths of duration. Simulation design in this chapter aimed to approximate the setting with the real world but could benefit from more elaborate configurations. The simulation specified the distributions of origin and destination factors using a uniform distribution and the flow generation using a multinomial distribution based on the output of spatial interaction model. So, the variance of simulated data is determined by these distributions, which may not reflect reality. The different characteristics of the input data may affect the delay time and the sensitivity of event detection. This may possibly explain why simulation experiments yielded a mean delay of 10 frames but in the experiments with the real-world bike share data, the delay is often 0 or 1. Future work can further explore this issue.

Another limitation is the use of a consistent subset of origin-destination pairs in the system. A consistent set of origin-destination pairs is needed to avoid the noise of too many zero flows but this limits in representing the entire system and could possibly cause bias in the event detection. For example, local events caused by transport disruptions from constructions or sport events like marathons are not detected with the current model specification. Future work may integrate a

model specification that can better account for zero flows so that without compromising on the consistent OD pairs, the regression model may better address the entire system. Alternatively, demonstrated by F. Cai and E. Koutsoukos (2020) in their analysis of image input streams, the idea of using generative models to retain local differences could be explored by converting spatial interactions into a model that can generate pseudo OD flow matrices that approximate all previous input OD flow matrices. Then strangeness can be effectively calculated with the mathematical distance between the generated OD matrices and input matrix, where any local changes may increase the strangeness measure.

The proposed framework can fit any regression model which gives great capacity for extending the framework. In this study, a gravity-type spatial interaction model was used but has limitations in explaining the trip generating processes. Results of LASSO regression in the second study showed that the gravity-type models with all available variables before variable selection can explain up to 60% of deviance in the spatial interactions. The unexplained deviance produces significant residuals even during normal times and leaves less room for events. Future work may adopt advanced trip prediction models, such as LSTM or Transformer, to get a more precise explanation of the input spatial interaction data and thus increase the sensitivity of the event detection process (i.e., deviations from the learned model).

4.6 Conclusion

To meet the increasing need to understand the high-frequency changes in the bike share system that may cause trend breaks in the trip demand generation, this study introduced and evaluated an event detection method by combining the martingale framework with spatial interaction data and

models. As the first-ever application of the martingale framework in the spatial interaction domain, essential adaptations were deployed, including the selection of regression function in the strangeness metric and dimension reduction of the residual matrix. Simulations were designed to validate that changes from a model-based proxy for behavioral events using the spatial interaction model could be detected effectively with simple adaptations. Simulation results were also informative about the basic characteristics of the martingale framework in the event detection task of spatial interaction data streams. Characteristics included the recall rate of known events when the changes are subtle as well as the delay time that reflects how prompt an event could be identified in a continuous deployment. Empirical work in NYC, Washington DC, and San Francisco showed a variety of events can be detected, such as extreme weather changes, holiday breaks, and different pandemic phases. Furthermore, detected events can be associated with behavioral changes from dynamic determinants using the same model from the second study. Detected events from different cities also highlight the subtle differences in the role of the bike share systems. With the highest usage of bike share in the US, NYC is carrying both recreational and commute trips. DC has more concentration on recreational trips around the National Mall, while San Francisco bears more commuting trips that are stable during the weekdays except for public holidays. Options to tune the proposed framework for different sensitivities were also discussed as an important takeaway in future applications. Future work in updating the regression function, optimizing the adaptations, and experimenting with more datasets are suggested to continue exploring the proposed framework. Detected events may further inform the bike share operators or researchers toward a more robust event prediction model by including the variables that have not been considered.

Chapter 5: Conclusion

5.1 Review of dissertation

Ongoing global urbanization creates a demand for an in-depth understanding of spatial interactions that describe origin-destination flows within urban systems. Advances in information technology and IOTs have resulted in new forms of transportation, such as bike share systems. The infrastructures of bike share systems are often lightweight and more affordable to upgrade or expand than traditional transportation such as metro stations. Meanwhile, methods used for traditional transportation cannot address the need to understand and predict the dynamic demand within bike share systems. With the availability of geo-located and detailed time information, bike share trips are often used to study urban mobility, especially the high-frequency changes in human activities. Existing methods are limited for analyzing more modern systems. This dissertation identified three challenges and related research objectives for three essays in Chapter 2, 3, and 4. New methodological and analytical frameworks were proposed and evaluated with real-world bike share data to increase understanding of spatial interaction processes, especially high-frequency changes. Spatial interaction modeling not only served as the theoretical and conceptual framework throughout the dissertation, but also was practically expanded. Bike share trip records were collected from the New York City Citi Bike system used in Chapter 2, 3, and 4. Trip records from other systems with substantial usage such as Washington, DC and San Francisco were used in Chapter 4.

The first study of the dissertation (Chapter 2) proposed a hybrid approach to address the 'cold start' problem that predicts trip demand at new stations. Flow interpolation models based on Kriging statistics were proposed for the first time in the flow domain and compared to areal interpolation

models. Exploratory data analysis revealed that the majority of the bike stations in NYC were added at a later time, between 2015 and the present, revealing the prediction of 'cold start' trips at newly added stations as an important research question. A group of flow interpolation and spatial interaction methods were examined at those 'cold start' stations, including areal natural neighbor, ordinary kriging, regression kriging, and gravity-type spatial interaction model. Results showed that a regression kriging method that used a spatial interaction model as the regression model and used the residual from the regression model as the kriging interpolation input can adaptively balance between the local effect and the global trend. By selecting the best method for each 'cold start' station, a spatially aware strategy can be summarized as: 1) stations added within the range of system coverage can benefit more from spatial dependence from nearby stations, so interpolation methods are preferred; 2) stations added to the new areas beyond the existing spatial range of the system can hardly rely on the spatial dependence with no nearby stations, so spatial interaction models are preferred.

The second study of the dissertation (Chapter 3) focused on the changes of determinants of bike share trips from the spatial interaction models in the context of the COVID-19 pandemic. Bike share trip numbers in NYC experienced a decrease during the lockdown period but recovered with more trips in 2021 than the pre-pandemic reference in 2019. This study deployed a disaggregated comparative framework to discover the long-term and short-term dynamics of determinants in the bike trip generating process underlying the up and down of the trip numbers. This comparative framework calibrated spatial interaction model with important variables over time periods across either years or weeks. Yearly models implied the determinants of trips in 2021 were different from the 2019 levels while more dynamic evolution paths of determinants can be extracted from weekly models. The weekly dynamics of determinants changed according to the development of the

COVID-19 pandemic with different impacts on each determinant. For example, the relationship between bike trips and stations with more recreation opportunities almost recovered to the pre-pandemic level. However, the absolute value of the distance decay factor remained lower than pre-pandemic levels, suggesting a long-term impact of COVID-19 on the travel behaviors regarding travel distance by the end of 2021.

The third and the last study (Chapter 4) is motivated by the trend breaks in spatial interaction behavior that are related to specific events. The research objective for this chapter was conceptualized as event detection in the spatial interaction data stream. This study combined the martingale test with the spatial interaction data and models and implemented essential adaptations to the input of spatial interaction data streams. As a novel approach in the domain of spatial interactions, the framework was first evaluated with simulated data to measure its basic performance to provide basic intuition to apply to real-world datasets. Empirical work with bike share trips from multiple US cities was performed to compare results. Event detection results not only revealed common events, such as holiday breaks and the COVID-19 pandemic, but also differed in other types of events due to the discrepancy in the geography and functional role of the bike share systems. Selected results demonstrated that the NYC system is more sensitive to extreme weather; local events like cherry blossoms are highlighted in Washington, DC; San Francisco experiences fewer fluctuations from the weather, but is more sensitive to public holidays as the key function of the system is for daily commuting.

5.2 Significant contributions

A number of significant findings about bike share usage and methodological innovations for the spatial interaction modeling framework are significant contributions from this dissertation.

Significant contribution 1: Chapter 2 focused on the 'cold start' problem which is under-discussed in a dock-based bike share system. The method presented here to solve the problem advances flow interpolation with kriging methods that are novel in the flow domain. Ordinary kriging and regression kriging methods for flow interpolation were implemented by establishing a relationship of flows to/from all the other stations from nearby stations. The proposed kriging implementation gave comparative or better results when compared to existing methods like areal natural neighbor interpolation and spatial interaction models. Being able to capture the spatial dependence from spatial interaction at nearby stations, the proposed kriging models can benefit future work when spatial interactions for higher spatial resolution become available.

Significant contribution 2: Chapter 2 suggested a spatially aware strategy in finding the best method for each 'cold start' station, e.g., for the stations within the system coverage, interpolation methods could achieve better results than a spatial interaction model. For the stations added beyond the system coverage, spatial dependence from the closest stations in the system are too far for interpolation methods to rely on. Regression-based spatial interaction models from exogenous variables are more accurate. Out of the proposed kriging-based interpolation methods from Chapter 2, regression kriging has demonstrated its advantage as an adaptive approach that can provide decent prediction at both inner and outer stations in terms of the location of the added station.

Significant contribution 3: Bike share usage was heavily impacted by the COVID-19 pandemic, but the determinants of the trip generation processes are not fully examined for the time period after the lockdown and compared to the pre-pandemic routine. In the second study (Chapter 3), a disaggregated comparative framework is proposed to track the dynamic determinants of bike trips at long-term and short-term intervals. The short-term weekly dynamics revealed more detailed changes in the trip generation processes associated with the COVID-19 pandemic, suggesting the necessity of exhaustive modeling over a refined time resolution to match the scale of the event. Comparison between the long-term and short-term results also showed changes from a shorter time scale may be hidden under the long-term horizon. Variable selection and collinearity analysis for the model determinants are shown as necessary steps in the framework because including variables that are correlated to each other risks biased conclusions.

Significant contribution 4: Determinants of bike share trips in NYC have shown long-term behavioral changes despite the recovery in bike trip volume. A "new normal" pattern can be seen as evidence from Chapter 3 showed at least by the end of 2021, impacts of the COVID-19 pandemic were still steering the bike trip generation in multiple factors. For instance, work-from-home opportunities likely affected the association between trips and places with more jobs for an extended period before resuming the pre-pandemic routine relationship.

Significant contribution 5: The final study (Chapter 4) proposed an event detection framework combining martingale test with spatial interaction data. After reviewing the past studies on the martingale framework, essential adaptations are integrated to accommodate the framework for event detection within spatial interaction data streams. The simulated data with controlled changes

was used to evaluate the performance of the method. Both the adaptation process and simulation experiments helped prepare for empirical applications. The simplicity and scalability of the method are advantages.

Significant contribution 6: Empirical results from three bike share systems have demonstrated the generalization ability of the proposed framework and that similar events can be captured with a few adjustments in the model configuration. In addition, the discrepancy in the detected events also reflected the heterogeneity in the functional role of bike share systems in human mobility across different metropolitan areas. The consistent spatial interaction origin and destination pairs showed NYC as a well-developed system with participation from both commuting and recreational trips. DC results highlight the recreational trips around the National Mall while the San Francisco system mainly supports commuting trips from and to train stations.

5.3 Future work

At the time of the dissertation, docked bike share systems keep thriving and are contributing to transportation systems, along with the other micro-mobility options of electric-powered scooters and bikes. This dissertation plays an important role in helping researchers and urban planners understand and predict bike share usage as human mobility. The dissertation focuses only on bike share given that micro mobility data often comes from a limited proportion of population but could be applied with other sources of spatial interaction, such as with the general mobility dataset from SafeGraph (2020). Future work with less biased data would contribute to the understanding of urban mobility at a higher level of accuracy and significance.

The entire dissertation is conducted with open data from the bike share systems and with support on places of interest from the commercial data providers during the COVID-19 pandemic. However, urban mobility studies are still restrained by the availability of dynamic data, as the prevalent open data for population and employment are only updated yearly from the US Census. As population experienced changes in NYC during the COVID-19[13], spatial interaction models with fix population may produce different results from the model with actual dynamics of population. Another constraint for data quality is also reflected in the collinearity between variables constructed from different type of locations. Techniques to unpack the association between POIs or extra information on each bike trip would enhance the data quality in Chapter 3. One goal of the dissertation is to keep promoting the openness and timeliness of geospatial data. With better accessibility of high-frequency data, wider applications of the methods proposed in the dissertation can be achieved in future work.

Apart from the suggested future work discussed in each chapter, an integrated framework connecting the proposed methods for trip demand modeling of bike share trips could be developed in future studies. Specifically, underlying Chapter 2 and Chapter 4 are the pathways to clearing roadblocks that hinder the deployment of a spatial interaction prediction framework from bike share and general spatial interaction. In future work, a spatial interaction demand model could take the method from Chapter 2 to produce pseudo flows at the new stations in order to leverage the temporal dependence from the deep neural networks like LSTMs or Transformers. By using the

[13] https://www.thecity.nyc/2022/5/31/23145072/nycs-population-plummeted-during-peak-covid-and-its-still-likely-shrinking

method from Chapter 4, such a model can help to locate the events that can result in long-term or short-term impact on the spatial interaction processes and instruct the deployment and operation of such spatial interaction models by alarming the model failure to those events. Lastly, Chapter three's framework could enhance the explainability of this integrated framework, providing insights into dynamic human mobility patterns. Limitations from using the gravity model as the only spatial interaction model also urges further work using advanced spatial interaction models that carry better accuracy without sacrificing interpretation ability.

5.4 Concluding remarks

Bike share systems are an important and increasingly popular transportation mode, providing detailed time and location data that can shed new light on the dynamics of spatial interaction processes and the interconnectedness of different transportation modes within cities. This dissertation advances innovations in spatial interaction theory and tools that can be applied to a complex and dynamic transportation system. These methods and strategies could be reused and extended to another study area to meet the increasing demand for the development of a bike share system in different urban environments all around the world. Furthermore, proposed methods for high-frequency spatial interaction modeling are not restricted to the application scenario of a bike share system but could be extended to application scenarios like charging stations for electric vehicles, providing great potential for future validation and application of the methodologies proposed in the dissertation.

Appendices

Appendix A. Supplementary materials for Chapter 3

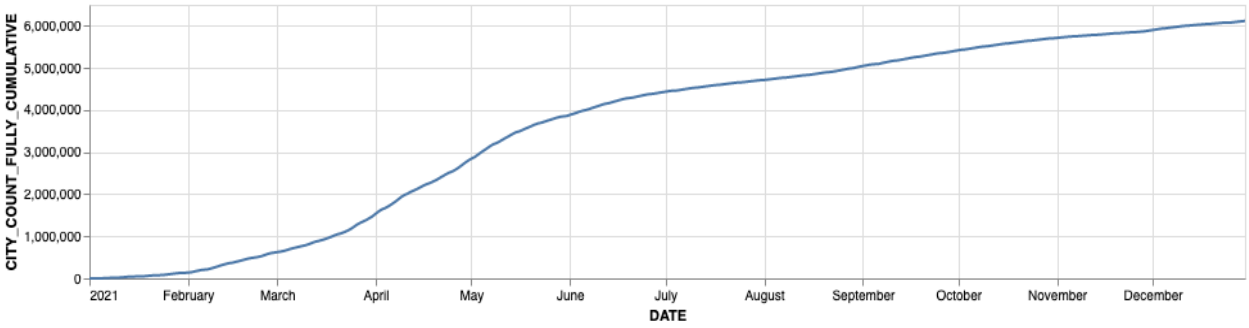

Figure A.1. Cumulative daily number of individuals fully vaccinated against COVID-19 in New York City in 2021

Appendix B. Supplementary materials for Chapter 4

Table B.1. Results of variable selection for three different cities using the method in section 3.3.4.

Cities	New York City	Washington, DC	San Francisco
Variable names	Distance cost	Distance cost	Distance cost
	Station capacity	Station capacity	Station capacity
	Recreation	Recreation	Recreation
	Employment	Employment	Subway access
		Population	Population
			Housing

Bibliography

Ai, Y., Li, Z., Gan, M., Zhang, Y., Yu, D., Chen, W., & Ju, Y. (2019). A deep learning approach on short-term spatiotemporal distribution forecasting of dockless bike-sharing system. *Neural Computing and Applications*, *31*(5), 1665–1677. https://doi.org/10.1007/s00521-018-3470-9

Alippi, C., & Roveri, M. (2006). An adaptive CUSUM-based test for signal change detection. *2006 IEEE International Symposium on Circuits and Systems*, 4 pp.-. https://doi.org/10.1109/ISCAS.2006.1693942

Barbour, N., Zhang, Y., & Mannering, F. (2019). A statistical analysis of bike sharing usage and its potential as an auto-trip substitute. *Journal of Transport & Health*, 12, 253–262. https://doi.org/10.1016/j.jth.2019.02.004

Bassolas, A., Barbosa-Filho, H., Dickinson, B., Dotiwalla, X., Eastham, P., Gallotti, R., Ghoshal, G., Gipson, B., Hazarie, S. A., Kautz, H., Kucuktunc, O., Lieber, A., Sadilek, A., & Ramasco, J. J. (2019). Hierarchical organization of urban mobility and its connection with city livability. *Nature Communications*, *10*(1), Article 1. https://doi.org/10.1038/s41467-019-12809-y

Bayraktar, H., & Turalioglu, F. S. (2005). A Kriging-based approach for locating a sampling site—In the assessment of air quality. *Stochastic Environmental Research and Risk Assessment*, 19(4), 301–305.

Bean, R., Pojani, D., & Corcoran, J. (2021). How does weather affect bikeshare use? A comparative analysis of forty cities across climate zones. *Journal of Transport Geography*, *95*, 103155. https://doi.org/10.1016/j.jtrangeo.2021.103155

Botella, P., Gora, P., Sosnowska, M., Karsznia, I., & Querol, S. C. (2021). Modelling mobility and visualizing people's flow patterns in rural areas for future infrastructure development as a good transnational land-governance practice (arXiv:2103.01777). *arXiv*. https://doi.org/10.48550/arXiv.2103.01777

Cai, F., & Koutsoukos, X. (2020). Real-time Out-of-distribution Detection in Learning-Enabled Cyber-Physical Systems. *2020 ACM/IEEE 11th International Conference on Cyber-Physical Systems (ICCPS)*, 174–183. https://doi.org/10.1109/ICCPS48487.2020.00024

Cai, L., Janowicz, K., Mai, G., Yan, B., & Zhu, R. (2020). Traffic transformer: Capturing the continuity and periodicity of time series for traffic forecasting. *Transactions in GIS*, *24*(3), 736–755. https://doi.org/10.1111/tgis.12644

Calafiore, A., Palmer, G., Comber, S., Arribas-Bel, D., & Singleton, A. (2021). A geographic data science framework for the functional and contextual analysis of human dynamics within global cities. *Computers, Environment and Urban Systems*, *85*, 101539. https://doi.org/10.1016/j.compenvurbsys.2020.101539

Campbell, K. B., & Brakewood, C. (2017). Sharing riders: How bikesharing impacts bus ridership in New York City. *Transportation Research Part A: Policy and Practice*, 100, 264–282. https://doi.org/10.1016/j.tra.2017.04.017

Chai, D., Wang, L., & Yang, Q. (2018). Bike flow prediction with multi-graph convolutional networks. *Proceedings of the 26th ACM SIGSPATIAL International Conference on Advances in Geographic Information Systems*, 397–400. https://doi.org/10.1145/3274895.3274896

Chawla, S., Zheng, Y., & Hu, J. (2012). Inferring the Root Cause in Road Traffic Anomalies. *2012 IEEE 12th International Conference on Data Mining*, 141–150.

https://doi.org/10.1109/ICDM.2012.104
Chen, L., Jakubowicz, J., Yang, D., Zhang, D., & Pan, G. (2017). Fine-Grained Urban Event Detection and Characterization Based on Tensor Cofactorization. *IEEE Transactions on Human-Machine Systems*, *47*(3), 380–391. https://doi.org/10.1109/THMS.2016.2596103
Chen, P.-C., Hsieh, H.-Y., Su, K.-W., Sigalingging, X. K., Chen, Y.-R., & Leu, J.-S. (2020). Predicting station level demand in a bike-sharing system using recurrent neural networks. *IET Intelligent Transport Systems*, *14*(6), 554–561. https://doi.org/10.1049/iet-its.2019.0007
Chen, X., & Jiang, H. (2022). Detecting the Demand Changes of Bike Sharing: A Bayesian Hierarchical Approach. *IEEE Transactions on Intelligent Transportation Systems*, *23*(5), 3969–3984. https://doi.org/10.1109/TITS.2020.3037791
Cheng, T., & Wicks, T. (2014). Event Detection using Twitter: A Spatio-Temporal Approach. *PLOS ONE*, *9*(6), e97807. https://doi.org/10.1371/journal.pone.0097807
Cheng, Z., Trepanier, M., & Sun, L. (2021). Real-time forecasting of metro origin-destination matrices with high-order weighted dynamic mode decomposition. *ArXiv:2101.00466 [Stat]*. http://arxiv.org/abs/2101.00466
Cherubin, G., Baldwin, A., & Griffin, J. (2018). Exchangeability martingales for selecting features in anomaly detection. *Proceedings of the Seventh Workshop on Conformal and Probabilistic Prediction and Applications*, 157–170. https://proceedings.mlr.press/v91/cherubin18a.html
Chu, K.-F., Lam, A. Y. S., & Li, V. O. K. (2020). Deep Multi-Scale Convolutional LSTM Network for Travel Demand and Origin-Destination Predictions. *IEEE Transactions on Intelligent Transportation Systems*, 21(8), 3219–3232. https://doi.org/10.1109/TITS.2019.2924971
Cressie, N. (1993). *Statistics for Spatial Data*. John Wiley & Sons.
Cui, Z., Ke, R., Pu, Z., & Wang, Y. (2019). Deep Bidirectional and Unidirectional LSTM Recurrent Neural Network for Network-wide Traffic Speed Prediction. *ArXiv:1801.02143 [Cs]*. http://arxiv.org/abs/1801.02143
Dang, T. T., Ngan, H. Y. T., & Liu, W. (2015). Distance-based k-nearest neighbors outlier detection method in large-scale traffic data. *2015 IEEE International Conference on Digital Signal Processing (DSP)*, 507–510. https://doi.org/10.1109/ICDSP.2015.7251924
Djenouri, Y., Belhadi, A., Lin, J. C.-W., Djenouri, D., & Cano, A. (2019). A Survey on Urban Traffic Anomalies Detection Algorithms. *IEEE Access*, *7*, 12192–12205. https://doi.org/10.1109/ACCESS.2019.2893124
Do, L. N. N., Vu, H. L., Vo, B. Q., Liu, Z., & Phung, D. (2019). An effective spatial-temporal attention based neural network for traffic flow prediction. *Transportation Research Part C: Emerging Technologies*, *108*, 12–28. https://doi.org/10.1016/j.trc.2019.09.008
Doraiswamy, H., Ferreira, N., Damoulas, T., Freire, J., & Silva, C. T. (2014). Using Topological Analysis to Support Event-Guided Exploration in Urban Data. *IEEE Transactions on Visualization and Computer Graphics*, *20*(12), 2634–2643. https://doi.org/10.1109/TVCG.2014.2346449
Dormann, C. F., Elith, J., Bacher, S., Buchmann, C., Carl, G., Carré, G., Marquéz, J. R. G., Gruber, B., Lafourcade, B., Leitão, P. J., Münkemüller, T., McClean, C., Osborne, P. E., Reineking, B., Schröder, B., Skidmore, A. K., Zurell, D., & Lautenbach, S. (2013). Collinearity: A review of methods to deal with it and a simulation study evaluating their performance. *Ecography*, *36*(1), 27–46. https://doi.org/10.1111/j.1600-0587.2012.07348.x
El-Assi, W., Salah Mahmoud, M., & Nurul Habib, K. (2017). Effects of built environment and

weather on bike sharing demand: A station level analysis of commercial bike sharing in Toronto. *Transportation*, 44(3), 589–613. https://doi.org/10.1007/s11116-015-9669-z

Emery, X. (2005). Simple and ordinary multigaussian kriging for estimating recoverable reserves. *Mathematical Geology*, 37(3), 295–319.

Eom, J. K., Park, M. S., Heo, T.-Y., & Huntsinger, L. F. (2006). Improving the Prediction of Annual Average Daily Traffic for Nonfreeway Facilities by Applying a Spatial Statistical Method. *Transportation Research Record*, 1968(1), 20–29. https://doi.org/10.1177/0361198106196800103

Eren, E., & Uz, V. E. (2020). A review on bike-sharing: The factors affecting bike-sharing demand. *Sustainable Cities and Society*, 54, 101882. https://doi.org/10.1016/j.scs.2019.101882

Faghih-Imani, A., Anowar, S., Miller, E. J., & Eluru, N. (2017). Hail a cab or ride a bike? A travel time comparison of taxi and bicycle-sharing systems in New York City. *Transportation Research Part A: Policy and Practice*, *101*, 11–21. https://doi.org/10.1016/j.tra.2017.05.006

Faghih-Imani, A., Hampshire, R., Marla, L., & Eluru, N. (2017). An empirical analysis of bike sharing usage and rebalancing: Evidence from Barcelona and Seville. *Transportation Research Part A: Policy and Practice*, *97*, 177–191. https://doi.org/10.1016/j.tra.2016.12.007

Farmer, C., & Oshan, T. (2017). Spatial Interactions. *Geographic Information Science & Technology Body of Knowledge*, 2017(Q4). https://doi.org/10.22224/gistbok/2017.4.5

Fedorova, V., Gammerman, A., Nouretdinov, I., & Vovk, V. (2012). Plug-in Martingales for Testing Exchangeability on-Line. *Proceedings of the 29th International Coference on International Conference on Machine Learning*, 923–930.

Fotheringham, A. S., & O'Kelly, M. E. (1989). *Spatial interaction models: Formulations and applications*. Kluwer Academic Publishers.

Gao, S., Liu, Y., Wang, Y., & Ma, X. (2013). Discovering Spatial Interaction Communities from Mobile Phone Data. *Transactions in GIS*, *17*(3), 463–481. https://doi.org/10.1111/tgis.12042

Geng, X., Li, Y., Wang, L., Zhang, L., Yang, Q., Ye, J., & Liu, Y. (2019). Spatiotemporal Multi-Graph Convolution Network for Ride-Hailing Demand Forecasting. *Proceedings of the AAAI Conference on Artificial Intelligence*, *33*(01), Article 01. https://doi.org/10.1609/aaai.v33i01.33013656

Guo, S., Lin, Y., Li, S., Chen, Z., & Wan, H. (2019). Deep Spatial–Temporal 3D Convolutional Neural Networks for Traffic Data Forecasting. *IEEE Transactions on Intelligent Transportation Systems*, *20*(10), 3913–3926. https://doi.org/10.1109/TITS.2019.2906365

Guo, Y., Zhou, J., Wu, Y., & Li, Z. (2017). Identifying the factors affecting bike-sharing usage and degree of satisfaction in Ningbo, China. *PLOS ONE*, 12(9), e0185100. https://doi.org/10.1371/journal.pone.0185100

Heydari, S., Konstantinoudis, G., & Behsoodi, A. W. (2021). Effect of the COVID-19 pandemic on bike-sharing demand and hire time: Evidence from Santander Cycles in London. *PLOS ONE*, *16*(12), e0260969. https://doi.org/10.1371/journal.pone.0260969

Ho, S.-S. (2005). A martingale framework for concept change detection in time-varying data streams. *Proceedings of the 22nd International Conference on Machine Learning*, 321–327. https://doi.org/10.1145/1102351.1102392

Ho, S.-S., Schofield, M., Sun, B., Snouffer, J., & Kirschner, J. (2019). A Martingale-Based Approach for Flight Behavior Anomaly Detection. *2019 20th IEEE International*

Conference on Mobile Data Management (MDM), 43–52. https://doi.org/10.1109/MDM.2019.00-75

Ho, S.-S., & Wechsler, H. (2010). A Martingale Framework for Detecting Changes in Data Streams by Testing Exchangeability. *IEEE Transactions on Pattern Analysis and Machine Intelligence*, *32*(12), 2113–2127. https://doi.org/10.1109/TPAMI.2010.48

Hoffimann, J., Zortea, M., de Carvalho, B., & Zadrozny, B. (2021). Geostatistical Learning: Challenges and Opportunities. *Frontiers in Applied Mathematics and Statistics*, *7*, 689393. https://doi.org/10.3389/fams.2021.689393

Hu, S., Chen, M., Jiang, Y., Sun, W., & Xiong, C. (2022). Examining factors associated with bike-and-ride (BnR) activities around metro stations in large-scale dockless bikesharing systems. *Journal of Transport Geography*, 98, 103271. https://doi.org/10.1016/j.jtrangeo.2021.103271

Jang, W., & Yao, X. (2011). Interpolating Spatial Interaction Data. *Transactions in GIS*, *15*(4), 541–555. https://doi.org/10.1111/j.1467-9671.2011.01273.x

Kang, Y., Gao, S., Liang, Y., Li, M., Rao, J., & Kruse, J. (2020). Multiscale dynamic human mobility flow dataset in the U.S. during the COVID-19 epidemic. *Scientific Data*, *7*(1), 390. https://doi.org/10.1038/s41597-020-00734-5

Kar, A., Le, H. T. K., & Miller, H. J. (2021). What Is Essential Travel? Socioeconomic Differences in Travel Demand in Columbus, Ohio, during the COVID-19 Lockdown. *Annals of the American Association of Geographers*, *0*(0), 1–24. https://doi.org/10.1080/24694452.2021.1956876

Karbalaie, A., Abtahi, F., & Sjöström, M. (2022). Event detection in surveillance videos: A review. *Multimedia Tools and Applications*, *81*(24), 35463–35501. https://doi.org/10.1007/s11042-021-11864-2

Ke, J., Qin, X., Yang, H., Zheng, Z., Zhu, Z., & Ye, J. (2019). Predicting origin-destination ride-sourcing demand with a spatio- temporal encoder-decoder residual multi-graph convolutional network. *ArXiv: 1910.09103*, 26. arXiv.

Khadaroo, J., & Seetanah, B. (2008). The role of transport infrastructure in international tourism development: A gravity model approach. *Tourism Management*, *29*(5), 831–840. https://doi.org/10.1016/j.tourman.2007.09.005

Kingan, R. J., & Westhuis, T. B. (2006). Robust Regression Methods for Traffic Growth Forecasting. *Transportation Research Record*, *1957*(1), 51–55. https://doi.org/10.1177/0361198106195700108

Kong, H., Jin, S. T., & Sui, D. Z. (2020). Deciphering the relationship between bikesharing and public transit: Modal substitution, integration, and complementation. *Transportation Research Part D: Transport and Environment*, *85*, 102392. https://doi.org/10.1016/j.trd.2020.102392

Krings, G., Calabrese, F., Ratti, C., & Blondel, V. D. (2009). Urban gravity: A model for inter-city telecommunication flows. *Journal of Statistical Mechanics: Theory and Experiment*, *2009*(07), L07003. https://doi.org/10.1088/1742-5468/2009/07/L07003

Kubaľák, S., Kalašová, A., & Hájnik, A. (2021). The Bike-Sharing System in Slovakia and the Impact of COVID-19 on This Shared Mobility Service in a Selected City. *Sustainability*, *13*(12), Article 12. https://doi.org/10.3390/su13126544

Lam, A., Schofield, M., & Ho, S.-S. (2019). Detecting (Unusual) Events in Urban Areas using Bike-Sharing Data. *Proceedings of the 3rd ACM SIGSPATIAL International Workshop on Analytics for Local Events and News*, 1–7. https://doi.org/10.1145/3356473.3365190

Le, N. D., & Zidek, J. V. (2006). *Statistical Analysis of Environmental Space-Time Processes*. Springer New York. https://doi.org/10.1007/0-387-35429-8

Lenormand, M., Bassolas, A., & Ramasco, J. J. (2016). Systematic comparison of trip distribution laws and models. *Journal of Transport Geography*, 51, 158–169. https://doi.org/10.1016/j.jtrangeo.2015.12.008

Li, A., & Axhausen, K. W. (2020). Short-term Traffic Demand Prediction using Graph Convolutional Neural Networks. *AGILE: GIScience Series*, *1*, 1–14. https://doi.org/10.5194/agile-giss-1-12-2020

Li, A., Zhao, P., Haitao, H., Mansourian, A., & Axhausen, K. W. (2021). How did micro-mobility change in response to COVID-19 pandemic? A case study based on spatial-temporal-semantic analytics. *Computers, Environment and Urban Systems*, 101703. https://doi.org/10.1016/j.compenvurbsys.2021.101703

Li, A., Zhao, P., Huang, Y., Gao, K., & Axhausen, K. W. (2020). An empirical analysis of dockless bike-sharing utilization and its explanatory factors: Case study from Shanghai, China. *Journal of Transport Geography*, *88*, 102828. https://doi.org/10.1016/j.jtrangeo.2020.102828

Li, Y., & Shuai, B. (2020). Origin and destination forecasting on dockless shared bicycle in a hybrid deep-learning algorithms. *Multimedia Tools and Applications*, 79(7), 5269–5280. https://doi.org/10.1007/s11042-018-6374-x

Lin, Z., Feng, J., Lu, Z., Li, Y., & Jin, D. (2019). DeepSTN+: Context-Aware Spatial-Temporal Neural Network for Crowd Flow Prediction in Metropolis. *Proceedings of the AAAI Conference on Artificial Intelligence*, *33*(01), Article 01. https://doi.org/10.1609/aaai.v33i01.33011020

Liu, J., Sun, L., Chen, W., & Xiong, H. (2016). Rebalancing Bike Sharing Systems: A Multi-source Data Smart Optimization. *Proceedings of the 22nd ACM SIGKDD International Conference on Knowledge Discovery and Data Mining*, 1005–1014. https://doi.org/10.1145/2939672.2939776

Liu, L., Qiu, Z., Li, G., Wang, Q., Ouyang, W., & Lin, L. (2019). Contextualized Spatial-Temporal Network for Taxi Origin-Destination Demand Prediction. *ArXiv:1905.06335 [Cs, Stat]*. http://arxiv.org/abs/1905.06335

Liu, X., Kang, C., Gong, L., & Liu, Y. (2016). Incorporating spatial interaction patterns in classifying and understanding urban land use. *International Journal of Geographical Information Science*, 30(2), 334–350. https://doi.org/10.1080/13658816.2015.1086923

Liu, Z., & Oshan, T. (2022). Comparing spatial interaction models and flow interpolation techniques for predicting "cold start" bike-share trip demand. *Transactions in GIS*, *26*(4), 2081–2098. https://doi.org/10.1111/tgis.12933

Lu, M., Hsu, S.-C., Chen, P.-C., & Lee, W.-Y. (2018). Improving the sustainability of integrated transportation system with bike-sharing: A spatial agent-based approach. *Sustainable Cities and Society*, *41*, 44–51. https://doi.org/10.1016/j.scs.2018.05.023

Ma, X., Zhang, J., Du, B., Ding, C., & Sun, L. (2019). Parallel Architecture of Convolutional Bi-Directional LSTM Neural Networks for Network-Wide Metro Ridership Prediction. *IEEE Transactions on Intelligent Transportation Systems*, *20*(6), 2278–2288. https://doi.org/10.1109/TITS.2018.2867042

Maas, S., Nikolaou, P., Attard, M., & Dimitriou, L. (2021). Spatial and temporal analysis of shared bicycle use in Limassol, Cyprus. *Journal of Transport Geography*, *93*, 103049. https://doi.org/10.1016/j.jtrangeo.2021.103049

Marrocu, E., & Paci, R. (2013). Different tourists to different destinations. Evidence from spatial interaction models. *Tourism Management*, *39*, 71–83. https://doi.org/10.1016/j.tourman.2012.10.009

Meyer, M., Farei-Campagna, T., Pasztor, A., Forno, R. D., Gsell, T., Faillettaz, J., Vieli, A., Weber, S., Beutel, J., & Thiele, L. (2019). Event-triggered natural hazard monitoring with convolutional neural networks on the edge. *Proceedings of the 18th International Conference on Information Processing in Sensor Networks*, 73–84. https://doi.org/10.1145/3302506.3310390

Miranda, F., Doraiswamy, H., Lage, M., Zhao, K., Goncalves, B., Wilson, L., Hsieh, M., & Silva, C. T. (2017). Urban Pulse: Capturing the Rhythm of Cities. *IEEE Transactions on Visualization and Computer Graphics*, *23*(1), 791–800. https://doi.org/10.1109/TVCG.2016.2598585

Mitas, L., & Mitasova, H. (1999). Spatial interpolation. *Geographical Information Systems: Principles, Techniques, Management and Applications*, 1(2).

Noland, R. B., Smart, M. J., & Guo, Z. (2016). Bikeshare trip generation in New York City. *Transportation Research Part A: Policy and Practice*, *94*, 164–181. https://doi.org/10.1016/j.tra.2016.08.030

Noland, R. B., Smart, M. J., & Guo, Z. (2019). Bikesharing Trip Patterns in New York City: Associations with Land Use, Subways, and Bicycle Lanes. *International Journal of Sustainable Transportation*, *13*(9), 664–674. https://doi.org/10.1080/15568318.2018.1501520

NYC Department of Transportation. (2019). New York City Mobility Report. *NYC Department of Transportation*.

Oja, P., Titze, S., Bauman, A., Geus, B. de, Krenn, P., Reger-Nash, B., & Kohlberger, T. (2011). Health benefits of cycling: A systematic review. *Scandinavian Journal of Medicine & Science in Sports*, *21*(4), 496–509. https://doi.org/10.1111/j.1600-0838.2011.01299.x

Oshan, T. M. (2016). A primer for working with the Spatial Interaction modeling (SpInt) module in the python spatial analysis library (PySAL). *REGION*, *3*(2), 11. https://doi.org/10.18335/region.v3i2.175

Oshan, T. M. (2020). Potential and Pitfalls of Big Transport Data for Spatial Interaction Models of Urban Mobility. *The Professional Geographer*, *72*(4), 468–480. https://doi.org/10.1080/00330124.2020.1787180

Oshan, T. M. (2021). The spatial structure debate in spatial interaction modeling: 50 years on. *Progress in Human Geography*, *45*(5), 925–950. https://doi.org/10.1177/0309132520968134

Otero, I., Nieuwenhuijsen, M. J., & Rojas-Rueda, D. (2018). Health impacts of bike sharing systems in Europe. *Environment International*, *115*, 387–394. https://doi.org/10.1016/j.envint.2018.04.014

Padmanabhan, V., Penmetsa, P., Li, X., Dhondia, F., Dhondia, S., & Parrish, A. (2021). COVID-19 effects on shared-biking in New York, Boston, and Chicago. *Transportation Research Interdisciplinary Perspectives*, *9*, 100282. https://doi.org/10.1016/j.trip.2020.100282

Pan, L., Cai, Q., Fang, Z., Tang, P., & Huang, L. (2019). A Deep Reinforcement Learning Framework for Rebalancing Dockless Bike Sharing Systems. *Proceedings of the AAAI Conference on Artificial Intelligence*, *33*, 1393–1400. https://doi.org/10.1609/aaai.v33i01.33011393

Pan, Y., Darzi, A., Kabiri, A., Zhao, G., Luo, W., Xiong, C., & Zhang, L. (2020). Quantifying

human mobility behaviour changes during the COVID-19 outbreak in the United States. *Scientific Reports*, *10*(1), Article 1. https://doi.org/10.1038/s41598-020-77751-2

Pan, Z., Zhang, W., Liang, Y., Zhang, W., Yu, Y., Zhang, J., & Zheng, Y. (2020). Spatio-Temporal Meta Learning for Urban Traffic Prediction. *IEEE Transactions on Knowledge and Data Engineering*, 1–1. https://doi.org/10.1109/TKDE.2020.2995855

Pang, L. X., Chawla, S., Liu, W., & Zheng, Y. (2011). On Mining Anomalous Patterns in Road Traffic Streams. In J. Tang, I. King, L. Chen, & J. Wang (Eds.), *Advanced Data Mining and Applications* (pp. 237–251). Springer. https://doi.org/10.1007/978-3-642-25856-5_18

Papadopoulos, H., Proedrou, K., Vovk, V., & Gammerman, A. (2002). Inductive Confidence Machines for Regression. In T. Elomaa, H. Mannila, & H. Toivonen (Eds.), *Machine Learning: ECML 2002* (pp. 345–356). Springer. https://doi.org/10.1007/3-540-36755-1_29

Pareja, A., Domeniconi, G., Chen, J., Ma, T., Suzumura, T., Kanezashi, H., Kaler, T., Schardl, T., & Leiserson, C. (2020). EvolveGCN: Evolving Graph Convolutional Networks for Dynamic Graphs. *Proceedings of the AAAI Conference on Artificial Intelligence*, *34*(04), 5363–5370. https://doi.org/10.1609/aaai.v34i04.5984

Pittino, F., Puggl, M., Moldaschl, T., & Hirschl, C. (2020). Automatic Anomaly Detection on In-Production Manufacturing Machines Using Statistical Learning Methods. *Sensors*, *20*(8), Article 8. https://doi.org/10.3390/s20082344

Pourebrahim, N., Sultana, S., Thill, J.-C., & Mohanty, S. (2018). Enhancing Trip Distribution Prediction with Twitter Data: Comparison of Neural Network and Gravity Models. *Proceedings of the 2nd ACM SIGSPATIAL International Workshop on AI for Geographic Knowledge Discovery*, 5–8. https://doi.org/10.1145/3281548.3281555

Qu, L., Li, W., Li, W., Ma, D., & Wang, Y. (2019). Daily long-term traffic flow forecasting based on a deep neural network. *Expert Systems with Applications*, *121*, 304–312. https://doi.org/10.1016/j.eswa.2018.12.031

Ranco, G., Aleksovski, D., Caldarelli, G., Grčar, M., & Mozetič, I. (2015). The Effects of Twitter Sentiment on Stock Price Returns. *PLOS ONE*, *10*(9), e0138441. https://doi.org/10.1371/journal.pone.0138441

Ren, Y., Chen, H., Han, Y., Cheng, T., Zhang, Y., & Chen, G. (2019). A hybrid integrated deep learning model for the prediction of citywide spatio-temporal flow volumes. *International Journal of Geographical Information Science*, 1–22. https://doi.org/10.1080/13658816.2019.1652303

Ren, Y., Cheng, T., & Zhang, Y. (2019). Deep spatio-temporal residual neural networks for road-network-based data modeling. *International Journal of Geographical Information Science*, *33*(9), 1894–1912. https://doi.org/10.1080/13658816.2019.1599895

Ross-Perez, A., Walton, N., & Pinto, N. (2022). Identifying trip purpose from a dockless bike-sharing system in Manchester. *Journal of Transport Geography*, *99*, 103293. https://doi.org/10.1016/j.jtrangeo.2022.103293

Saberi, M., Ghamami, M., Gu, Y., Shojaei, M. H. (Sam), & Fishman, E. (2018). Understanding the impacts of a public transit disruption on bicycle sharing mobility patterns: A case of Tube strike in London. *Journal of Transport Geography*, *66*, 154–166. https://doi.org/10.1016/j.jtrangeo.2017.11.018

SafeGraph. (2020). The Impact of Coronavirus (COVID-19) on Foot Traffic [Data set]. *In U.S. Consumer Activity During COVID-19 Pandemic*.

Schimohr, K., & Scheiner, J. (2021). Spatial and temporal analysis of bike-sharing use in Cologne

taking into account a public transit disruption. *Journal of Transport Geography*, *92*, 103017. https://doi.org/10.1016/j.jtrangeo.2021.103017

Schuessler, N., & Axhausen, K. W. (2009). Processing Raw Data from Global Positioning Systems without Additional Information. *Transportation Research Record, 2105*(1), 28–36. https://doi.org/10.3141/2105-04

Sevtsuk, A., Hudson, A., Halpern, D., Basu, R., Ng, K., & Jong, J. de. (2021). The impact of COVID-19 on trips to urban amenities: Examining travel behavior changes in Somerville, MA. *PLOS ONE*, *16*(9), e0252794. https://doi.org/10.1371/journal.pone.0252794

Shaw, S.-L., & Sui, D. Z. (Eds.). (2018). *Human Dynamics Research in Smart and Connected Communities*. Springer International Publishing. https://doi.org/10.1007/978-3-319-73247-3

Shen, Y., Zhang, X., & Zhao, J. (2018). Understanding the usage of dockless bike sharing in Singapore. *International Journal of Sustainable Transportation, 12*(9), 686–700. https://doi.org/10.1080/15568318.2018.1429696

Shleifer, S., McCreery, C., & Chitters, V. (2019). Incrementally Improving Graph WaveNet Performance on Traffic Prediction. *ArXiv:1912.07390 [Cs, Eess]*. http://arxiv.org/abs/1912.07390

Si, H., Shi, J., Wu, G., Chen, J., & Zhao, X. (2019). Mapping the bike sharing research published from 2010 to 2018: A scientometric review. *Journal of Cleaner Production, 213*, 415–427. https://doi.org/10.1016/j.jclepro.2018.12.157

Sibson, R. (1981). A Brief Description of Natural Neighbor Interpolation. In *Interpreting Multivariate Data* (p. pp 21-36). Chichester: John Wiley.

Signorino, G., Pasetto, R., Gatto, E., Mucciardi, M., La Rocca, M., & Mudu, P. (2011). Gravity models to classify commuting vs. Resident workers. An application to the analysis of residential risk in a contaminated area. *International Journal of Health Geographics, 10*(1), 11. https://doi.org/10.1186/1476-072X-10-11

Šimbera, J., & Aasa, A. (2019). Areal interpolation of spatial interaction data. *Adjunct Proceedings of the 15th International Conference on Location Based Services (LBS 2019)*, 8. https://doi.org/10.34726/lbs2019.61

Stopher, P., Jiang, Q., & FitzGerald, C. (2005). Processing GPS Data from Travel Surveys. *2nd International Colloqium on the Behavioural Foundations of Integrated Land-Use and Transportation Models: Frameworks, Models and Applications*, Toronto, 17.

Su, X., & Khoshgoftaar, T. M. (2009). A Survey of Collaborative Filtering Techniques. *Advances in Artificial Intelligence, 2009*, e421425. https://doi.org/10.1155/2009/421425

Sun, J., Zhang, J., Li, Q., Yi, X., Liang, Y., & Zheng, Y. (2020). Predicting Citywide Crowd Flows in Irregular Regions Using Multi-View Graph Convolutional Networks. *IEEE Transactions on Knowledge and Data Engineering*, 1–1. https://doi.org/10.1109/TKDE.2020.3008774

Takeuchi, J., & Yamanishi, K. (2006). A unifying framework for detecting outliers and change points from time series. *IEEE Transactions on Knowledge and Data Engineering*, *18*(4), 482–492. https://doi.org/10.1109/TKDE.2006.1599387

Teixeira, J. F., & Lopes, M. (2020). The link between bike sharing and subway use during the COVID-19 pandemic: The case-study of New York's Citi Bike. *Transportation Research Interdisciplinary Perspectives*, *6*, 100166. https://doi.org/10.1016/j.trip.2020.100166

Tobler, W. R. (1970). A Computer Movie Simulating Urban Growth in the Detroit Region. *Economic Geography, 46*(sup1), 234–240. https://doi.org/10.2307/143141

Ukil, A., Bandyoapdhyay, S., Puri, C., & Pal, A. (2016). IoT Healthcare Analytics: The Importance of Anomaly Detection. *2016 IEEE 30th International Conference on Advanced Information Networking and Applications (AINA)*, 994–997. https://doi.org/10.1109/AINA.2016.158

United Nations, Department of Economic and Social Affairs, Population Division. (2019). *World Urbanization Prospects: The 2018 Revision (ST/ESA/SER.A/420)*. United Nations. https://esa.un.org/unpd/wup

Vioulès, M. J., Moulahi, B., Azé, J., & Bringay, S. (2018). Detection of suicide-related posts in Twitter data streams. *IBM Journal of Research and Development*, *62*(1), 7:1-7:12. https://doi.org/10.1147/JRD.2017.2768678

Volkovs, M., Yu, G., & Poutanen, T. (2017). DropoutNet: Addressing Cold Start in Recommender Systems. *Advances in Neural Information Processing Systems*, *10*.

Vovk, V., Nouretdinov, I., & Gammerman, A. (2003). Testing exchangeability on-line. *Proceedings of the Twentieth International Conference on International Conference on Machine Learning*, 768–775.

Wang, H., & Noland, R. B. (2021). Bikeshare and subway ridership changes during the COVID-19 pandemic in New York City. *Transport Policy*, *106*, 262–270. https://doi.org/10.1016/j.tranpol.2021.04.004

Wang, M., & Zhou, X. (2017). Bike-sharing systems and congestion: Evidence from US cities. *Journal of Transport Geography*, *65*, 147–154. https://doi.org/10.1016/j.jtrangeo.2017.10.022

Wang, X., Cheng, Z., Trépanier, M., & Sun, L. (2021). Modeling bike-sharing demand using a regression model with spatially varying coefficients. *Journal of Transport Geography*, *93*, 103059. https://doi.org/10.1016/j.jtrangeo.2021.103059

Wang, X., & Kockelman, K. M. (2009). Forecasting Network Data: Spatial Interpolation of Traffic Counts from Texas Data. *Transportation Research Record*, *2105*(1), 100–108. https://doi.org/10.3141/2105-13

Wang, Y., Yin, H., Chen, H., Wo, T., Xu, J., & Zheng, K. (2019). Origin-Destination Matrix Prediction via Graph Convolution: A New Perspective of Passenger Demand Modeling. *Proceedings of the 25th ACM SIGKDD International Conference on Knowledge Discovery & Data Mining*, 1227–1235. https://doi.org/10.1145/3292500.3330877

van Wee, B., & Witlox, F. (2021). COVID-19 and its long-term effects on activity participation and travel behaviour: A multiperspective view. *Journal of Transport Geography*, *95*, 103144. https://doi.org/10.1016/j.jtrangeo.2021.103144

Werner, P. A., Kęsik-Brodacka, M., Nowak, K., Olszewski, R., Kaleta, M., & Liebers, D. T. (2022). Modeling the Spatial and Temporal Spread of COVID-19 in Poland Based on a Spatial Interaction Model. *ISPRS International Journal of Geo-Information*, *11*(3), 195. https://doi.org/10.3390/ijgi11030195

Wilson, A. G. (1971). A family of spatial interaction models and associated developments", Environment and Planning. *Environment and Planning*, *3*, 1–32.

Wu, Y., Zhuang, D., Labbe, A., & Sun, L. (2020). Inductive Graph Neural Networks for Spatiotemporal Kriging. *ArXiv:2006.07527 [Cs, Stat]*. http://arxiv.org/abs/2006.07527

Xie, Y., Zhou, X., & Shekhar, S. (2020). Discovering Interesting Subpaths with Statistical Significance from Spatiotemporal Datasets. *ACM Transactions on Intelligent Systems and Technology*, *11*(1), 1–24. https://doi.org/10.1145/3354189

Xiong, X., Ozbay, K., Jin, L., & Feng, C. (2020). Dynamic Origin-Destination Matrix Prediction

with Line Graph Neural Networks and Kalman Filter. *ArXiv:1905.00406 [Cs, Stat]*. http://arxiv.org/abs/1905.00406

Yang, B., Sun, S., Li, J., Lin, X., & Tian, Y. (2019). Traffic flow prediction using LSTM with feature enhancement. *Neurocomputing*, *332*, 320–327. https://doi.org/10.1016/j.neucom.2018.12.016

Yang, H., Zhang, Y., Zhong, L., Zhang, X., & Ling, Z. (2020). Exploring spatial variation of bike sharing trip production and attraction: A study based on Chicago's Divvy system. *Applied Geography*, *115*, 102130. https://doi.org/10.1016/j.apgeog.2019.102130

Yang, Y., Heppenstall, A., Turner, A., & Comber, A. (2019). A spatiotemporal and graph-based analysis of dockless bike sharing patterns to understand urban flows over the last mile. *Computers, Environment and Urban Systems*, *77*, 101361. https://doi.org/10.1016/j.compenvurbsys.2019.101361

Yang, Y., Heppenstall, A., Turner, A., & Comber, A. (2020). Using graph structural information about flows to enhance short-term demand prediction in bike-sharing systems. *Computers, Environment and Urban Systems*, *83*, 101521. https://doi.org/10.1016/j.compenvurbsys.2020.101521

Yang, Y., Beecham, R., Heppenstall, A., Turner, A., & Comber, A. (2022). Understanding the impacts of public transit disruptions on bikeshare schemes and cycling behaviours using spatiotemporal and graph-based analysis: A case study of four London Tube strikes. *Journal of Transport Geography*, *98*, 103255. https://doi.org/10.1016/j.jtrangeo.2021.103255

Yang, Y., Zha, K., Chen, Y., Wang, H., & Katabi, D. (2021). Delving into Deep Imbalanced Regression. *Proceedings of the 38th International Conference on Machine Learning*, 11842–11851. https://proceedings.mlr.press/v139/yang21m.html

Yao, X., Zhu, D., Gao, Y., Wu, L., Zhang, P., & Liu, Y. (2018). A Stepwise Spatio-Temporal Flow Clustering Method for Discovering Mobility Trends. *IEEE Access*, *6*, 44666–44675. https://doi.org/10.1109/ACCESS.2018.2864662

Younes, H., Nasri, A., Baiocchi, G., & Zhang, L. (2019). How transit service closures influence bikesharing demand; lessons learned from SafeTrack project in Washington, D.C. metropolitan area. *Journal of Transport Geography*, *76*, 83–92. https://doi.org/10.1016/j.jtrangeo.2019.03.004

Younes, H., Zou, Z., Wu, J., & Baiocchi, G. (2020). Comparing the Temporal Determinants of Dockless Scooter-share and Station-based Bike-share in Washington, D.C. *Transportation Research Part A: Policy and Practice*, *134*, 308–320. https://doi.org/10.1016/j.tra.2020.02.021

Zacharias, J., & Meng, S. (2021). Environmental correlates of dock-less shared bicycle trip origins and destinations. *Journal of Transport Geography*, *92*, 103013. https://doi.org/10.1016/j.jtrangeo.2021.103013

Zhang, L., Cheng, J., & Jin, C. (2019). Spatial Interaction Modeling of OD Flow Data: Comparing Geographically Weighted Negative Binomial Regression (GWNBR) and OLS (GWOLSR). *ISPRS International Journal of Geo-Information*, *8*(5), Article 5. https://doi.org/10.3390/ijgi8050220

Zhang, Y., Cheng, T., Ren, Y., & Xie, K. (2020). A novel residual graph convolution deep learning model for short-term network-based traffic forecasting. *International Journal of Geographical Information Science*, *34*(5), 969–995. https://doi.org/10.1080/13658816.2019.1697879

Zhang, Y., & Mi, Z. (2018). Environmental benefits of bike sharing: A big data-based analysis. *Applied Energy*, *220*, 296–301. https://doi.org/10.1016/j.apenergy.2018.03.101

Zhang, Y., Thomas, T., Brussel, M., & van Maarseveen, M. (2017). Exploring the impact of built environment factors on the use of public bikes at bike stations: Case study in Zhongshan, China. *Journal of Transport Geography*, *58*, 59–70. https://doi.org/10.1016/j.jtrangeo.2016.11.014

Zhang, Y., & Xin, D. (2020). Dynamic Optimization Long Short-Term Memory Model Based on Data Preprocessing for Short-Term Traffic Flow Prediction. *IEEE Access*, *8*, 91510–91520. https://doi.org/10.1109/ACCESS.2020.2994655

Zhou, T., Huang, B., Liu, X., He, G., Gou, Q., Huang, Z., & Xie, C. (2020). Spatiotemporal Exploration of Chinese Spring Festival Population Flow Patterns and Their Determinants Based on Spatial Interaction Model. ISPRS *International Journal of Geo-Information*, *9*(11), Article 11. https://doi.org/10.3390/ijgi9110670

Zhou, X., Wang, M., & Li, D. (2019). Bike-sharing or taxi? Modeling the choices of travel mode in Chicago using machine learning. *Journal of Transport Geography*, *79*, 102479. https://doi.org/10.1016/j.jtrangeo.2019.102479

Zhou, Y., Chen, H., Li, J., Wu, Y., Wu, J., & Chen, L. (2019). Large-Scale Station-Level Crowd Flow Forecast with ST-Unet. *ISPRS International Journal of Geo-Information*, *8*(3), Article 3. https://doi.org/10.3390/ijgi8030140

Zhou, Y., Liu, X. C., & Grubesic, T. (2021). Unravel the impact of COVID-19 on the spatio-temporal mobility patterns of microtransit. *Journal of Transport Geography*, *97*, 103226. https://doi.org/10.1016/j.jtrangeo.2021.103226

Zhu, D., Cheng, X., Zhang, F., Yao, X., Gao, Y., & Liu, Y. (2020). Spatial interpolation using conditional generative adversarial neural networks. *International Journal of Geographical Information Science*, *34*(4), 735–758. https://doi.org/10.1080/13658816.2019.1599122

Zhu, R., Zhang, X., Kondor, D., Santi, P., & Ratti, C. (2020). Understanding spatio-temporal heterogeneity of bike-sharing and scooter-sharing mobility. *Computers, Environment and Urban Systems*, 81, 101483. https://doi.org/10.1016/j.compenvurbsys.2020.101483

Zhu, X., & Guo, D. (2017). Urban event detection with big data of taxi OD trips: A time series decomposition approach. *Transactions in GIS*, *21*(3), 560–574. https://doi.org/10.1111/tgis.12288

Zimmerman, D., De Marsily, G., Gotway, C. A., Marietta, M. G., Axness, C. L., Beauheim, R. L., Bras, R. L., Carrera, J., Dagan, G., Davies, P. B., & others. (1998). A comparison of seven geostatistically based inverse approaches to estimate transmissivities for modeling advective transport by groundwater flow. *Water Resources Research*, 34(6), 1373–1413.